KIT SCIENTIFIC REPORTS 7663

Large Scale Separate Effects Tests on Hydrogen Combustion during Direct Containment Heating Events

Leonhard Meyer, Giancarlo Albrecht,
Max Kirstahler, Markus Schwall, Ernst Wachter

KIT Scientific Publishing

Leonhard Meyer, Giancarlo Albrecht,
Max Kirstahler, Markus Schwall, Ernst Wachter

Large Scale Separate Effects Tests on Hydrogen Combustion during Direct Containment Heating Events

Karlsruhe Institute of Technology
KIT SCIENTIFIC REPORTS 7663

Large Scale Separate Effects Tests on Hydrogen Combustion during Direct Containment Heating Events

by
Leonhard Meyer, Giancarlo Albrecht,
Max Kirstahler, Markus Schwall, Ernst Wachter

KIT Scientific Publishing

Report-Nr. KIT-SR 7663

Hinweis
Die vorliegende wissenschaftliche Kurzdarstellung wurde im Auftrag
des Umweltministeriums Baden-Württemberg durchgeführt.
Die Verantwortung für den Inhalt dieser Veröffentlichung liegt bei den Autoren.

Impressum

Scientific Publishing

Karlsruher Institut für Technologie (KIT)
KIT Scientific Publishing
Straße am Forum 2
D-76131 Karlsruhe

www.ksp.kit.edu

Print on Demand 2014

ISSN 1869-9669
ISBN 978-3-7315-0195-4
DOI: 10.5445/KSP/1000039484

ABSTRACT

In the frame of severe accident research for light water reactors Karlsruhe Institute of Technology (KIT), formerly Forschungszentrum Karlsruhe (FZK), operates the facility DISCO-H since 1998, conceived to investigate the high pressure melt ejection (HPME) and direct containment heating (DCH) issue. Previous experiments have investigated the corium dispersion and containment pressurization in different reactor geometries using an iron-alumina melt and steam as model fluids. The analysis of these experiments showed that the containment was pressurized by the debris-to-gas heat transfer but also to a large part by hydrogen combustion.

The need was identified to better characterize the hydrogen combustion during DCH. To address this issue separate effect tests in the DISCO-H facility were conducted at a scale of 1:18 relative to a large European reactor. These tests reproduced phenomena occurring during DCH (injection of a hot steam-hydrogen mixture jet into the containment and ignition of the air-steam-hydrogen mixture) with the exception of corium dispersion. The hydrogen was blown out of a pressure vessel into a small compartment, simulating the reactor pit, and from there into a large vessel, simulating the containment. A number of distributed igniters simulated hot melt particles. Tests with and without steam and with concentrations of pre-existing hydrogen in the containment atmosphere between 0 and 8% were conducted.

Combustion codes were applied to reproduce the experimental data from tests in DISCO-H. The code calculations revealed shortcomings of the existing models which made an application of the code for reactor calculations unfeasible because of the required up-scaling. Combustion and heat loss models need further improvements. However, data from experiments at a single scale are not sufficient to reach this goal; therefore additional tests at a larger scale (1:7) in the A2 facility at the Institute for Nuclear and Energy Technologies (IKET) were performed.

The most important variables measured were the increase in pressure in the containment vessel, gas temperatures and the number of moles of hydrogen burnt. The experiments have shown that there is no scaling effect relative to the pressure increase in the containment. The pressure increase correlates with total hydrogen burned. The fraction of hydrogen that burns depends on the ratio of pre-existing to blow-down hydrogen and on the total amount of hydrogen and varies between 46% and 100%.

Großmaßstäbliche Experimente zur Wasserstoffverbrennung bei DCH-Prozessen

ZUSAMMENFASSUNG

Im Rahmen der Forschung zu schweren Unfällen in Leichtwasserreaktoren wird im Karlsruher Institut für Technologie (KIT), früher Forschungszentrum Karlsruhe (FZK), seit 1998 die Versuchsanlage DISCO-H betrieben. Vorangegangene Experimente haben die Schmelzeverteilung und Druckerhöhung im Containment nach Versagen des Reaktordruckbehälters (RDB) für verschiedene Reaktorgeometrien untersucht (Direct Containment Heating, DCH), unter Anwendung von Eisen-Aluminium-Schmelzen und Dampf als Modellfluide.

Die Analyse dieser Experimente hat gezeigt, dass der Druckanstieg sowohl durch den Wärmeübergang von der Schmelze an das Gas, aber auch zum nicht unerheblichen Teil durch Wasserstoffverbrennung verursacht wurde. So hat sich die Notwendigkeit ergeben, die charakteristischen Eigenschaften der Wasserstoffverbrennung während des DCH-Prozesses besser beschreiben zu können. Um diese Fragen zu klären, wurden Einzeleffektexperimente in der DISCO-H Versuchsanlage durchgeführt. Mit Ausnahme der Schmelzedispersion laufen in diesen Experimenten die gleichen Prozesse ab, wie sie während des DCH-Vorganges auftreten, das ist das Abblasen einer heißen Wasserstoff-Dampf Mischung in den Sicherheitsbehälter und die Zündung und Verbrennung dieses Gasgemisches in einer Luft-Dampf-Wasserstoff Atmosphäre. Der Effekt der Schmelzepartikel als Zünder wurde mit Thermitkerzen simuliert. Experimente mit und ohne Dampf, und Wasserstoffkonzentrationen in der Atmosphäre des Sicherheitsbehälters zwischen 0 und 8% wurden durchgeführt.

Die experimentellen Daten aus DISCO-H Experimenten im Maßstab 1:18 wurden benutzt, um Modelle in Verbrennungscodes zu verifizieren und um die Ergebnisse auf Reaktormaßstab zu extrapolieren. Dabei hat sich gezeigt, dass die bestehenden Modelle verfeinert und kalibriert werden müssen. Dies ist jedoch mit Daten aus Experimenten bei einem einzigen Maßstab nicht möglich. Deshalb wurden zusätzliche Experimente bei einem größeren Maßstab (1:7) in der A2-Anlage im Institute für Kern- und Energietechnik (IKET) durchgeführt.

Die wichtigsten gemessenen Größen waren der Druckanstieg im Sicherheitsbehälter, die Gastemperaturen und die Anzahl der verbrannten Wasserstoffmole. Die Experimente haben ergeben, dass es in Bezug auf den Druckanstieg im Sicherheitsbehälter keinen Skalierungseffekt gibt. Der Druckanstieg korreliert mit der Masse des verbrannten Wasserstoffs. Der Bruchteil des Wasserstoffs, der tatsächlich verbrennt, hängt ab vom Verhältnis von im Containment bereits vorhandenen Wasserstoff zur Menge des in das Containment eingeblasenen Wasserstoffs, und von der Wasserstoff-Gesamtmenge, und variiert zwischen 46% und 100%.

TABLE OF CONTENTS

LIST OF TABLES

LIST OF FIGURES

1 Introduction

In case of a core melt accident in light water cooled nuclear reactors (LWR) depressurization is initiated, but the pressure vessel may fail at still elevated pressure of 1 to 2 MPa after the forming of a molten pool. Then, the molten core debris will be ejected forcefully into the reactor cavity and beyond, depending on the specific reactor design. This may pressurize the reactor containment building beyond its failure pressure.

Hydrogen combustion during high pressure melt ejection (HPME) can contribute more than half of the pressure increase in the containment [1, 2]. The most important role plays the time scale of hydrogen combustion [3, 4]. This effect has grown in importance since it was found that pre-existing hydrogen also burns in the same time scale if the concentration in the containment atmosphere is high [5].

Hydrogen is produced in the reactor pit during concurrent melt discharge and steam blow down by oxidation of the metal part of the corium. This reaction can be limited by the amount of available blow down steam or accessible metal. The latter either because of the limited amount of metal in the corium or because the particle sizes are too large to be fully oxidized. Depending on the limiting effects, there is either pure hydrogen flow or mixed hydrogen–steam flow out of the cavity into the neighboring reactor rooms. In these rooms and in the containment dome there is a mixed atmosphere of air, steam and hydrogen, whose composition depends on the accident history. Generally, an elevated pressure due to preceding steam release and a certain hydrogen concentration due to oxidation of fuel rod claddings can be assumed. Hot melt particles serve as igniters and the inflowing hydrogen burns as a flame, while mixing with the oxygen rich atmosphere. The combustion terminates when the oxygen concentration reaches a lower limit or the hydrogen supply ends. In the first case the subsequent hydrogen flows to the next reactor room or the containment dome, where it continues to burn. The release of thermal energy by hydrogen combustion contributes to the containment peak pressure when, firstly, it coincides with the bulk of the heat transfer from dispersed melt particles to the containment atmosphere, and secondly, the heat losses, i.e. heat transfer to structures, are lower than the heat release by combustion.

For an assessment of the effect of hydrogen combustion on the containment load the amount of hydrogen must be known that burns at the DCH time scale. The parameters are (1) the initially existing hydrogen in the containment, (2) the amount of hydrogen produced during blow down and (3) the cavity geometry. Calculations with the dedicated combustion code COM3D [6] revealed that, depending on initial concentration of hydrogen in the containment, three regimes of combustion can be distinguished. In the first regime, which is realized in case of low initial hydrogen concentration, the hydrogen injection will lead to the formation of an attached diffusion flame and the pressure rise in this case is defined by the hydrogen injection rate only. In the second regime the initial hydrogen concentration in the containment is slightly below the lower flammability limit (LFL). The containment atmosphere is not burnable; however an injection even of small amounts of hydrogen can lead to fast formation of large-scale burnable mixtures and thus drastically change the regime of heat release. The rate of heat release in this case is defined by the competition between hydrogen injection, mixing of the injected gas and burnout of the newly formed combustible mixture. After burn-

out of the volumetric hydrogen a formation of the attached diffusion flame, similar to the first regime, is expected. The third regime is characterized by higher initial hydrogen concentrations. In this regime the initial containment hydrogen concentration is higher than LFL. An ignition of the burnable cloud results in different modes of premixed combustion. The flame speed and connected pressure growth can be different depending on turbulence level, obstruction of the volume, etc. After burnout of the containment hydrogen, again formation of the attached diffusion flame is expected, if O_2 is still available.

Dedicated combustion codes (e. g. COM3D) were not capable to reproduce the results obtained in a first series of experiments with hydrogen release conducted in the DISCO facility at Forschungszentrum Karlsruhe (FZK, now KIT) at a geometrical scale of roughly 1:18 [5, 6]. The code calculations revealed shortcomings of the existing models which made an analysis of DCH in real reactors unfeasible due to up-scaling [3]. Combustion models and heat loss models need further improvements. The final objective is to obtain parameters for combustion rates under DCH conditions at reactor scale, to be used in lumped parameter codes as ASTEC. Experiments at a single scale are not sufficient to reach this goal, therefore additional tests at different scales were deemed necessary. Consequently, a second series of experiments under similar conditions in a similar geometry but at larger scale of approximately 1:7 were conducted (see Fig. 1 for comparison of size).

2 Geometry and Dimensions

The experiments were performed in the A2 test facility at the Institute for Nuclear and Energy Technology (IKET), which is shown in Fig. 2. Since the A2-pressure vessel modelled the containment vessel, which should contain steam, the A2-vessel was thermally insulated and equipped with an electrical heater (Fig. 3). The heater-blower apparatus worked in a closed cycle, drawing dry air from the vessel through the heater and blowing it back into the vessel. The lower calotte of the pressure vessel was filled with concrete with embedded draining lines.

The experimental setup and procedure, the instrumentation and data acquisition were arranged as similar as possible to the test series with the simplified geometry in the DISCO-H facility at the scale 1:18. Only the three components of a reactor, respectively their volumes were modelled, the reactor pressure vessel (RPV) including the volume of the primary cooling system (RCS), the reactor cavity and the containment. The main dimensions, flow areas and volumes of the two facilities can be taken from Table 2 and Table 3 and Fig. 67 - Fig. 9.

The opening mechanism in the exit tube located at the bottom of the RPV vessel was different in the two facilities. In the small facility it was a ball valve, which had opening times between 68 ms and 192 ms. In the large facility it was a rupture disk, which was fully open within less than 5 ms.

In these experiments, the fraction of hydrogen, that is produced during steam-corium blowdown by oxidation of the metal part with steam in DCH experiments or in real case, is filled into the vessel, which models the volumes of the reactor cooling system (RCS) and the reactor pressure vessel (RPV), and is blown out of it together with the other gases used, i.e. nitrogen or steam. This is an adequate simulation of hydrogen blowdown and production, since generally most of the metal oxidation and thereby hydrogen production takes place within the cavity. The atmosphere in the containment was varied in these tests, containing either air or a mixture of air and steam with different amounts of pre-existing hydrogen.

As in the test series in scale 1:18, the simplified geometry did not have sub-compartments and the eight exits from the cavity to the containment vessel were modelled by four pipes keeping the total flow cross section true to scale (Fig. 6).

Because of the absence of melt droplets no natural igniters for the hydrogen are available. Twelve distributed igniters simulated hot melt particles. One igniter each was above every single pipe exit (level 1), and four igniters each were at two higher levels (see **Table 4**, Fig. 6 and Fig. 10). Conventional thermite sparklers have been made steam-tight by coating with a water-resistant lacquer. They are started by electric resistance heating 1.2 seconds before initiating the blow down. They can ignite a hydrogen-air mixture in a radius of approximately 5 cm. They furnish sparks for a period of approximately 10 seconds, which is sufficient to guarantee ignition when the conditions are right.

3 Instrumentation

3.1 Temperature

Gas temperatures were measured with 24 K-type thermocouples having an outer diameter of 0.36 mm. One thermocouple was installed within the RPV pressure vessel. A total of 23 thermocouples were located at four levels in the containment pressure vessel. The exact positions are given in Table 5 and Fig. 11 through Fig. 15. Twelve additional thermocouples were installed at the inside wall of the containment pressure vessel. These temperatures were monitored at the heater control board to control the heat-up of the containment atmosphere prior to the test.

3.2 Pressure

A total of 8 strain gauge-type pressure transducers (6 Kulite® and 2 Kistler®) were used to measure steam and gas pressure. The compensated operating temperature range is 27°C – 232°C, with a thermal drift of +/- 5% of full scale output for the Kulite® transducers. The Kistler® transducers were mounted outside the facility in cold environment connected with a pipe to the measurement position. They were used as reference for the Kulite transducers during stationary periods of the experiment. During the transient period their response is slow due to the long connecting line. The Kulite transducers were adjusted at operating temperature before the start of the experiment. All gauges were mounted in tapped holes that were connected gas tight with the outside atmosphere at their backsides. In case of the transducers in the RCS-RPV pressure vessel and the cavity this connection was achieved by flexible steel hoses. The gauges in the containment pressure vessel were mounted in the blind flanges of the ports at different levels.

3.3 Data acquisition

The data acquisition system recorded data at a rate of 1000 data points per second per channel for a period of 40 seconds.

3.4 Gas composition

Twelve pre-evacuated 500-cm³ gas grab sample bottles were used to collect dry-basis gas samples before and after the test at six positions in the containment vessel at four levels (Fig. 17). The sample lines and the sample bottles were at room temperature, thus the bottles were filled with non-condensable gases and steam that later condensed. The ventilator inside the containment is running before and after the test to ensure a well-mixed atmosphere. The gas samples were analysed at the Engler-Bunte-Institut at the KIT.

3.5 Video observation

Four video cameras with 50 frames/second and one high speed video camera with 125 frames/second were used to record the strength and timing of hydrogen combustion. Two cameras were looking down from the top cover, one had a horizontal view from a level B port, and one used an endoscope introduced in a level A port (). The high speed camera also used an endoscope through a level B port, but yielded underexposed pictures due to the small aperture of the endoscope, so no information could be used from them.

4 Test parameters

Table 1. Test matrix with initial conditions of performed tests

		GL1	GL2	GL3	GL4	GL5	GL6	GL7	GL8	GL9
CON: Temperature	°C	32	118	91	93	111	112	122	123	115
CON: Pressure	MPa	0.200	0.205	0.206	0.155	0.165	0.178	0.221	0.212	0.170
CON: Steam		no	no	no	yes	yes	yes	no	no	yes
CON: H2 mass	g	0	814	700	711	1613	1497	2421	1607	1435
CON: H2 concentration	%	0	2.82	2.24	3.05	6.79	5.87	7.82	5.42	5.94
RPV: Pressure	MPa	1.80	1.79	1.80	1.77	1.77	1.77	-	1.75	1.69
RPV: Temperature	°C	31	118	91	91	117	113	-	126	124
RPV: Hydrogen mass	g	1596	1375	803	755	785	1378	-	808	1276
Total Hydrogen mass	g	1596	2189	1503	1466	2398	2875	2421	2415	2711

The main initial parameters of the nine tests performed are shown in Table 1. In all tests the initial pressure in the RPV was approximately 1.8 MPa, while the containment pressure was kept between 0.16 and 0.22 MPa. One basic combustion test was conducted (GL7), in a dry containment atmosphere with a high hydrogen concentration above the flammability limit (7.8%), without any blow-down of hydrogen or nitrogen. Four tests were performed in a dry containment atmosphere, without steam (GL1, GL2, GL3, GL8). In these four tests the hydrogen mass in the containment was varied in steps between 0, 800 and 1600 gram, leading to hydrogen concentrations of 0%, approximately 3% and 5.4%. Different amounts of hydrogen were stored in the RPV together with nitrogen to obtain the pressure of 1.8 MPa. Also, four tests were conducted with a wet containment atmosphere, approximately 0.1 MPa air and 0.1 MPa steam (GL4, GL5, GL6 GL9). In these tests the initial hydrogen concentration varied between 3.1 and 6.8%.

The complete initial conditions in the containment and RPV/RCS are given in Table 7 and 8.

5 Experimental procedure

The pressure vessel A2 (Fig. 2) modelling the containment was insulated and equipped with a closed cycle heating system (Fig. 3). Air is drawn from the upper dome inside the vessel (Fig. 4), led through an electric heater and blown back into the vessel in its lower region (Fig. 5).

Except for test No.1, the containment air, structures and wall were heated to 120°C at atmospheric pressure during several hours before the test. Then, the valves of the heating loop are closed, both at the entrance and exit sides. In test cases with a dry containment atmosphere, air was added until the pressure reached 0.2 MPa. In the test cases with wet containment atmosphere, steam was added over a prolonged time, while condensate water was drained from a bottom valve. The steam generation is stopped when the containment pressure remains constant at 0.2 MPa for a certain period of time. Finally, a metered amount of hydrogen is added to the containment vessel. During the whole procedure two fans are running inside the vessel and serve for a mixing of the containment atmosphere.

The pressure vessel modelling the RCS and the RPV volume (Fig. 6 and 8) attained the same temperature as the containment. The oxygen is removed from the vessel by flushing with nitrogen. Thereafter the vessel is closed at atmospheric pressure. This condition (1000 mbar) determines the initial nitrogen mass inside the RPV-vessel. Then hydrogen is filled into the vessel. The exact mass of added hydrogen was determined by weighing the hydrogen gas bottle before and after the filling process with 0.1 g resolution. If the pressure in the RPV-vessel is below 1.8 MPa, nitrogen is added until this pressure level is obtained.

Before the start of the test the pre-test gas samples are taken and the fans are turned off. The experiment is started computer controlled with the ignition of the thermitic sparklers. After two seconds a valve is opened at the top of the RPV-vessel which releases a plunger (pointed steel cylinder, 24 mm diameter, 40 mm length, Fig. 6). This cylinder falls through a guide tube and hits the rupture disk at the bottom of the vessel, which immediately opens fully within less than 5 ms. The blow down of the hydrogen-nitrogen mixture from the RPV vessel into the cavity commences and continues until pressure equilibrium with the containment pressure is reached. The only flow path out of the cavity is through the four pipes. After the data acquisition terminates, the fans are turned on again and after five minutes the post-test gas samples are taken.

6 Results

A compilation of all results regarding pressure and temperature histories is shown in figures 18 through 22. The detailed pressure and temperature curves of all sensors are shown for all tests individually in figures 27 through 71.

6.1 Pressure

The pressure blow down curves in Fig. 18 fall into two groups; one with a faster pressure decline (GL2, GL6, GL9) and the other one with a slower blow down. The first group is characterized by a blow down of almost pure hydrogen (88 mol% H_2), while the other group contains tests with about 50% hydrogen and 50% nitrogen. The curve of test GL1 lies in between, because the gas was at a lower temperature and the hydrogen content was 76%.

A compilation of the pressure rise in the containment is shown in figures 20, 21 and 22. For a better comparison the curves were shifted to the same initial pressure 0.2 MPa in Fig. 21 and 22. The most striking curve with a pressure rise of 0.32 MPa is that of the simple hydrogen combustion in dry atmosphere (GL7). The total hydrogen mass was similar as in test GL6, but all well mixed in the containment at time of ignition (see also Fig. 23).

Test GL5 had the highest concentration before blow-down (except in GL7), but it was already above the ignition limit. So, hydrogen started to burn, when the igniters were started. The pressure decreased already, when the blow-down commenced. Consequently, the pressure increase was relatively low.

Two tests with similar total hydrogen masses (GL2 and GL8) show different pressure increases. In GL2 the pre-existing hydrogen concentration in the containment was low and a large mass of hydrogen was blown down, resulting in a lower pressure increase (0.15 MPa) compared to test GL8 (0.20 MPa), where the conditions were vice versa.

In tests GL3 and GL4 similar amounts of hydrogen were involved in both, RPV and containment. While test GL3 had a dry atmosphere test GL4 had a wet atmosphere. However, the pressure increase is the same in both cases.

The simple blow down of almost pure hydrogen into a dry air atmosphere without pre-existing hydrogen in test GL1 resulted in a higher pressure increase than tests GL3 and GL4 with a slightly higher total hydrogen mass involved, but less pressure increase than in all other tests with substantial higher hydrogen mass.

6.2 Gas Temperature

The gas temperature in the RPV vessel (Fig. 19) initially drops due to the gas expansion, recovers and decreases again. The overall decrease is between 120 K and 160 K.

Figures 36 through 71 show the gas temperatures measured at four levels in the containment, level 1 being the highest position and level 4 the lowest, below the exit pipes (Fig.11-15).

All gas temperatures at all positions increase within the first second into blow down and reach a maximum within 1 and 4 seconds. The temperatures at level 4, below the pipe exits, are generally low and lie between 100°C and 300°C.

The temperatures at level 3, just above the pipe exits, show the most fluctuations over a prolonged period of time, depicting hydrogen flames at late times, which however do not contribute to the peak pressure anymore, but reduce the temperature and pressure drop over this period of time. The average temperature at this level is between 300 and 500°C in most cases.

The gas temperatures at level 2, higher up in the containment show the highest peaks, generally in the order of 1000°C, which correspond to the pressure peaks in the containment. The temperatures at the highest position, level 1, are similar to those at level 2, sometimes with less pronounced peaks.

The temperature histories in test GL7 show a different picture. This test was without blow down and had a hydrogen concentration of 7.82% in a dry atmosphere. All temperature traces at all levels are similar. They rise within 4 seconds by approximately 600 K and decrease by 200 K within the next 14 seconds. Only for the temperature at the lowest level 4, the decrease is higher with about 300 K.

6.3 Gas Analysis

The individual results of the gas sampling are listed in Table 9 through Table 17, each for the pretest sample and the posttest samples. These data are dry gas values, i.e. without steam fraction. The quantification limits for the components were as follows: 0.1 vol% for hydrogen, 0.3 vol% for oxygen, and 0.4 vol% for nitrogen.

For the gas analysis by the nitrogen ratio method (see appendix A) average values between the six measuring positions were taken. The results of the gas analysis are given in Table 18. There were differences between the evaluated amounts of initial hydrogen between the measured amount of added hydrogen and the results of the gas sampling. Although incomplete mixing of the atmosphere may have led to errors in the gas sampling method, for consistency with the post test data the values of this measuring method are stated throughout the report.

7 Analysis of Results and Comparison with G-series

A comparison of some tests from the G0-series in small scale with similar GL-tests in large scale is shown in Fig. 24. Although the pressure rises are similar in corresponding tests the time evolution is different. The picture changes if the time scale is scaled according to the linear scale of the facilities (Fig. 1). In Fig. 25 the time is scaled to prototype scale, i.e. multiplied by a factor of 18 for the G0 series and 7 for the GL series. GL1 and G02 are tests of blow-down in a dry atmosphere without pre-existing hydrogen, basically simple hydrogen torches. The peak pressures are identical. GL3 and G03 are both tests in a dry atmosphere with small pre-existing and small blow-down hydrogen masses, which show a small difference in the peak pressure, but this is within the experimental uncertainty in initial conditions. GL4 and G04 are the corresponding tests in a wet atmosphere; again identical pressure increase is found. There are no exactly matching tests with high hydrogen masses, which can be compared directly (as G06 with GL6); but taking into account the differences, the resulting peak pressures are similar again. In prototype scale the peak pressures would be reached about 16 to 25 seconds after blow down commenced. Also the decline of the pressure is similar in both scales, which means that the heat losses are similar in magnitude and time scaling, although different for different conditions.

For both test series, figure 26 shows the pressure increase in the containment vessel over the amount of hydrogen burnt during the entire duration of the test reduced by the containment volume. The pressure increases linearly with the amount of burned hydrogen, with some scatter and no scaling effect. The non-matching test GL7 was the test without blow-down, simple multi-ignited hydrogen combustion. The relation between the amount of burnt hydrogen and the total available (fraction burnt in Table 18), respectively the pre-existing or the blow-down hydrogen must be studied in detail and is not so simple. If there is only blow-down hydrogen (as in G01, G02 and GL1), the fraction which burns is very high; in case of GL1 it is even close to 100%. It is still high if the amount of blow-down hydrogen is higher than the pre-existing amount, as in GL2. Apart from this, the general trend seems to be: the higher the total amount of hydrogen, the higher the fraction which burns.

The theoretical possible pressure rise resulting from the energy release by hydrogen combustion can be approximated by combining the caloric equation of state with the ideal gas law, $\Delta p = \Delta Q(\kappa-1)/V$, with κ the ratio of gas specific heats and V the containment volume. The energy release by combustion is $\Delta Q = \Delta q\ N_H$, with Δq = 242 kJ/mol burnt H_2, and N_H the number of burnt hydrogen moles. The ratio of measured to theoretical pressure increase is the efficiency of the process, a measure for all heat losses involved. The efficiency lies between 42 and 71%, excluding the combustion without blow down (GL7); the average efficiency is 55%.

An extended comparison between the results of the hydrogen blow down tests in small scale and larger scale can be found is reference [7].

8 Conclusions

Hydrogen combustion tests at DCH conditions conducted in two different size facilities have shown that there is no scaling effect relative to the pressure increase in the containment. The pressure increase correlates with total hydrogen burned. The fraction of hydrogen that burns depends on the ratio of pre-existing to blow-down hydrogen and on the total amount of hydrogen and varies between 46% and 100%. Compartments may have an effect on the burnt fraction but this has not been investigated in depth. The efficiency of combustion energy conversion into pressure varies between 42 and 71% and again may be affected by compartments and structures in the containment. These effects can be analysed by code calculations, for which the experimental results may serve as a data base for code modelling and validation.

9 References

1. Meyer, L.; Albrecht, G.; Caroli, C.; Ivanov, I., Direct containment heating integral effects tests in geometries of European nuclear power plants. Nuclear Engineering and Design, 239(2009) pp.2070-84
2. L.Meyer, G.Albrecht, M.Kirstahler, M.Schwall, E.Wachter, G.Wörner, 2004, Melt Dispersion and Direct Containment Heating (DCH) Experiments in the DISCO-H Test Facility, FZKA 6988, Forschungszentrum Karlsruhe.
3. Meyer, L., Albrecht, G., Wilhelm, D., 2004, Direct containment heating investigations for European pressurized water reactors. NUTHOS-6, 2004, Nara, Japan, Proc. on CD-ROM Paper ID. N6P007
4. Wilhelm, D., 2003, Recalculation of corium dispersion experiments at low system pressure, NURETH-10, 2003, Seoul, Korea.
5. Meyer, L.; Albrecht, G.; Kirstahler, M.; Schwall, M.; Wachter, E., Separate effects tests on hydrogen combustion during direct containment heating, events. Wissenschaftliche Berichte, FZKA-7379 (Januar 2008)
6. Meyer, L.; Kotchourko, A., Separate effects tests on hydrogen combustion during direct containment heating events in European reactors. Gupta, A. [Hrsg.] Transactions 19th Internat.Conf.on Structural Mechanics in Reactor Technology, (SMiRT-19), Toronto, CDN, August 12-17, 2007,Madison, Wis. : Omnipress, 2007
7. Meyer, L.; Albrecht, G., Experimental study of hydrogen combustion during DCH events in two different scales, NURETH-14, Toronto, Ontario, Canada (2011)

TABLES

Table 2. Geometric parameters of the DISCO and A2 test facility

Containment Pressure Vessel		**DISCO**	**A2**
Diameter (inner)	m	2.17	5.95
Total empty volume of containment	m^3	14.18	234.5
Volume of internal structures (RRV/RCS, concrete)	m^3	0.30	7.5
Total freeboard volume	**m^3**	**13.88**	**227.0**
RCS and RPV pressure vessel			
Inner diameter of RCS	m	0.200	770
Height of RCS	m	1.593	2860
Volume of RCS	m^3	0.0500	1.278
Total volume of RCS and RPV	**m^3**	**0.0801**	**1.375**

Table 3. Geometrical flow parameters

		DISCO	A2
Height of cavity	m	0.612	1.507
Diameter of cavity (lower part, concrete wall)	m	0.342	0.905
Height of lower part (concrete wall)	m	0.462	1.241
Diameter of cavity (upper part, steel wall)	m	0.540	0.905
Length from RPV bottom (lower head) to cavity floor	m	0.066	0.165
Length of annular cross section	m	0.316	0.730
Gap width between RPV and cavity wall	m	0.021	0.052
Flow area of annulus (minimum flow cross section)	m^2	0.0212	0.141
Cut out diameter at nozzles (around main cooling lines)	m	0.086	0.215
Flow area at nozzles (4×cut out area)	m^2	0.0232	0.145
Diameter of connecting pipe attached to cut out	m	0.105	0.273
Flow cross section of 4 connecting pipes	m^2	0.0346	0.234
Empty volume of cavity (without RPV)	m^3	0.0748	0.969
Free volume of cavity	m^3	0.0365	0.378
RPV- exit hole / tube diameter	cm	2.50	6.25
RPV- exit hole area	cm^2	4.91	30.69

Table 4. Positions of igniters DISCO-A2

Level	Height [m]	Angle [°]	Distance to wall [m]
L1	2.25	45	1.774
L1	2.25	135	1.774
L1	2.25	225	1.774
L1	2.25	315	1.774
L2	2.70	0	1.174
L2	2.70	90	1.174
L2	2.70	180	1.174
L2	2.70	270	1.174
L3	4.10	45	874
L3	4.10	135	874
L3	4.10	225	874
L3	4.10	315	874

Table 5. Positions of Thermocouples DISCO-A2

Channel	Name	Level	Position	Height [m]	Angle [°]	Distance to wall [m]
0	T0	1 m above exit	RPV			
1	T1	L1*			18	1.5
2	T2	L1	Containment	5.85	0	3.0
3	T3	L1			198	0.3
4	T1	L2			315	2.0
5	T2	L2			270	1.0
6	T3	L2			225	2.0
7	T4	L2	Containment	4.24	180	0.3
8	T5	L2			135	2.0
9	T6	L2			90	1.5
10	T7	L2			45	0.3
11	T8	L2			0	2.0
12	T1	L3			315	2.0
13	T2	L3			270	0.1
14	T3	L3			225	2.0
15	T4	L3	Containment	2.90	180	1.5
16	T5	L3			135	2.0
17	T6	L3			90	1.5
18	T7	L3			45	0.1
19	T8	L3			0	1.0
20	T1	L4			45	1.3
21	T2	L4	Cavity	0.68	135	1.4
22	T3	L4			225	1.3
23	T4	L4			315	1.3

*in the Figures 9 – 10 they are labeled with E instead of L.

Table 6. Positions of pressure transducers

Name	Type	Range (MPa)	Position
P1	Kistler®	2.0	RPV connected with line to outside containment
P2	Kistler®	1.0	Containment vessel middle flange
P3	Kulite®	3.5	RPV top flange
P4	Kulite®	1.7	Upper cavity
P5	Kulite®	1.7	Lower cavity
P6	Kulite®	1.7	Containment top flange
P7	Kulite®	1.7	Containment lower flange
P8	Kulite®	1.7	Containment middle flange

Table 7. Initial Gas Composition in the Containment vessel

			GL1	GL2	GL3	GL4	GL5	GL6	GL7	GL8	GL9
Containment volume	V	m³	227	227	227	227	227	227	227	227	227
Initial air temperature	T_1	K	305	393	365	381	409	408	398	401	412
Initial pressure	p_1	MPa	0.2	0.2	0.202	0.105	0.106	***0.086***	0.205	0.203	***0.086***
Temperature at start	**T_2**	**K**	305	391	364	366	384	385	395	396	388
Pressure at start	**p_2**	**MPa**	0.2	0.205	0.206	0.155	0.165	0.178	0.221	0.212	0.170
Added hydrogen	**m_{H2}**	**kg**	0	0.814	0.700	0.711	1.610	1.497	2.421	1.607	1.435
Air mass	m_{air}	kg	518.5	402.4	437.4	217.1	203.9	167.4	409.0	402.0	165.0
Steam mass	**m_{steam}**	**kg**	**0**	**0**	**0**	**66.4**	**70.1**	**110.0**	**0**	**0**	**100.0**
Partial pressure of air	P_{2air}	MPa	0.200	0.199	0.201	0.100	0.099	0.082	0.203	0.200	0.081
Partial pressure H_2	p_{2H2}	MPa	0.000	0.006	0.005	0.005	0.011	0.011	0.017	0.012	0.010
Partial pressure steam	P_{steam}	MPa	0	0	0	0.049	0.055	0.086	0	0	0.079
Added hydrogen	**M_{H2}**	**kmol**	0.000	0.403	0.347	0.352	0.797	0.741	1.199	0.796	0.710
Steam moles	**M_{H2O}**	**kmol**	0.000	0.000	0.000	3.684	3.892	6.100	0.000	0.000	5.553
Air moles	M_{air}	kmol	17.90	13.89	15.10	7.495	7.042	5.781	14.12	13.86	5.699
Total gas moles	**M_{total}**	**k mol**	17.90	14.30	15.45	11.53	11.73	12.62	15.32	14.65	11.96
Nitrogen moles	M_{N2}	kmol	13.97	10.84	11.79	5.849	5.495	4.511	11.02	10.81	4.447
Oxygen moles	M_{O2}	kmol	3.758	2.916	3.170	1.573	1.478	1.214	2.965	2.908	1.196
Argon etc. moles	$M_{Ar\ etc.}$	kmol	0.172	0.134	0.145	0.072	0.068	0.056	0.136	0.133	0.055
Mol% of hydrogen	**M_{H2}/M_{tot}**	**%**	0.00	2.82	2.24	3.05	6.79	5.87	7.82	5.42	5.94
Mol% of steam	**M_{H2O}/M_{tot}**	**%**	0.00	0.00	0.00	31.95	33.17	48.33	0.00	0.00	46.42
Mol% of air	M_{air}/M_{tot}	%	100	97.18	97.76	65.00	60.03	45.80	92.18	94.57	47.64
Mol% of nitrogen	M_{N2}/M_{tot}	%	78.03	75.83	76.28	50.72	46.84	35.74	71.93	73.79	37.17
Mol% of oxygen	M_{O2}/M_{tot}	%	20.99	20.40	20.52	13.64	12.60	9.61	19.35	19.85	10.00
Mol% of argon	M_{Ar}/M_{tot}	%	0.96	0.94	0.94	0.63	0.58	0.44	0.89	0.91	0.46

Table 8. Compilation of main initial conditions in RPV/RCS

		GL1	GL2	GL3	GL4	GL5	GL6	GL7	GL8	GL9
RPV/RCS pressure	MPa	1.800	1.794	1.799	1.771	1.771	1.774	-	1.745	1.69
RPV/RCS temperature	K	304	390	364	364	390	385	-	399	398
RPV/RCS nitrogen	kg	5.300	2.248	11.76	12.07	10.15	2.220	-	9.050	2.212
RPV/RCS hydrogen	kg	1.596	1.375	0.803	0.755	0.785	1.379	-	0.808	1.276
RPV/RCS nitrogen	mol	189	80	420	431	362	79	-	323	79
RPV/RCS hydrogen	mol	790	681	397	374	389	683	-	400	632
Nitrogen blowdown*	**mol**	**161**	**71**	**360**	**377**	**319**	**71**	**-**	**284**	**70**
Hydrogen blowdown*	**mol**	**671**	**602**	**345**	**327**	**343**	**614**	**-**	**351**	**561**

* Note, that not all gas has been blow out of the RPV; the remainder has been calculated with pressure equilibrium being reached.

Table 9. Measured gas concentrations in GL1

Time	Location	Species (mole %)		
		N_2	O_2	H_2
Pretest	top: short	*(79.96*	*21.00*	*0)*
	top: long	79.17	20.83	0
	middle: short	79.10	20.90	0
	middle: long	78.94	21.06	0
	low: short	78.71	21.29	0
	low: long	78.77	21.23	0
	average	**78.95**	**21.05**	**0**
Posttest	top: short	*(82.35*	*19.58*	*< 0.1)*
	top: long	80.95	19.05	< 0.1
	middle: short	80.62	19.38	< 0.1
	middle: long	80.83	19.17	< 0.1
	low: short	80.24	19.76	< 0.1
	low: long	80.32	19.68	< 0.1
	average	**80.59**	**19.41**	**< 0.1**

Table 10. Measured gas concentrations in GL2

Time	Location	Species (mole %)		
		N_2	O_2	H_2
Pretest	top: short	77.66	19.35	2.99
	top: long	77.22	19.87	2.91
	middle: short	77.50	19.43	3.07
	middle: long	77.22	19.72	3.06
	low: short	77.34	19.71	2.95
	low: long	77.49	19.46	3.05
	average	**77.41**	**19.59**	**3.01**
Posttest	top: short	81.32	17.05	1.63
	top: long	81.87	16.56	1.56
	middle: short	81.35	17.00	1.65
	middle: long	81.04	17.15	1.81
	low: short	81.04	17.16	1.79
	low: long	80.46	17.53	2.01
	average	**81.18**	**17.08**	**1.74**

Table 11. Measured gas concentrations in GL3

Time	Location	Species (mole %)		
		N_2	O_2	H_2
Pretest	top: short	77.72	20.01	2.28
	top: long	77.94	19.92	2.14
	middle: short	77.61	20.16	2.23
	middle: long	77.38	20.42	2.20
	low: short	76.99	20.63	2.37
	low: long	77.85	19.87	2.27
	average	**77.58**	**20.17**	**2.25**
Posttest	top: short	79.40	18.72	1.88
	top: long	79.47	18.68	1.85
	middle: short	79.77	18.39	1.84
	middle: long	79.33	18.73	1.95
	low: short	79.15	18.96	1.89
	low: long	78.92	19.06	2.02
	average	**79.34**	**18.76**	**1.90**

Table 12. Measured gas concentrations in GL4

Time	Location	Species (mole %)		
		N_2	O_2	H_2
Pretest	top: short	75.51	19.90	4.59
	top: long	75.78	19.73	4.49
	middle: short	76.30	19.22	4.48
	middle: long	76.19	19.44	4.37
	low: short	75.92	19.70	4.38
	low: long	75.40	19.99	4.61
	average	**75.85**	**19.66**	**4.49**
Posttest	top: short	79.95	16.97	3.08
	top: long	*(80.10*	*17.49*	*2.41)*
	middle: short	80.01	16.81	3.18
	middle: long	80.78	15.93	3.29
	low: short	79.31	17.22	3.47
	low: long	78.75	17.40	3.85
	average	**79.76**	**16.87**	**3.37**

Table 13. Measured gas concentrations in GL5

Time	Location	Species (mole %)		
		N_2	O_2	H_2
Pretest	top: short	70.53	18.19	11.29
	top: long	70.84	17.80	11.35
	middle: short	71.93	17.94	10.14
	middle: long	71.91	18.22	9.87
	low: short	70.73	17.96	11.30
	low: long	*(74.06*	*19.02*	*6.92)*
	average	**71.18**	**18.02**	**10.79**
Posttest	top: short	81.56	15.40	3.05
	top: long	83.30	12.50	4.20
	middle: short	83.52	12.66	3.81
	middle: long	82.82	12.88	4.30
	low: short	81.66	15.82	2.52
	low: long	82.03	13.32	4.65
	average	**82.48**	**13.76**	**3.75**

Table 14. Measured gas concentrations in GL6

Time	Location	Species (mole %)		
		N_2	O_2	H_2
Pretest	top: short	71.44	17.49	11.07
	top: long	70.85	17.62	11.54
	middle: short	70.04	18.35	11.61
	middle: long	70.21	18.38	11.41
	low: short	71.04	17.91	11.06
	low: long	69.94	18.38	11.68
	average	**70.59**	**18.02**	**11.39**
Posttest	top: short	84.23	9.74	6.03
	top: long	*84.73*	*9.47*	*5.80*
	middle: short	82.94	10.76	6.30
	middle: long	79.98	11.69	*8.32*
	low: short	81.39	11.61	7.01
	low: long	*79.69*	*12.61*	7.69
	average	**82.16**	**10.98**	**6.86**

Table 15. Measured gas concentrations in GL7

Time	Location	Species (mole %)		
		N_2	O_2	H_2
Pretest	top: short	75.27	17.44	7.28
	top: long	75.09	17.58	7.34
	middle: short	75.30	17.66	7.05
	middle: long	74.44	18.55	7.02
	low: short	73.54	18.97	7.48
	low: long	*(77.37)*	*(18.50)*	*(4.14)*
	average	**74.73**	**18.04**	**7.23**
Posttest	top: short	82.71	16.21	1.08
	top: long	83.22	15.92	0.86
	middle: short	82.12	16.99	0.89
	middle: long	82.83	16.07	*1.10*
	low: short	83.51	15.79	0.71
	low: long	82.78	16.57	0.65
	average	**82.86**	**16.25**	**0.88**

Table 16. Measured gas concentrations in GL8

Time	Location	Species (mole %)		
		N_2	O_2	H_2
Pretest	top: short	74.58	20.00	5.43
	top: long	74.56	20.03	5.41
	middle: short	75.05	19.57	5.38
	middle: long	74.72	19.92	5.36
	low: short	75.61	19.06	5.33
	low: long	74.51	20.00	5.49
	average	**74.84**	**19.76**	**5.40**
Posttest	top: short	80.36	17.52	2.12
	top: long	80.71	17.38	1.90
	middle: short	80.33	17.63	2.03
	middle: long	80.49	17.27	2.24
	low: short	79.85	17.49	2.66
	low: long	79.38	17.91	2.71
	average	**80.19**	**17.53**	**2.28**

Table 17. Measured gas concentrations in GL9

Time	Location	Species (mole %)		
		N_2	O_2	H_2
Pretest	top: short	70.50	18.09	11.41
	top: long	70.67	17.95	11.38
	middle: short	69.99	18.60	11.41
	middle: long	69.84	18.73	11.43
	low: short	69.73	18.72	11.55
	low: long	69.49	18.70	11.81
	average	**70.04**	**18.46**	**11.50**
Posttest	top: short	82.73	11.14	6.13
	top: long	82.76	11.24	6.00
	middle: short	82.65	11.38	5.97
	middle: long	79.32	12.77	7.92
	low: short	81.19	11.97	6.84
	low: long	79.54	12.99	7.48
	average	**81.36**	**11.92**	**6.72**

Table 18. Initial Conditions, Results and Analysis of GL-series

		GL1	GL2	GL3	GL4	GL5	GL6	GL7	GL8	GL9
RPV pressure	MPa	1.800	1794	1.799	1.771	1.771	1.774	-	1.745	1.692
Steam concentration in cont.	mol %	0	0	0	31.95	33.17	48.33	0	0	46.42
H_2 concentration in cont.	mol %	0	2.82	2.24	3.05	6.79	5.87	7.82	5.43	5.94
Initial H_2 in containment	mol	0	403	347	352	797	741	1198	795	710
RPV-blow down H_2	mol	671	602	338	327	343	*650*	-	351	*610*
Total available H_2	mol	671	1005	692	679	1140	1391	1198	1146	1320
Burned H_2 (N_H)	mol	657	916	394	409	870	1059	1037	872	1031
Fraction burned	-	0.97	0.91	0.57	0.60	0.76	0.76	0.87	0.76	0.78
H_2 post test concentration	mol %	<0.1	1.7	1.9	2.2	2.2	3.2	0.8	2.1	3.1
Measured peak pressure increase	MPa	0.131	0.148	0.104	0.109	0.181	0.174	0.320	0.196	0.160
Theo. maximum $\Delta p = f(H_{2burn})$	MPa	0.245	0.342	0.147	0.152	0.325	0.395	0.385	0.325	0.385
Efficiency	-	0.53	0.43	0.71	0.71	0.56	0.44	0.83	0.60	0.42

FIGURES: Geometry

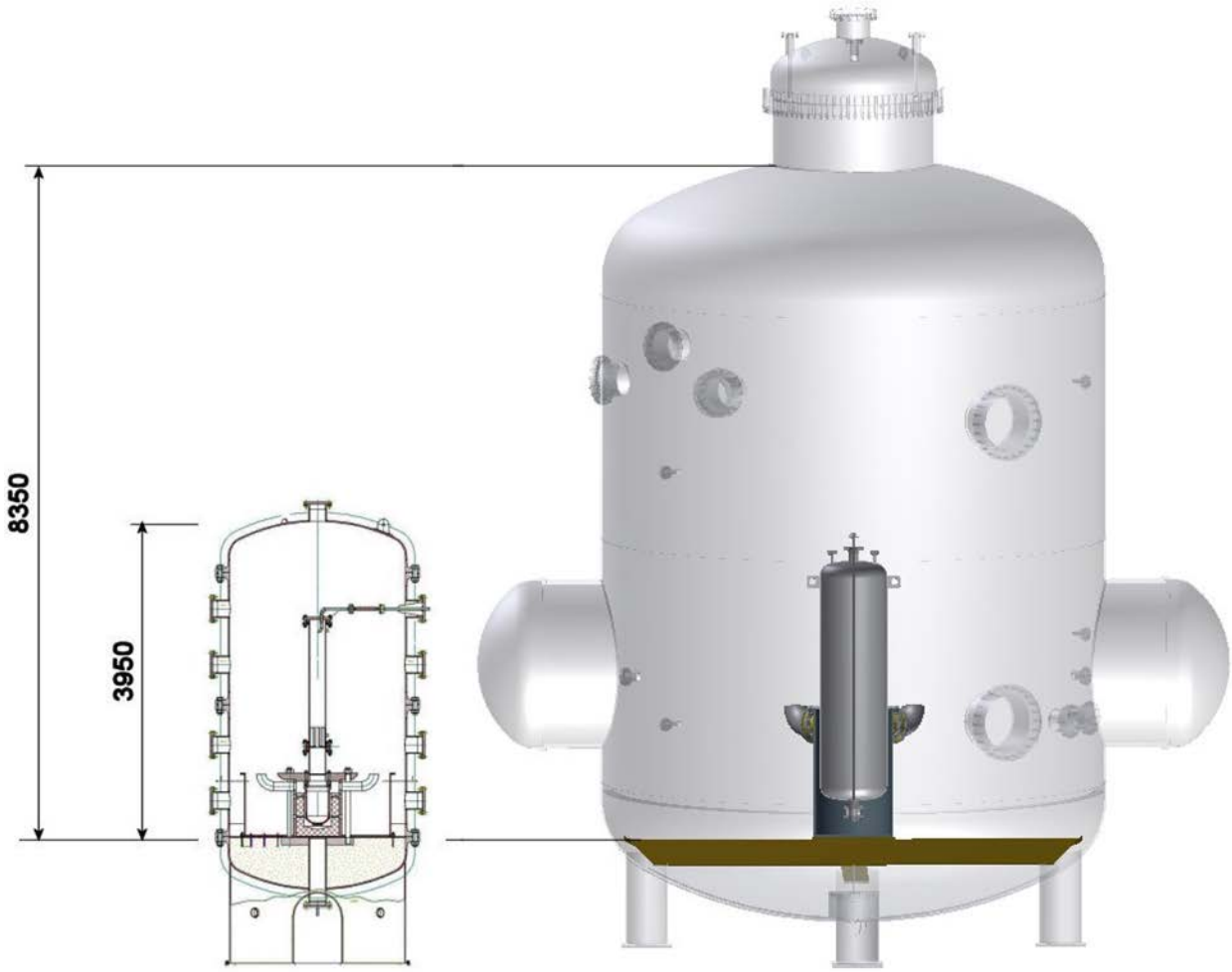

Fig. 1. The two test facilities in scale.

Fig. 2. Pressure vessel A2 without insulation and heating equipment

Fig. 3. Pressure vessel A2 with insulation and heating equipment

Fig. 4. Suction pipe of air heating equipment

Fig. 5. Air inlet coming from heater

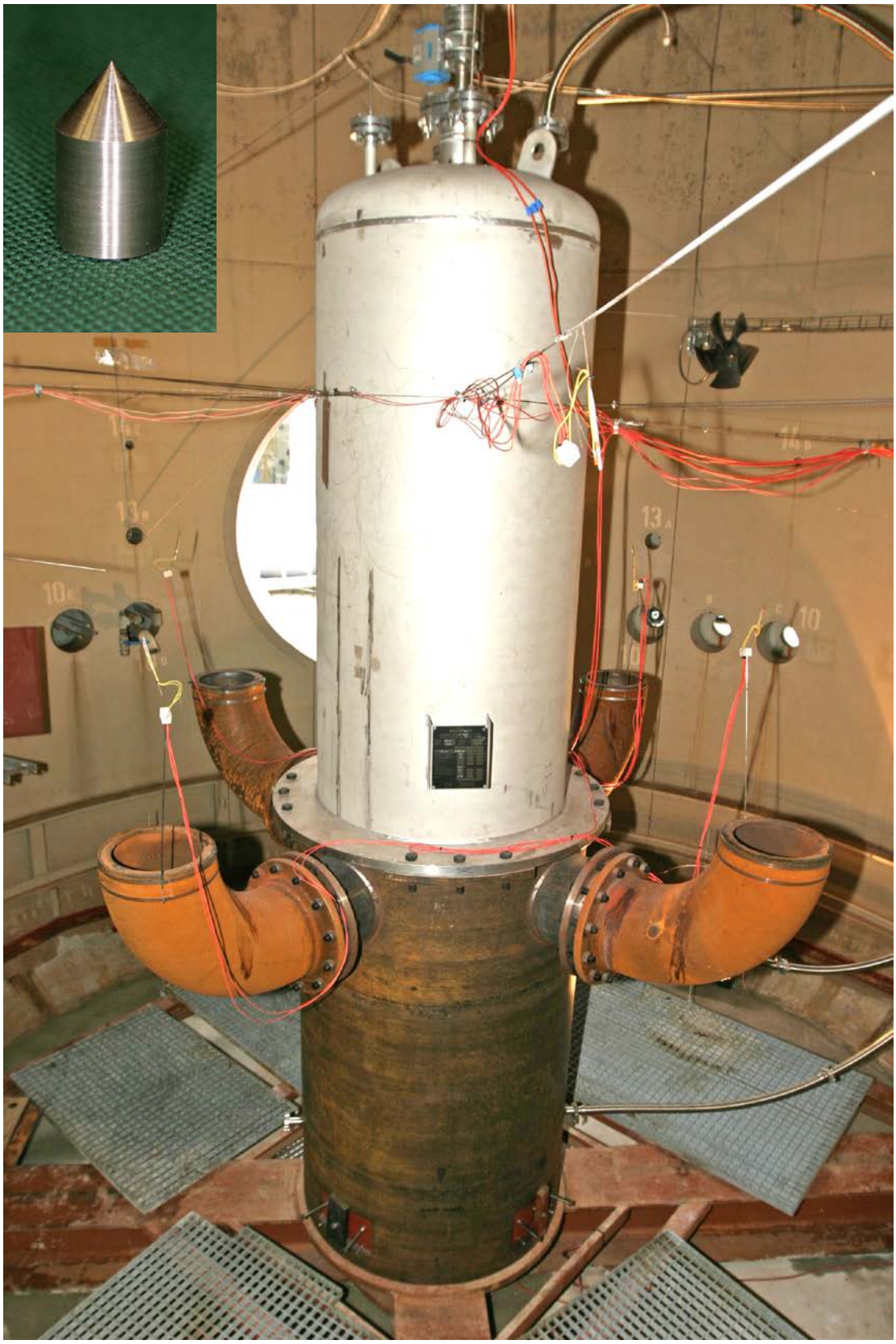

Fig. 6. Inside pressure containment vessel with RPV/RCS-vessel and cavity; plunger

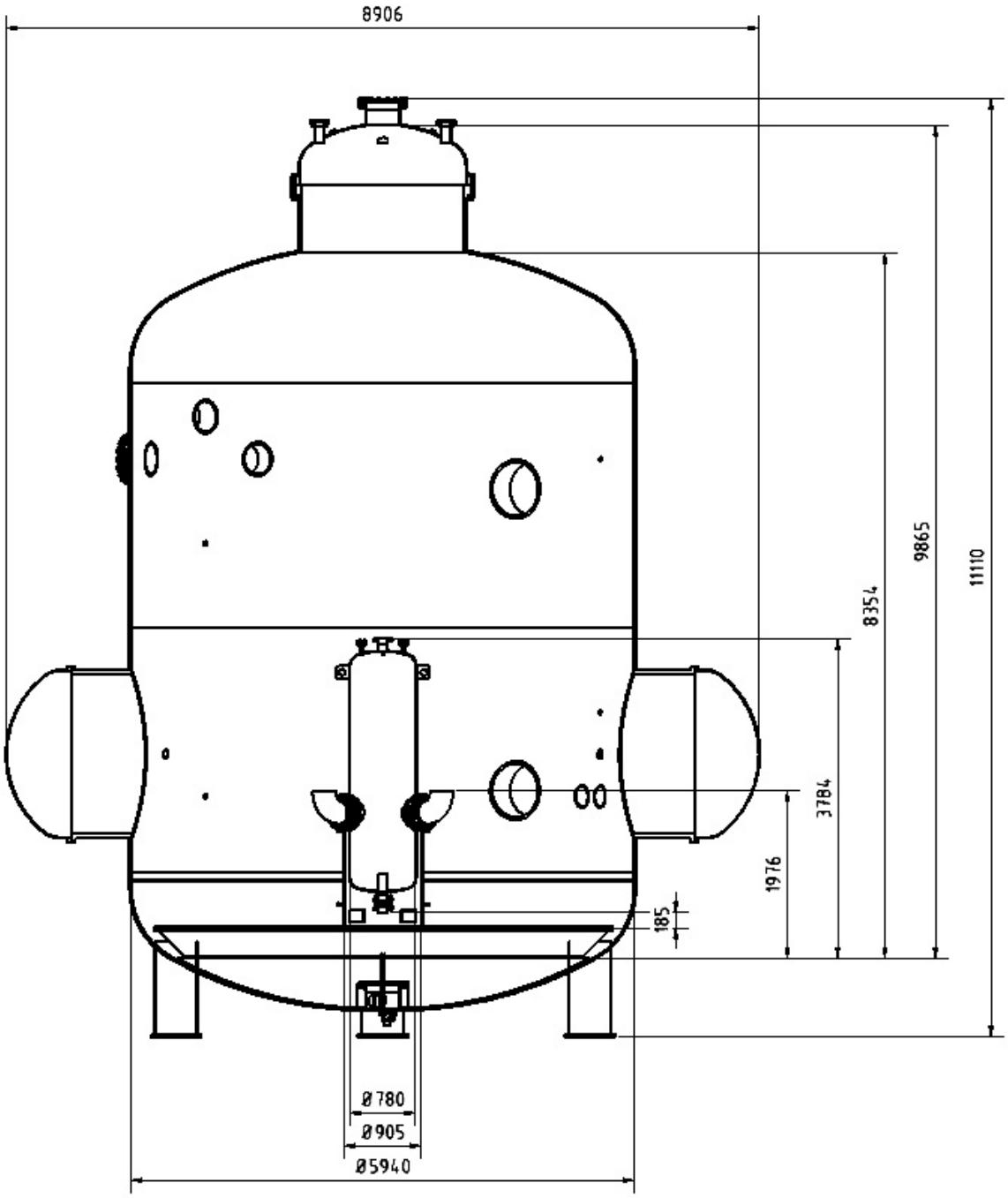

Fig. 7. The containment pressure vessel with internal structures

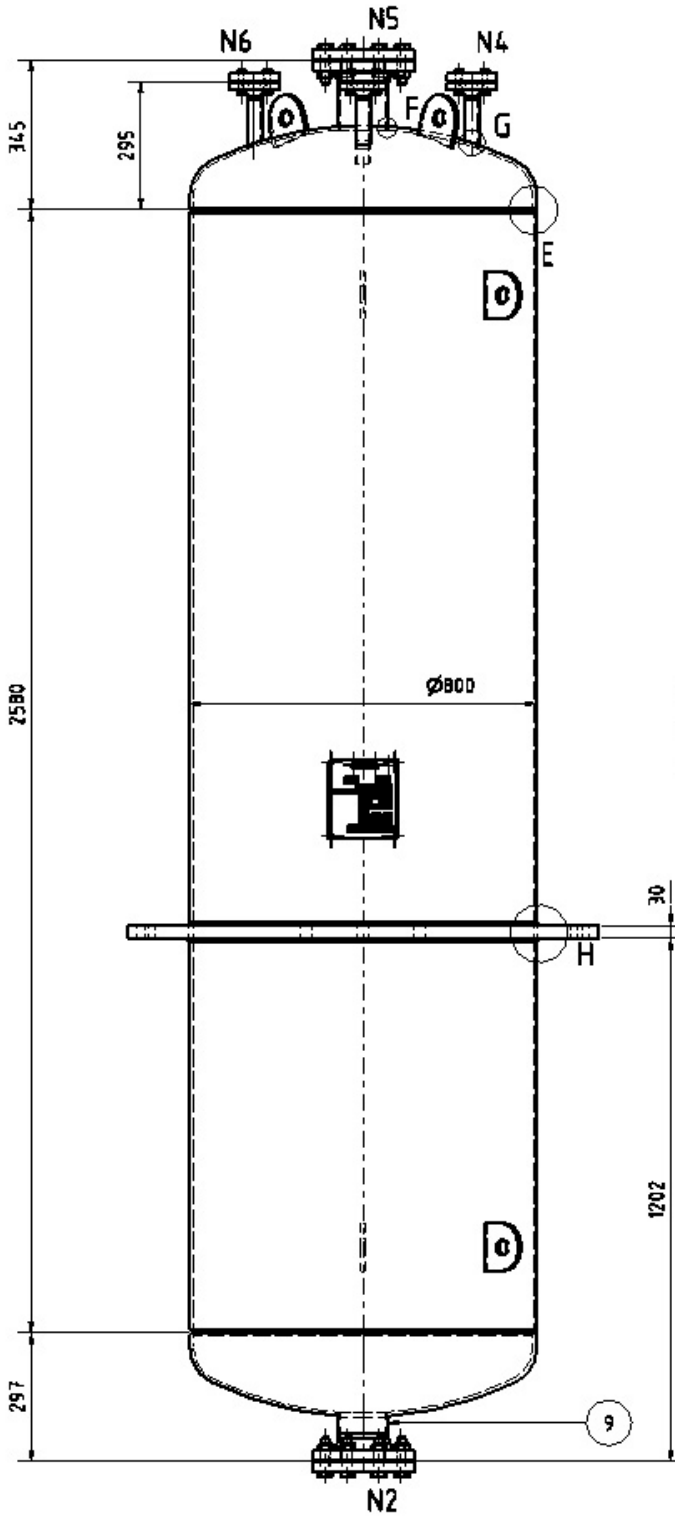

Fig. 8. Dimensions of the RPV vessel

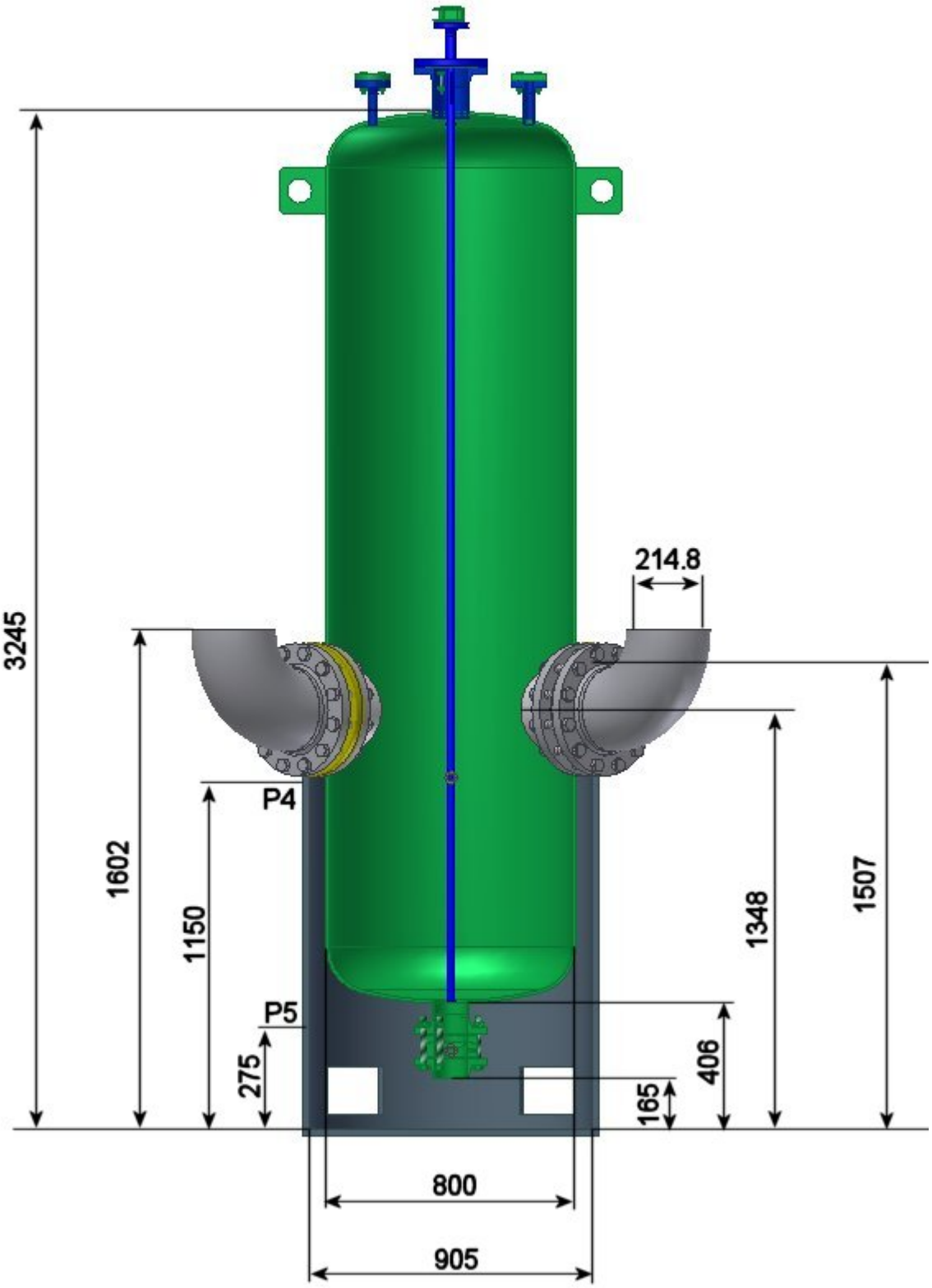

Fig. 9. Dimensions of the cavity and RPV (hand holes are closed during test)

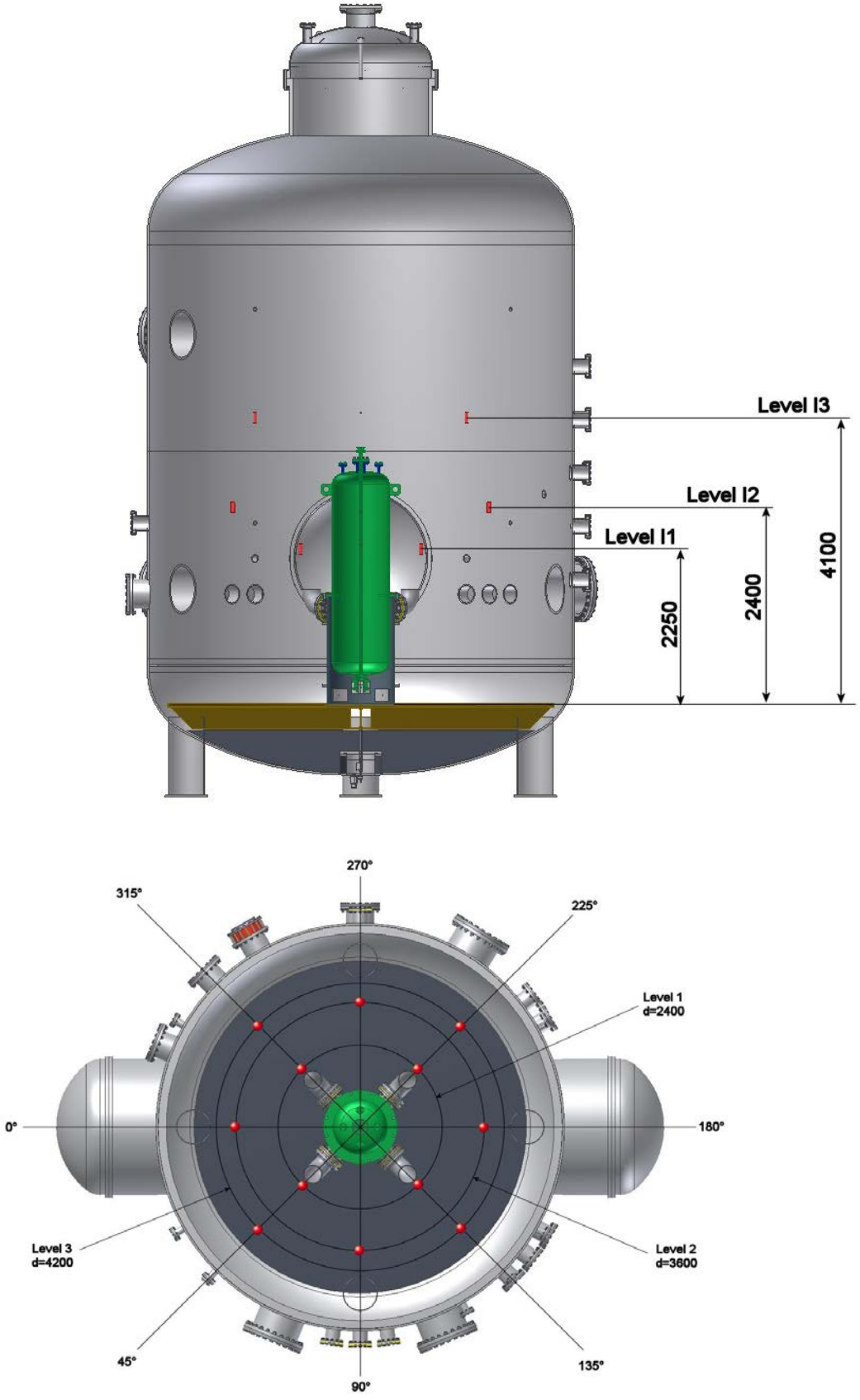

Fig. 10. Positions of igniters

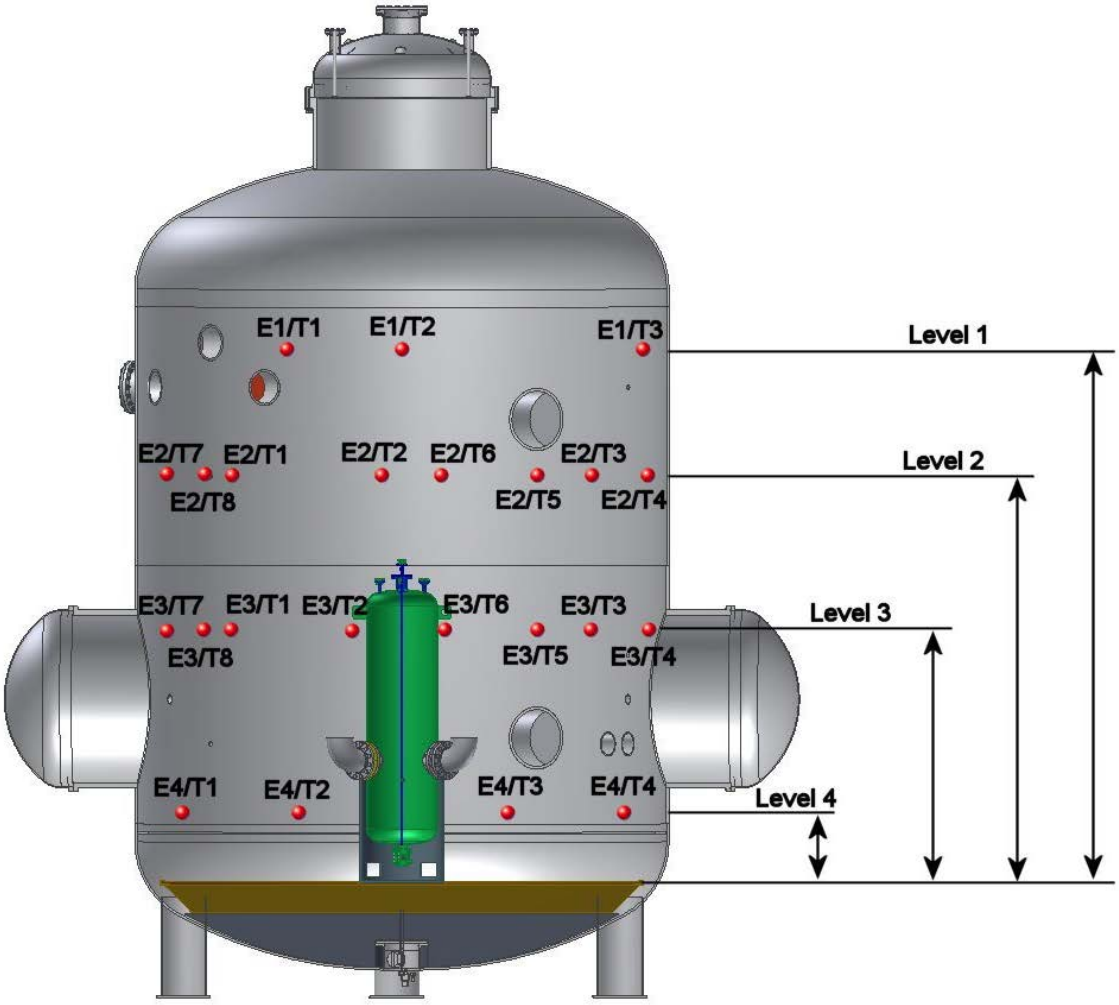

Fig. 11. Positions of thermocouples
(exact positions see **Table 5**)

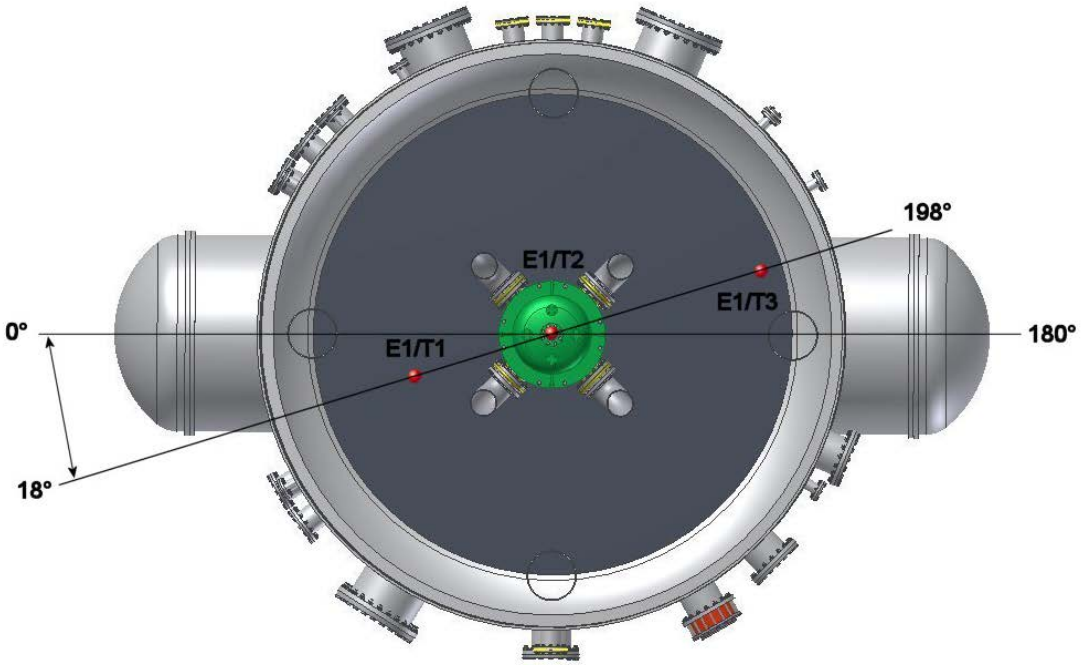

Fig. 12. Positions of thermocouples in level 1

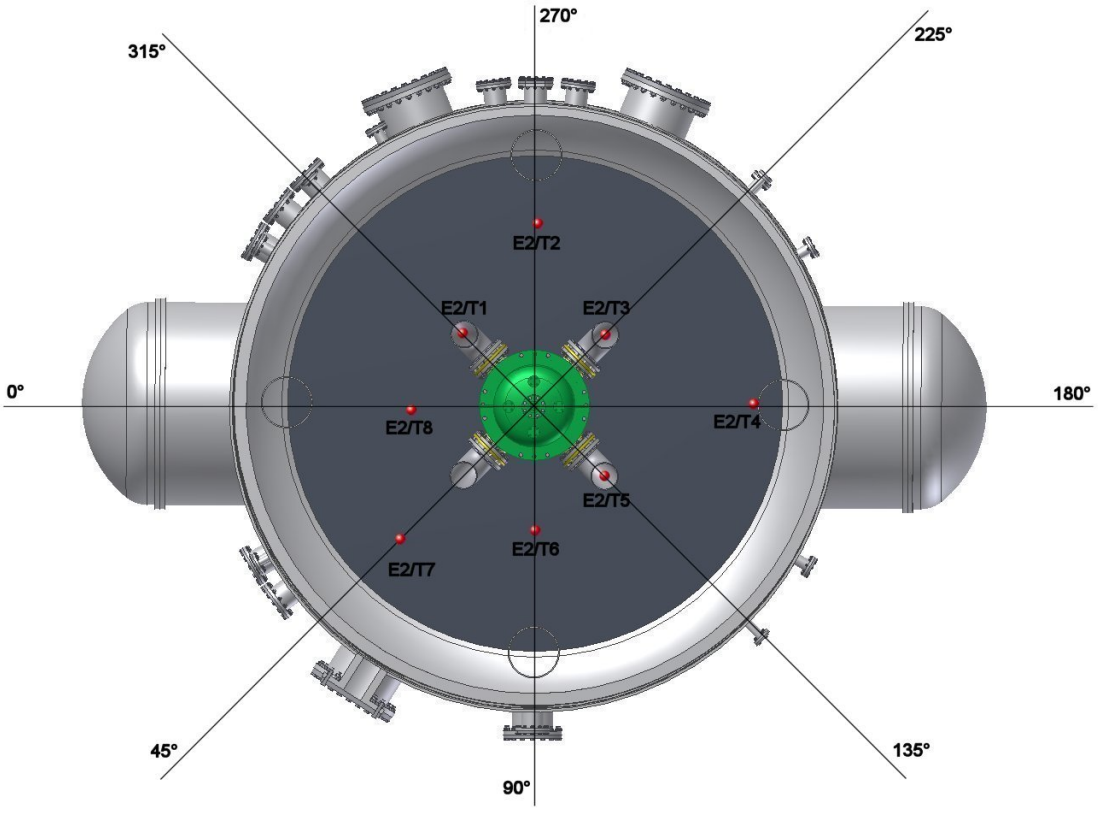

Fig. 13. Positions of thermocouples in level 2

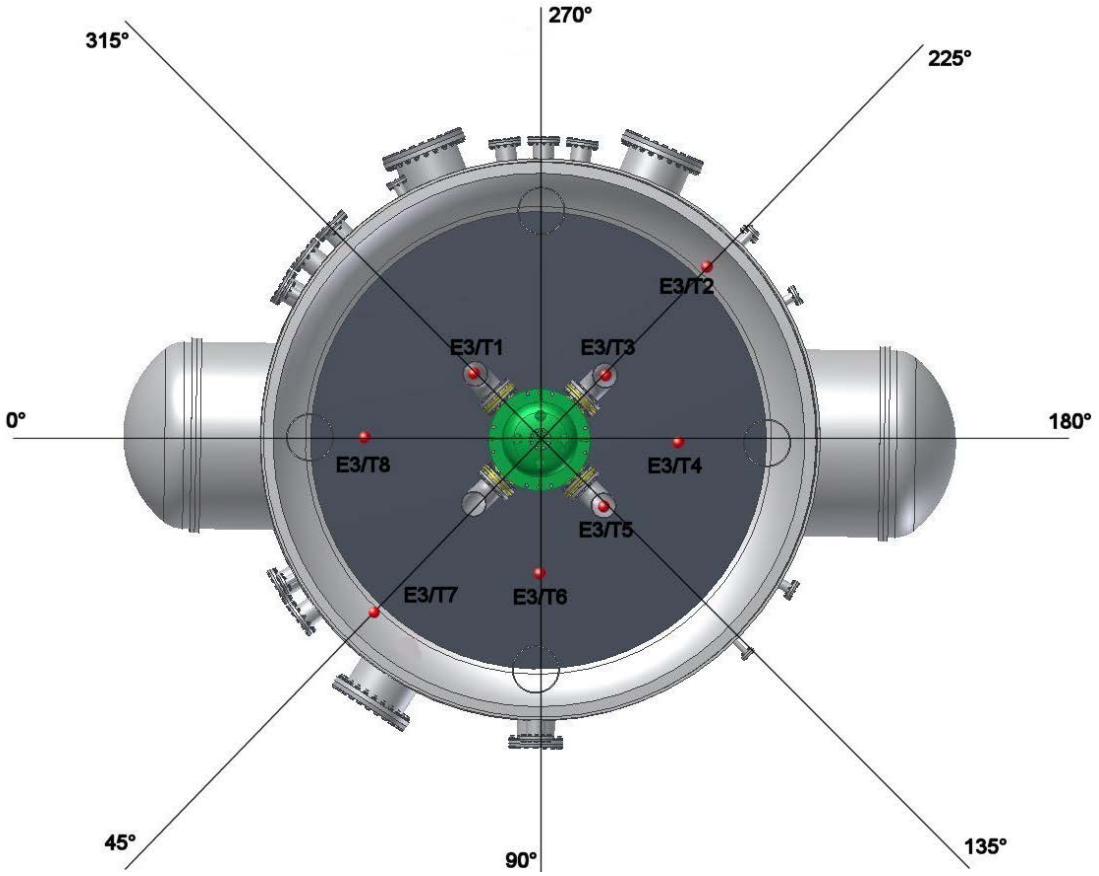

Fig. 14. Positions of thermocouples in level 3

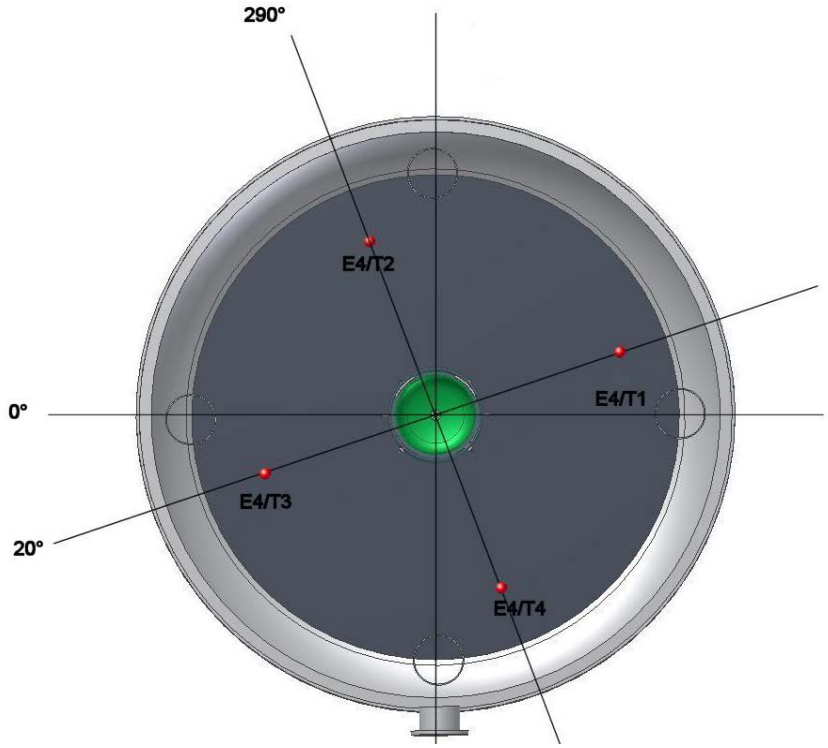

Fig. 15. Positions of thermocouples in level 4

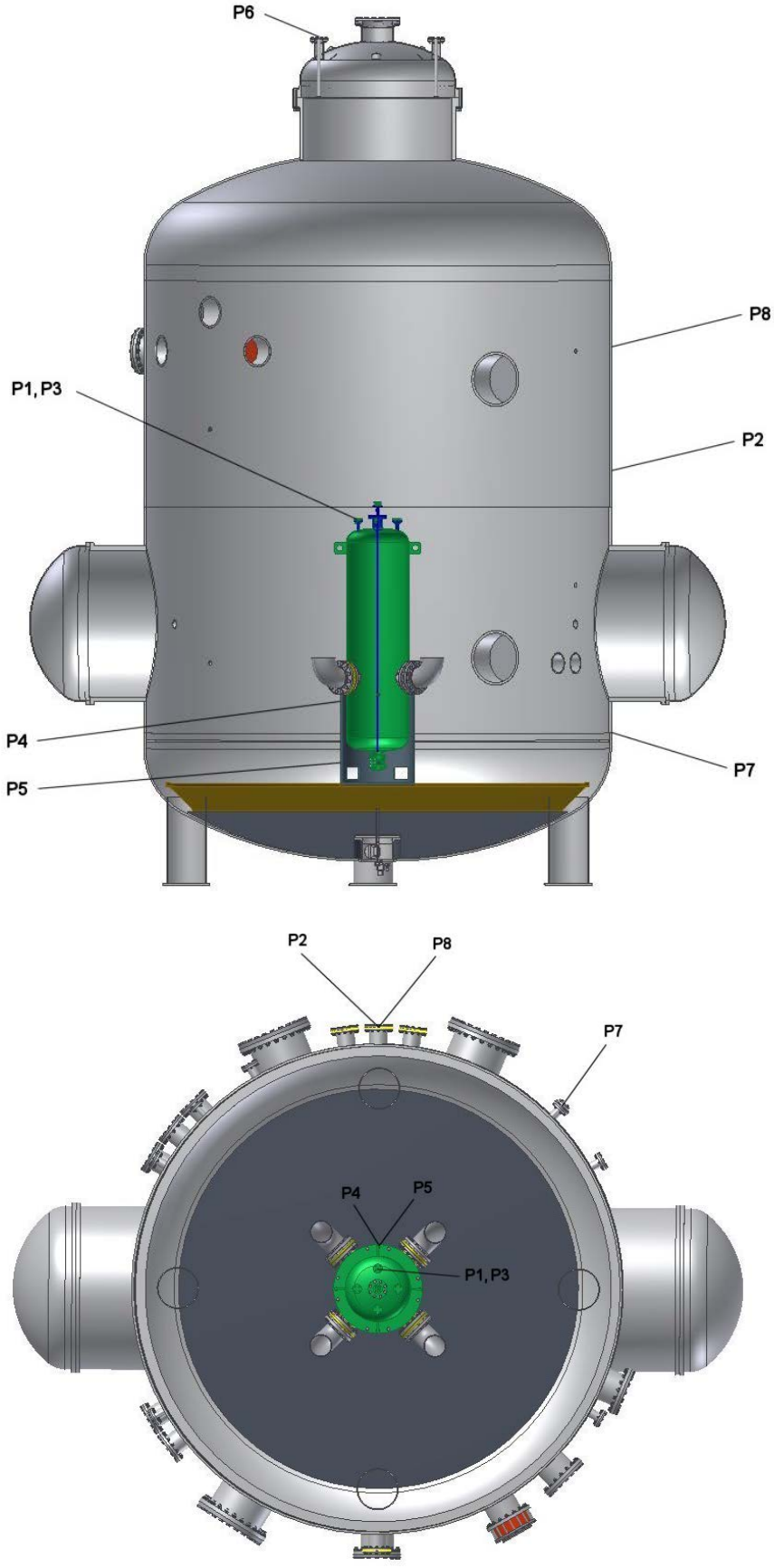

Fig. 16. Positions of pressure sensors

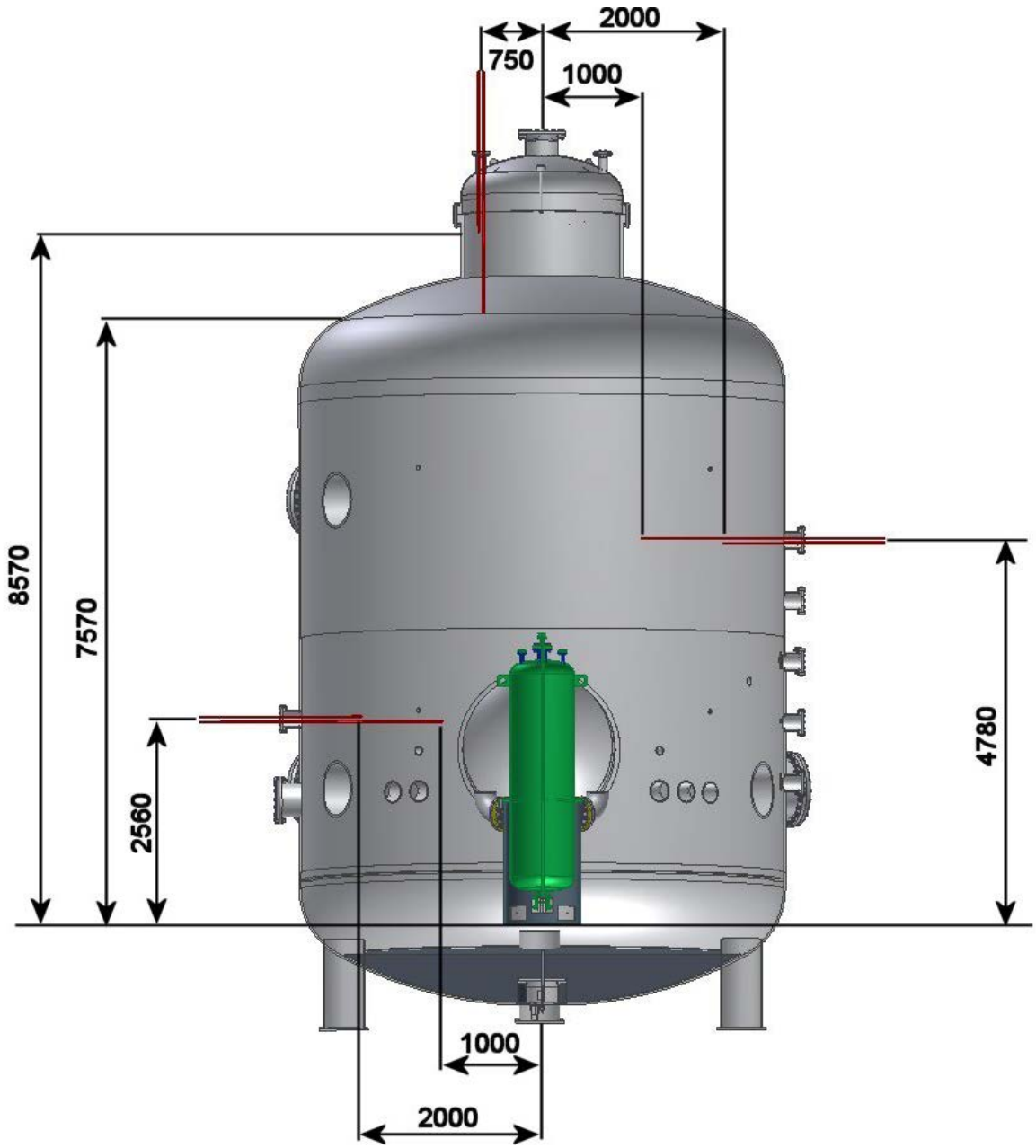

Fig. 17. Positions of gas sample lines (top: short/long; middle: short/long; low: short/long)

FIGURES: Results

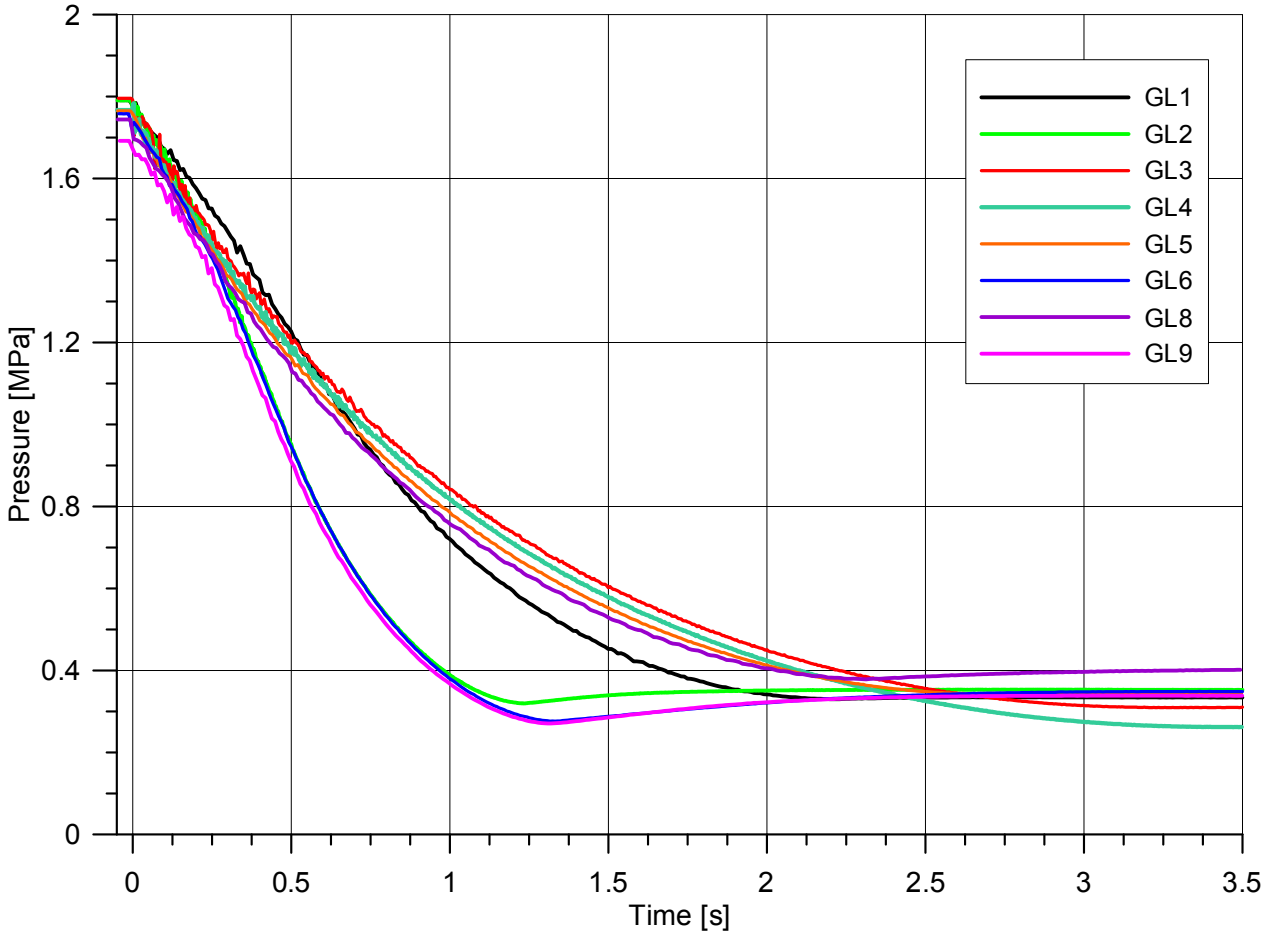

Fig. 18. Pressures in the RPV-vessel during blow down

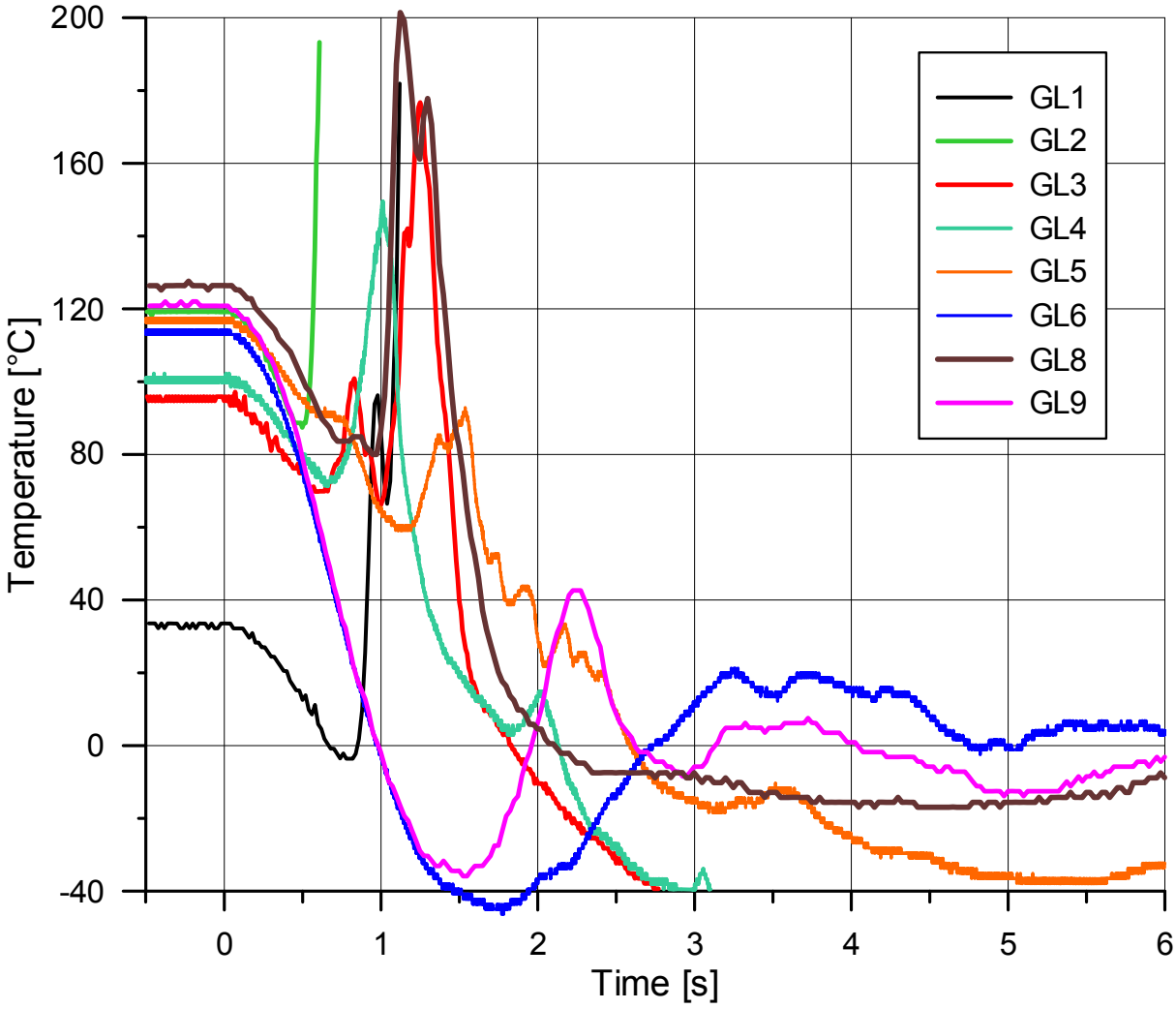

Fig. 19. Gas Temperature in the RPV vessel during blow down

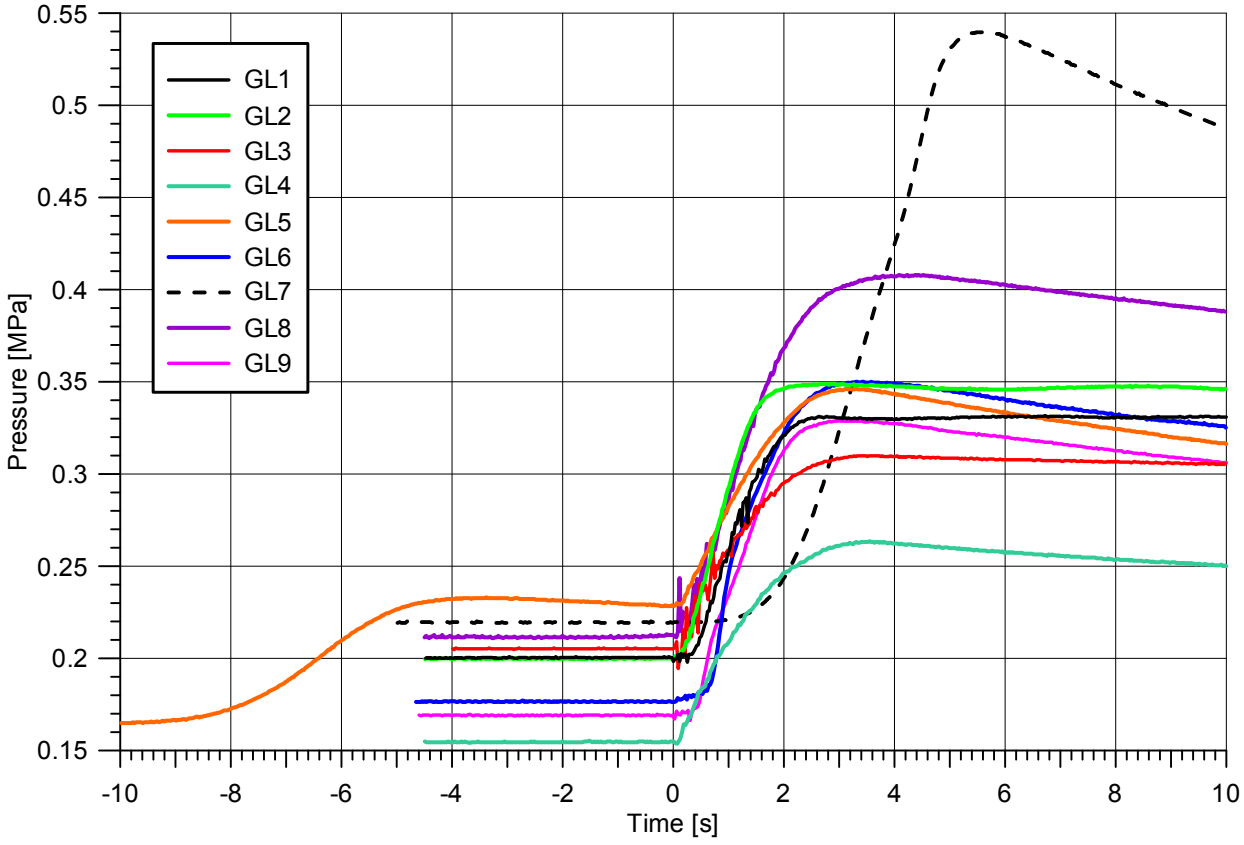

Fig. 20. Containment pressure rise

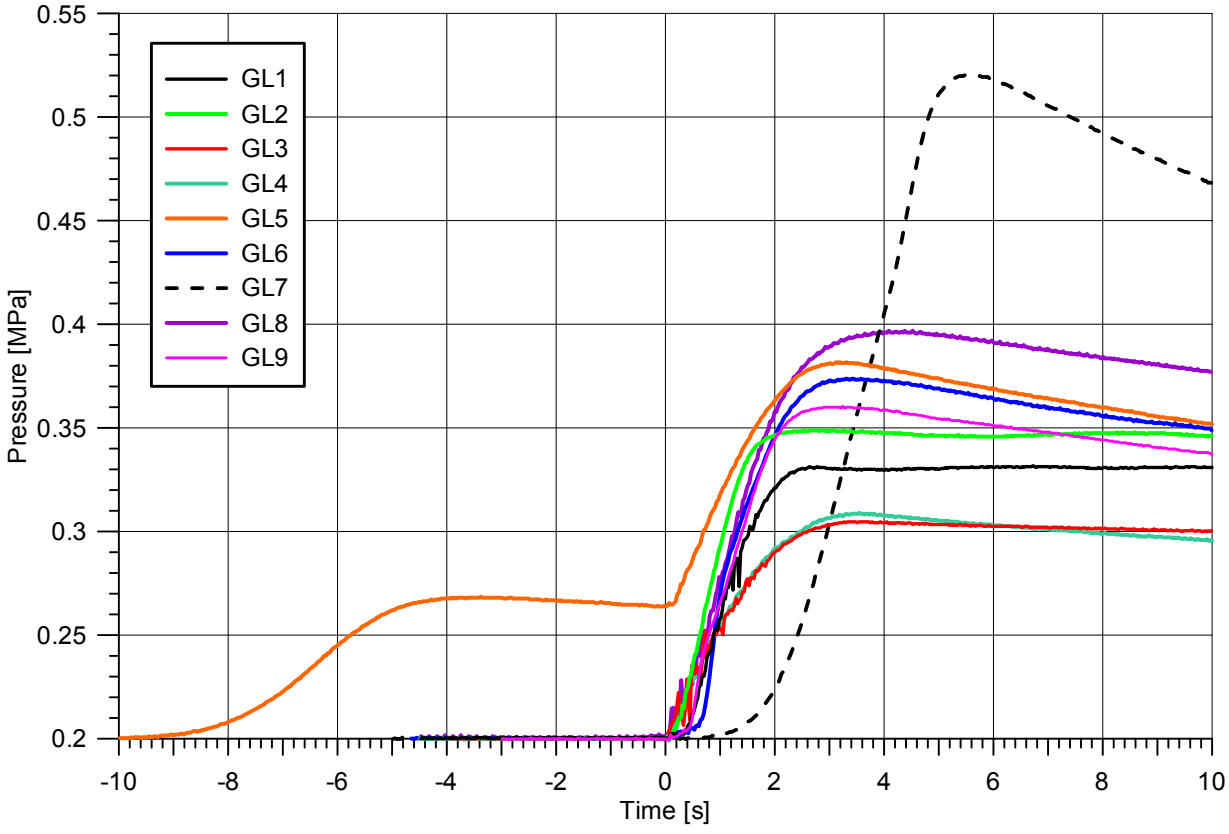

Fig. 21. Containment pressure rise, data shifted to 0.2 MPa initial containment pressure, short term

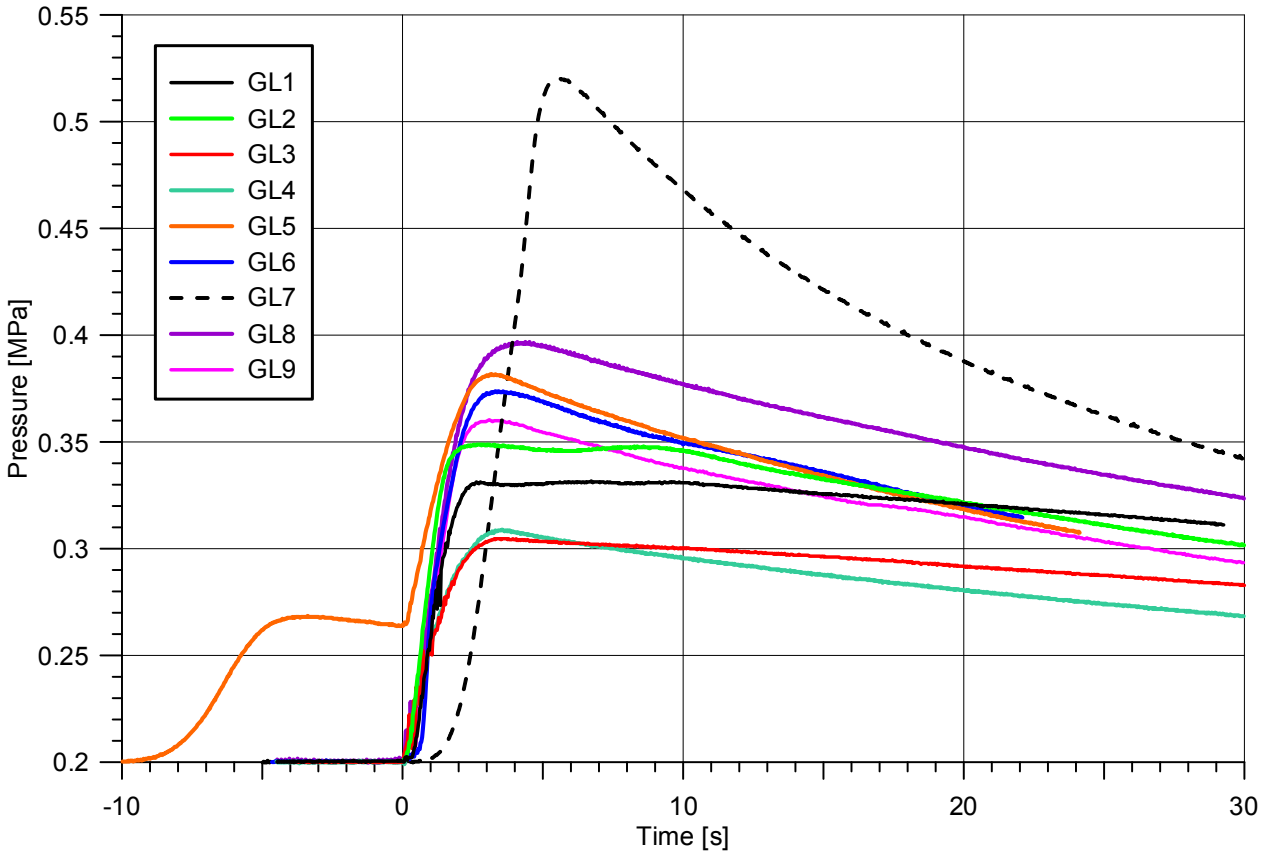

Fig. 22. Containment pressure rise, data shifted to 0.2 MPa initial containment pressure, long term

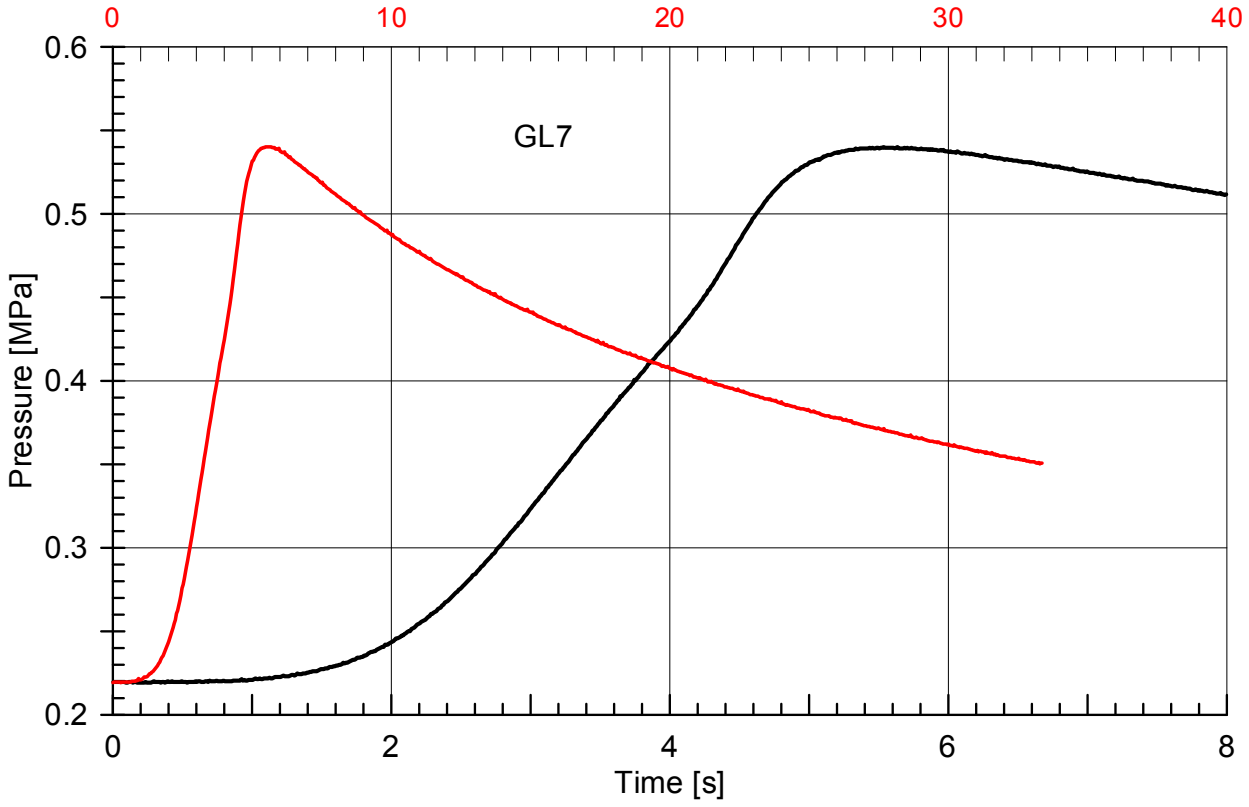

Fig. 23. Pressure rise in test GL7 (no blowdown), black: short time, red: long time scale

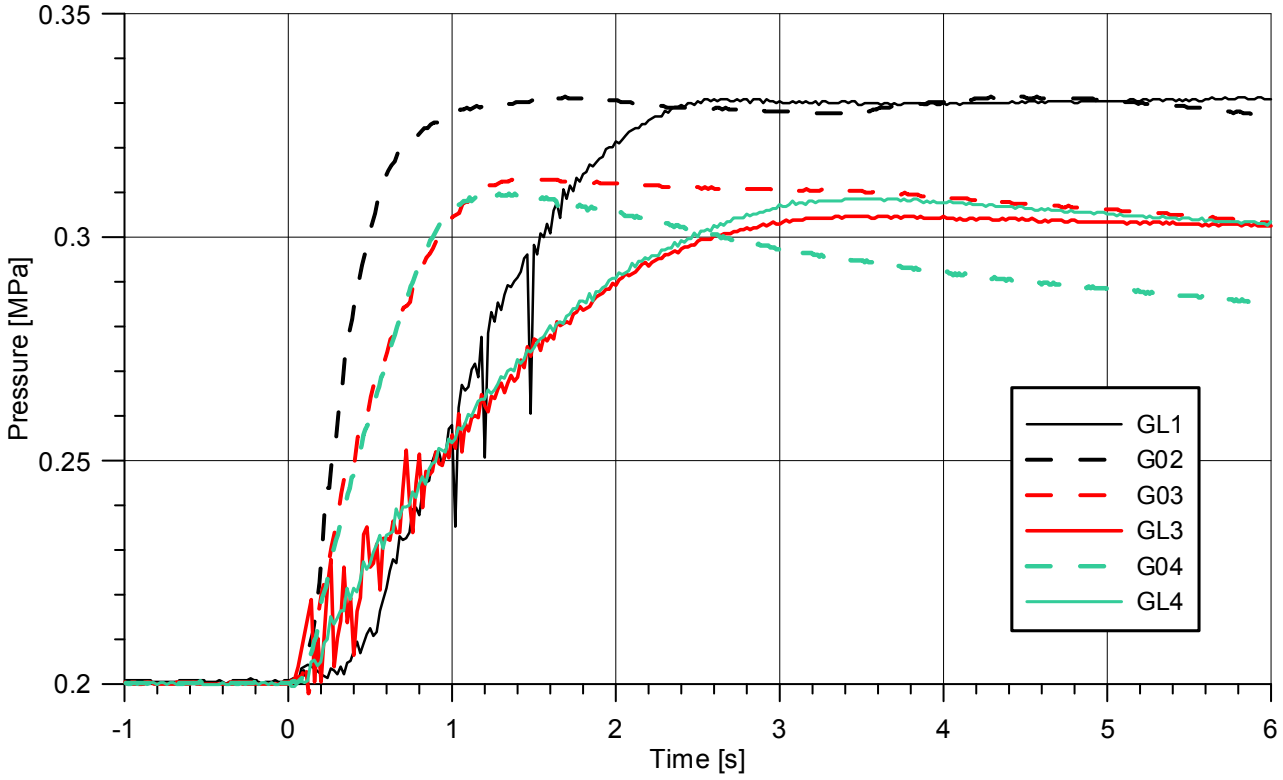

Fig. 24. Comparison of containment pressure rise
in 1:18 and 1:7 scale experiments

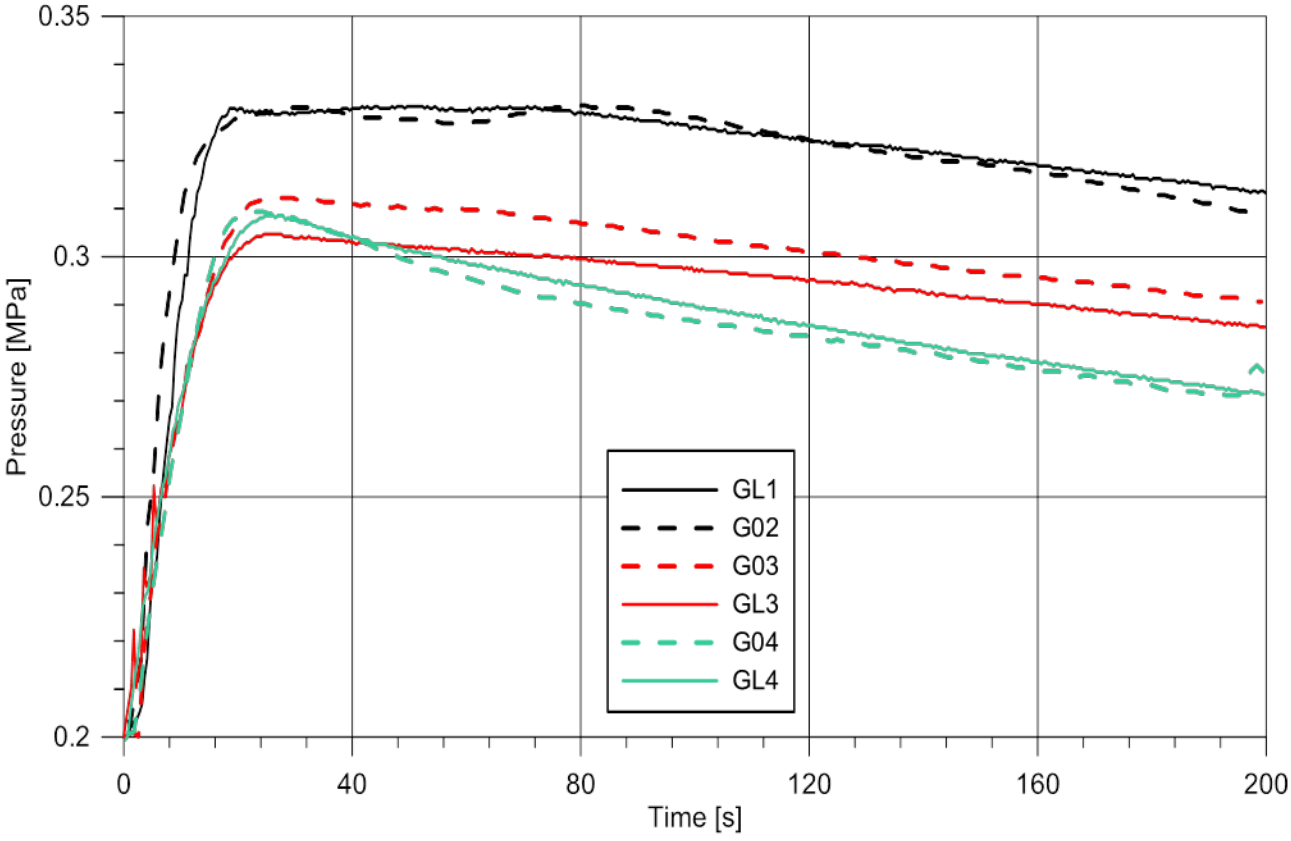

Fig. 25. Comparison of long term containment pressure in 1:18 and 1:7 scale experiments, time axis scaled to 1:1 scale.

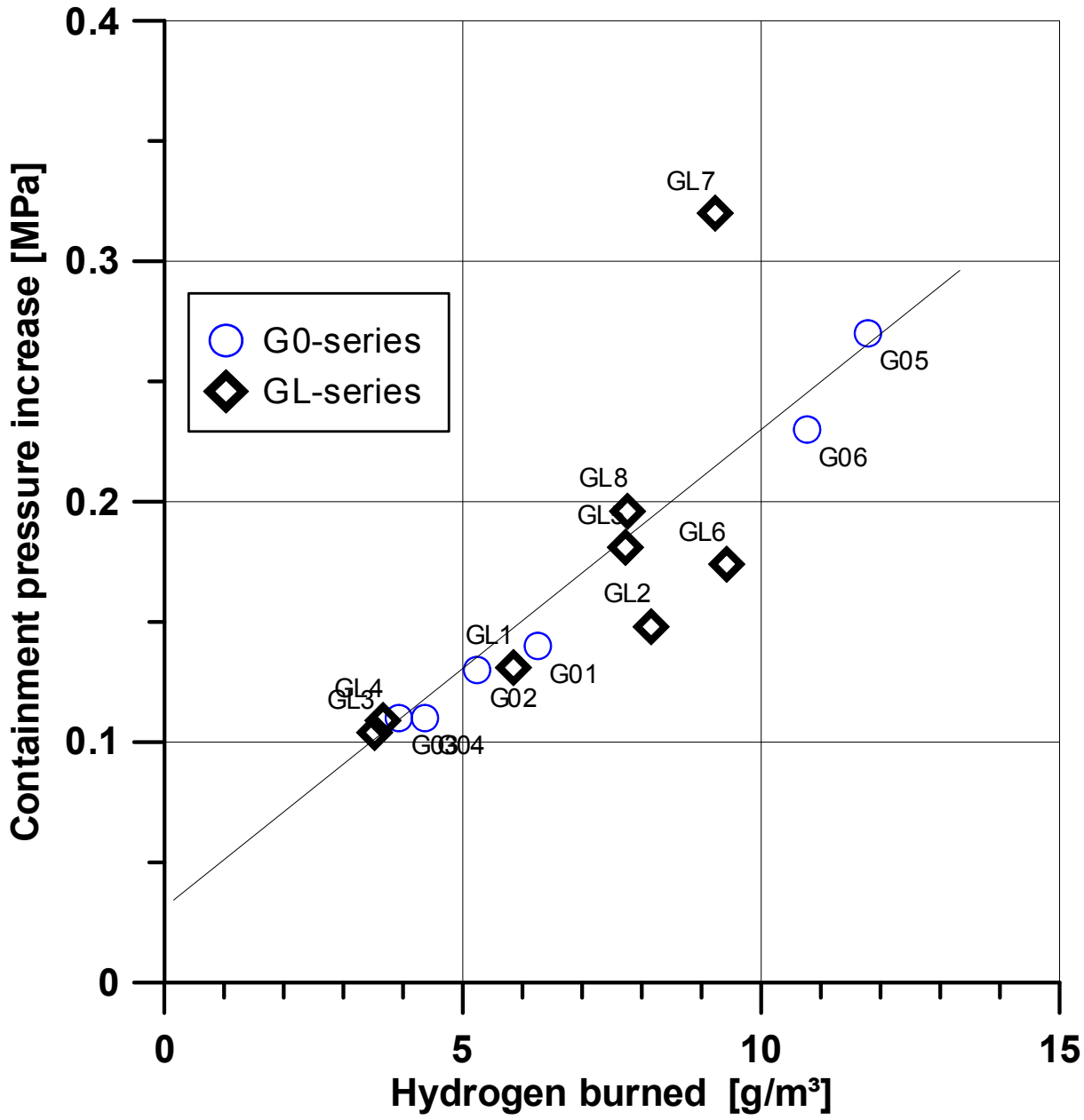

Fig. 26. Pressure increase versus burned hydrogen

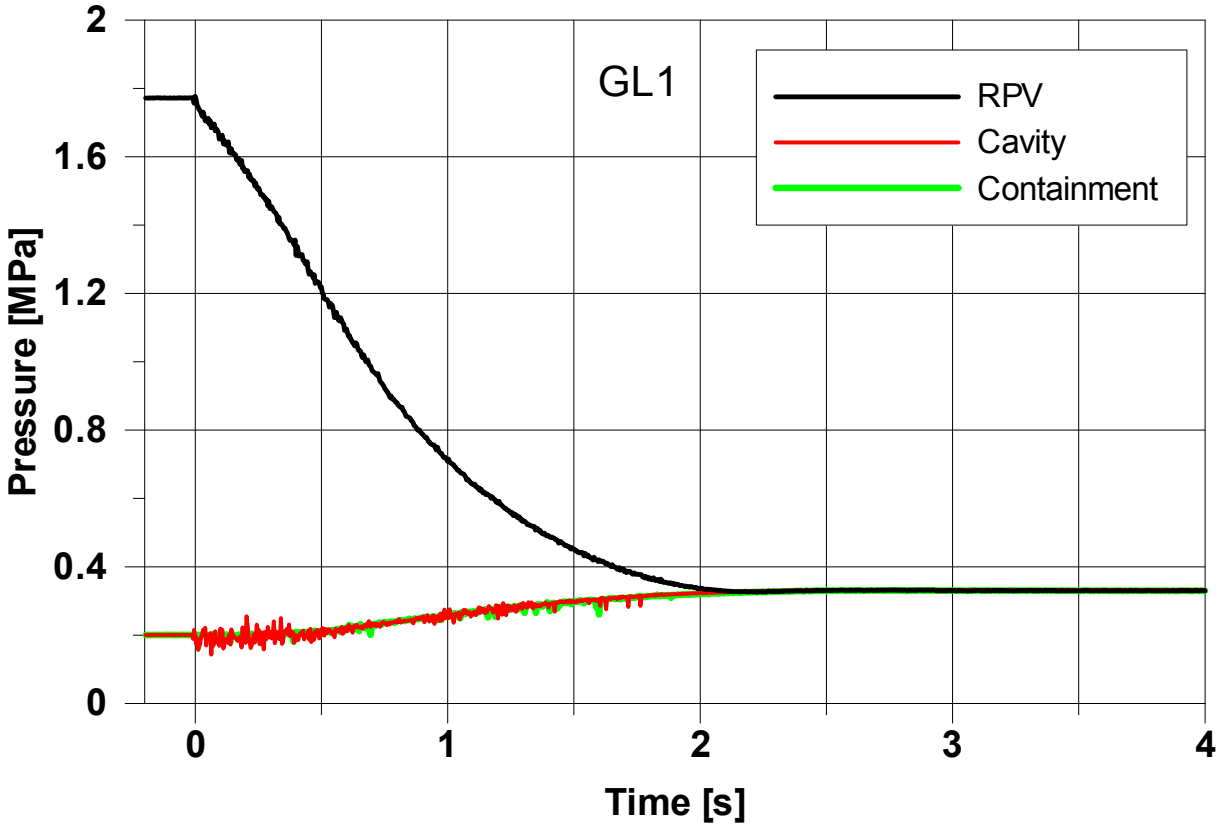

Fig. 27. Pressures in Test GL1

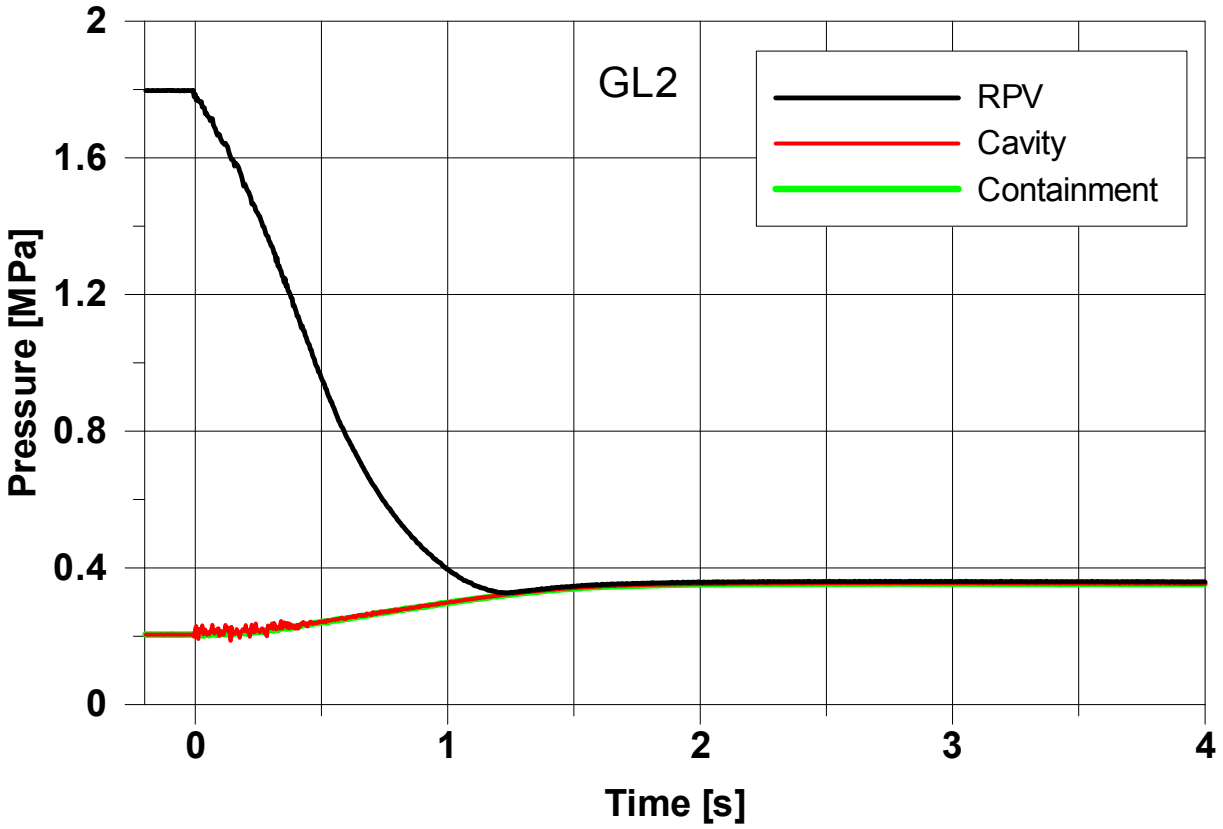

Fig. 28. Pressures in Test GL2

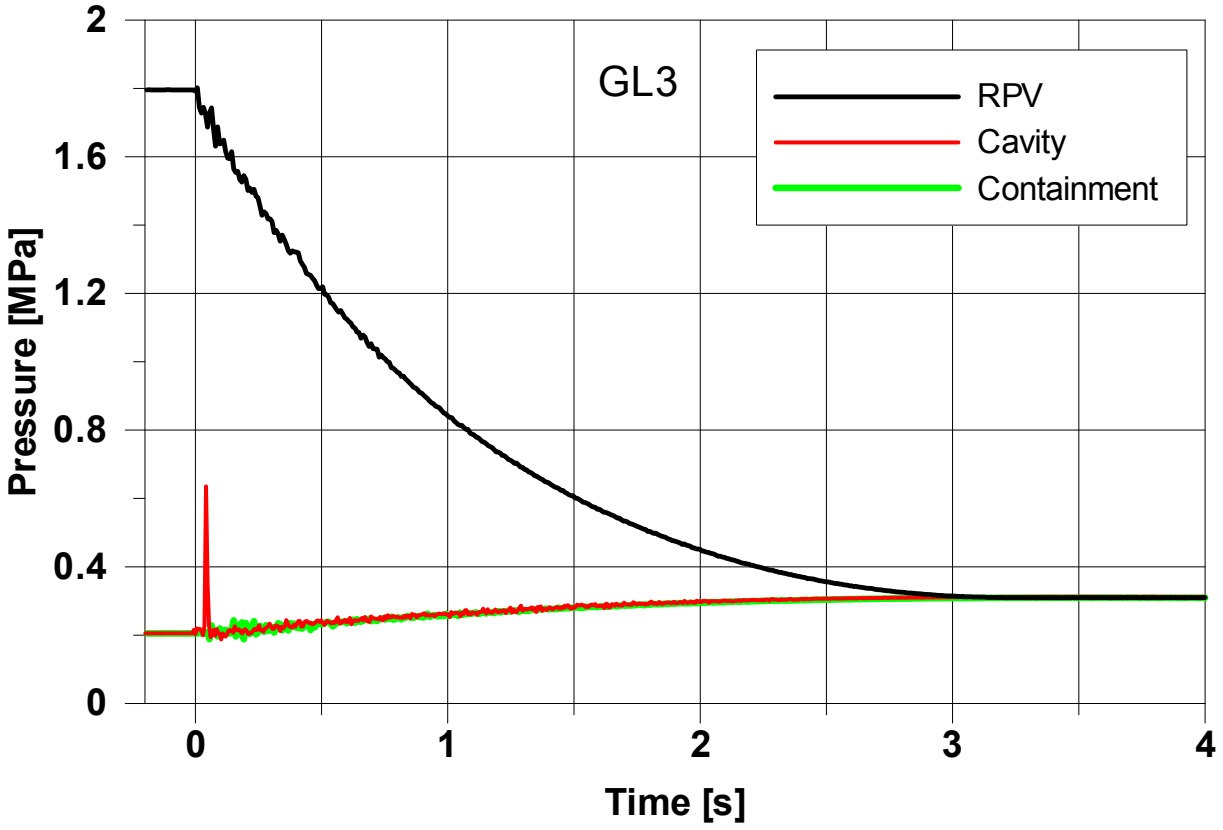

Fig. 29. Pressures in Test GL3

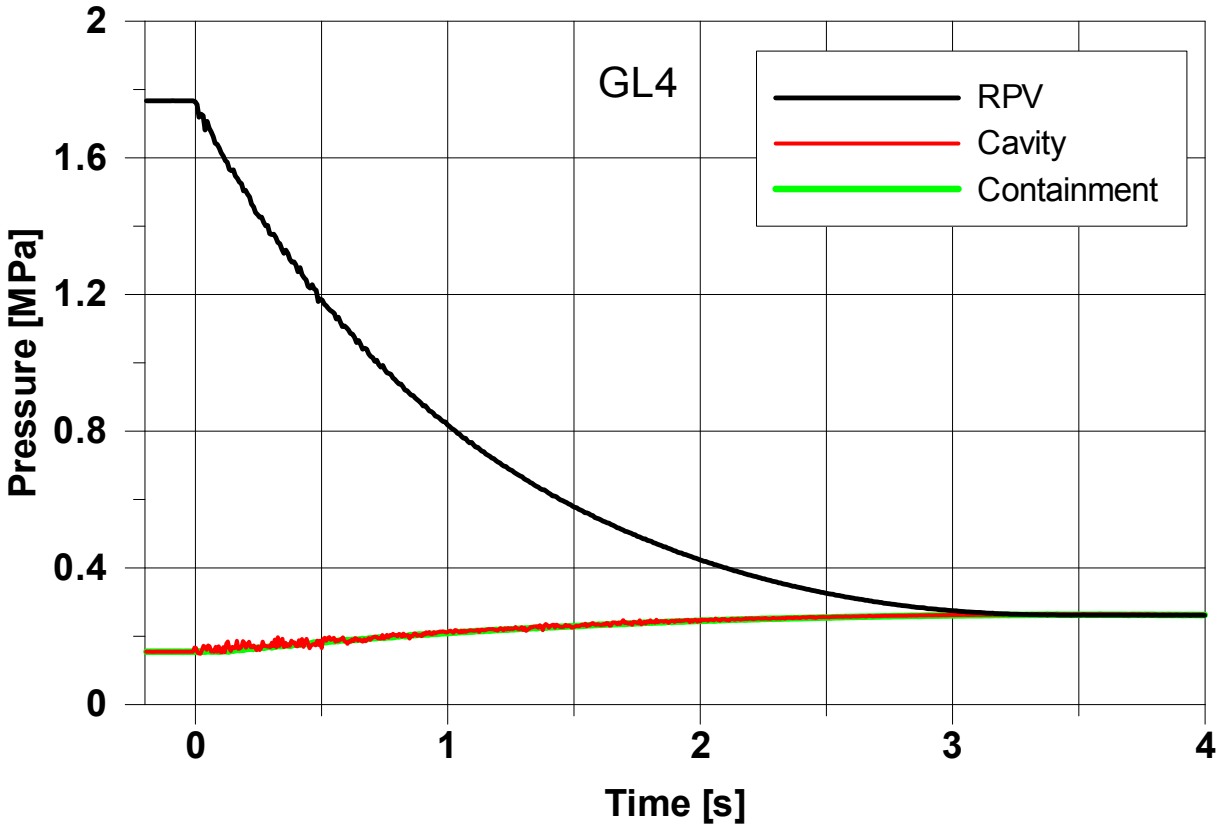

Fig. 30. Pressures in Test GL4

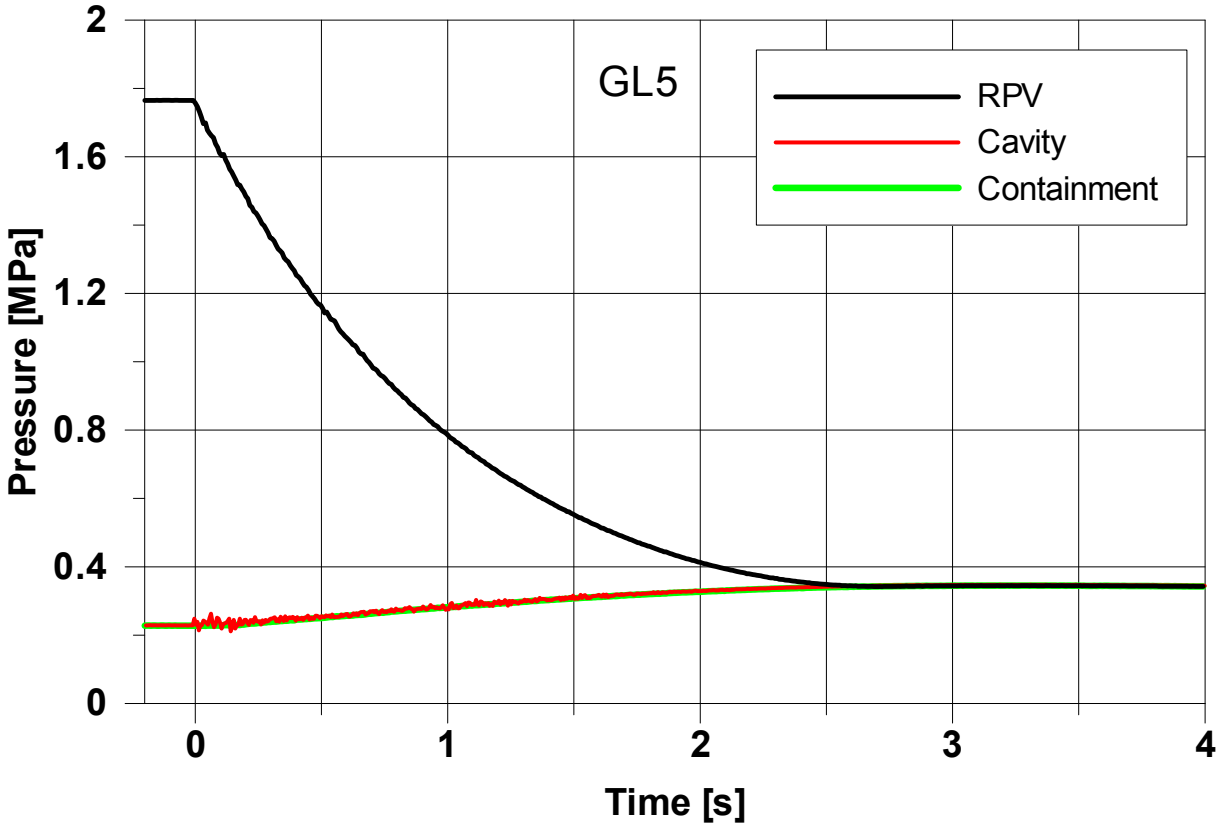

Fig. 31 Pressures in Test GL5.

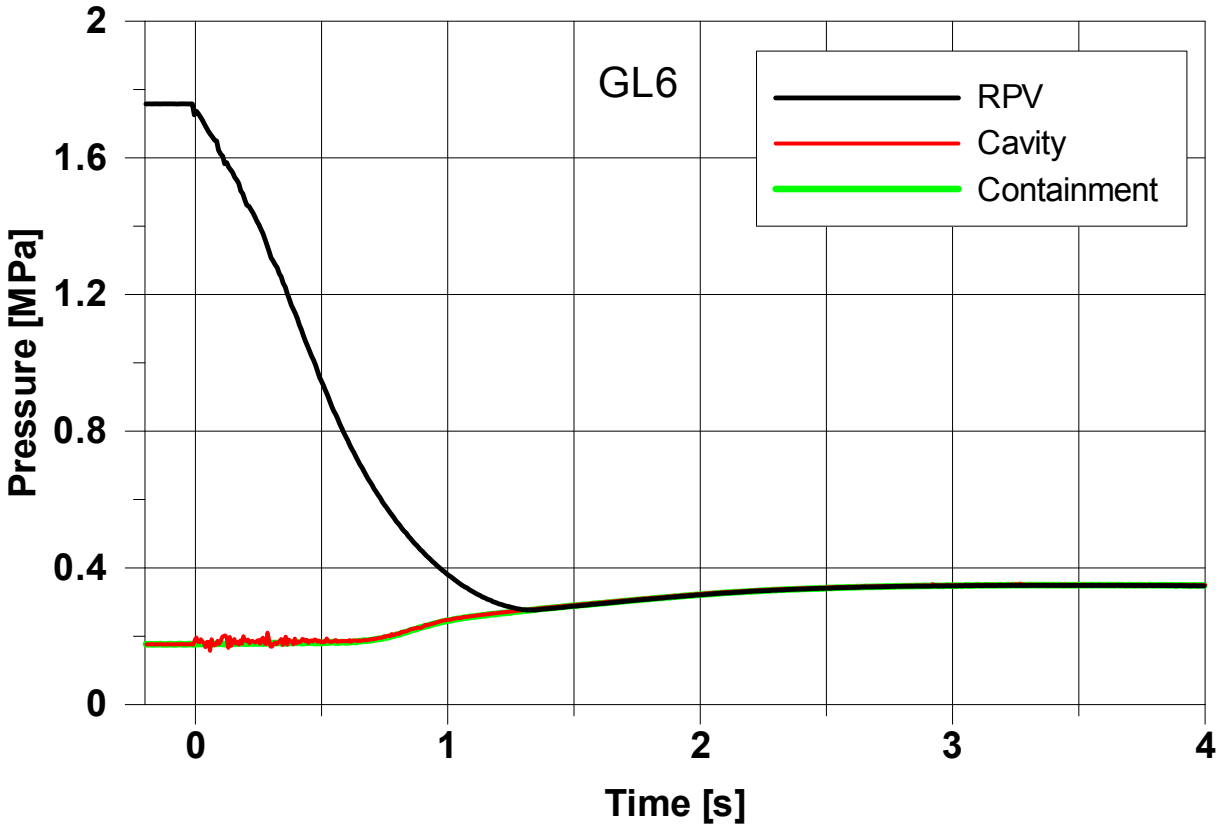

Fig. 32. Pressures in Test GL6

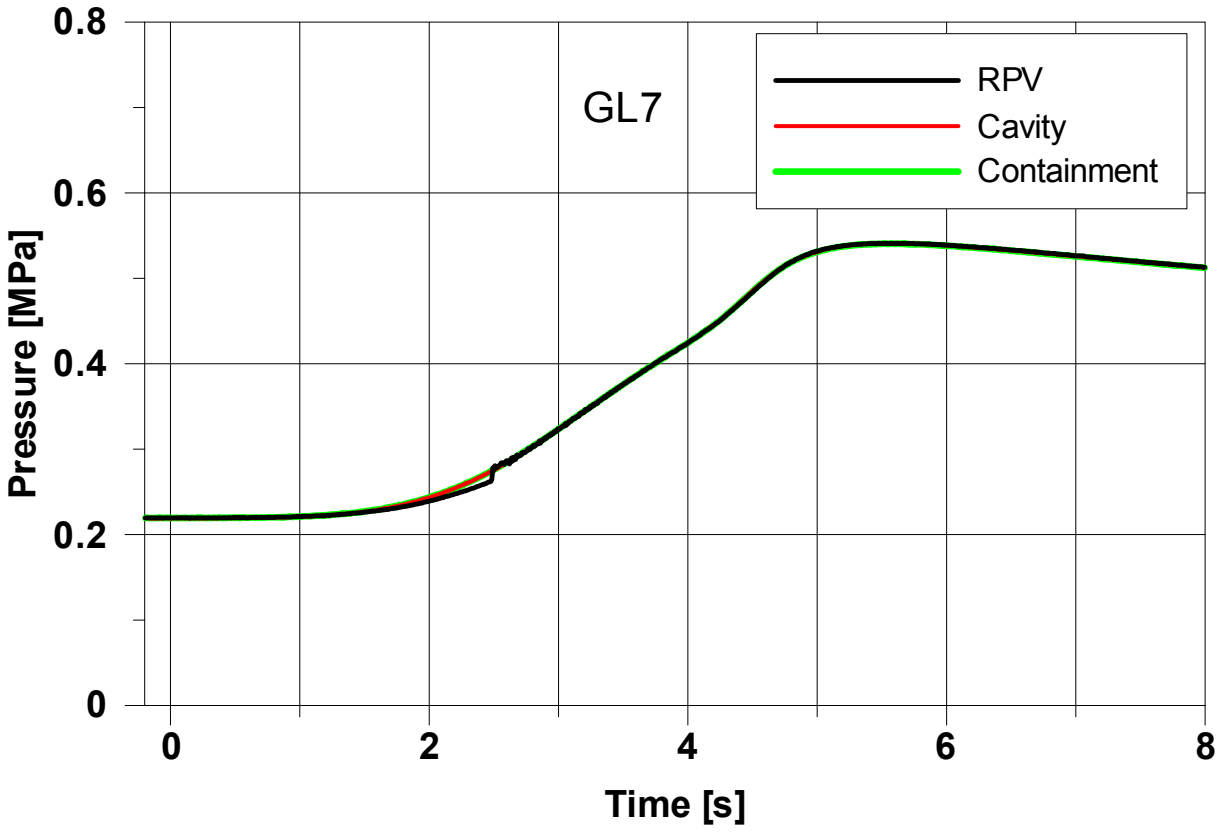

Fig. 33. Pressures in Test GL7

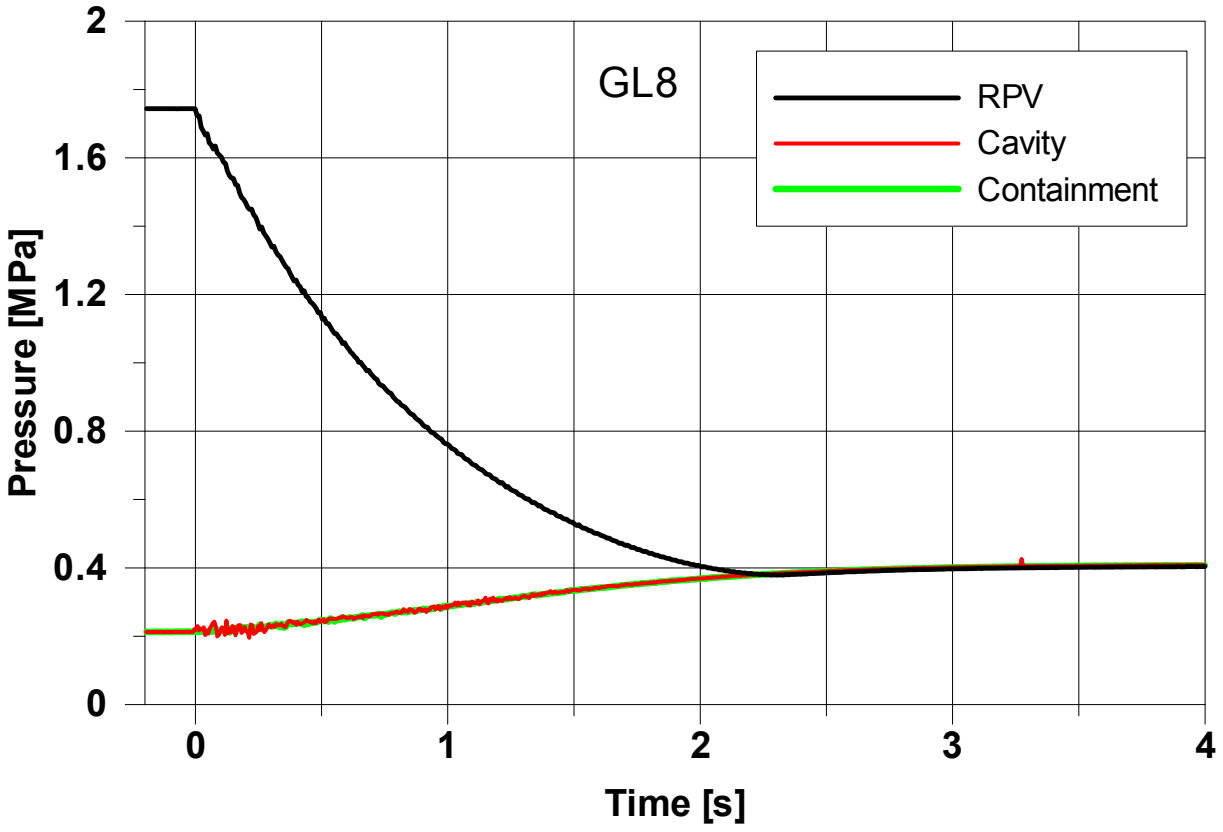

Fig. 34. Pressures in Test GL8

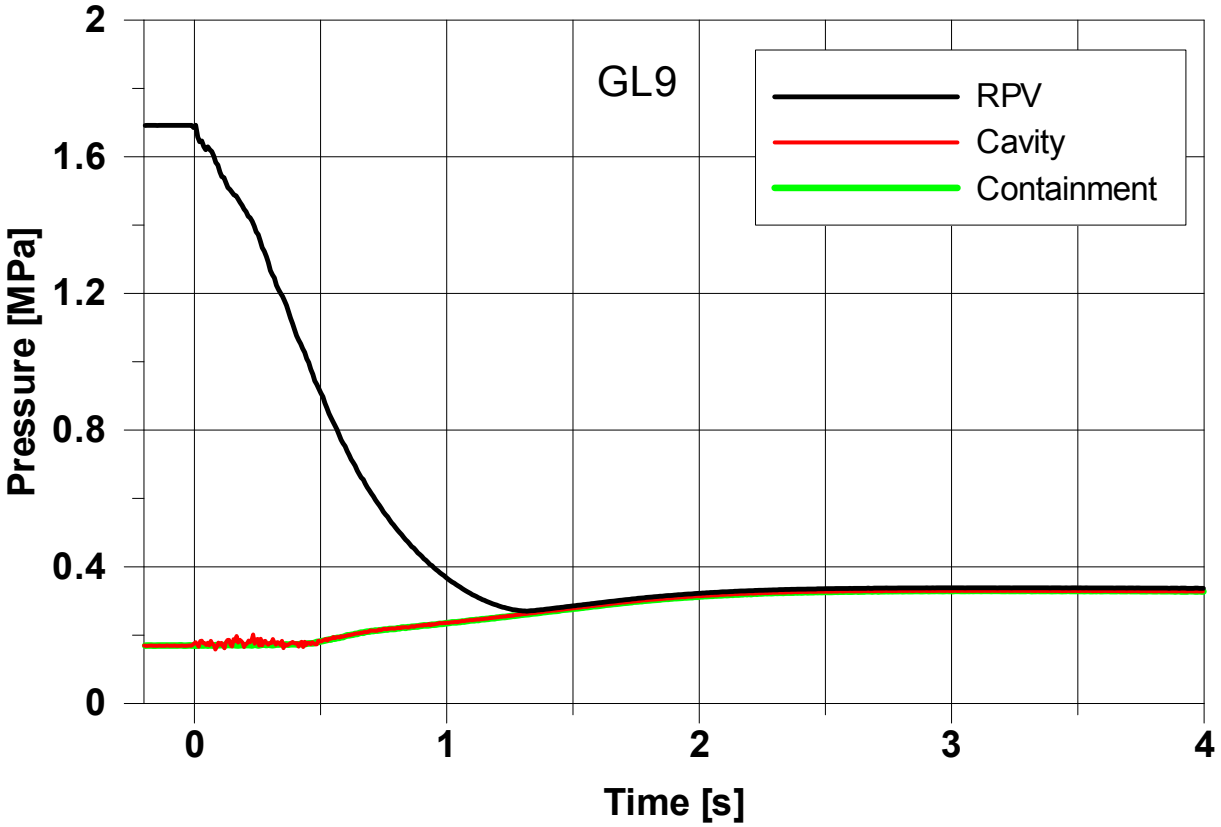

Fig. 35. Pressures in Test GL9

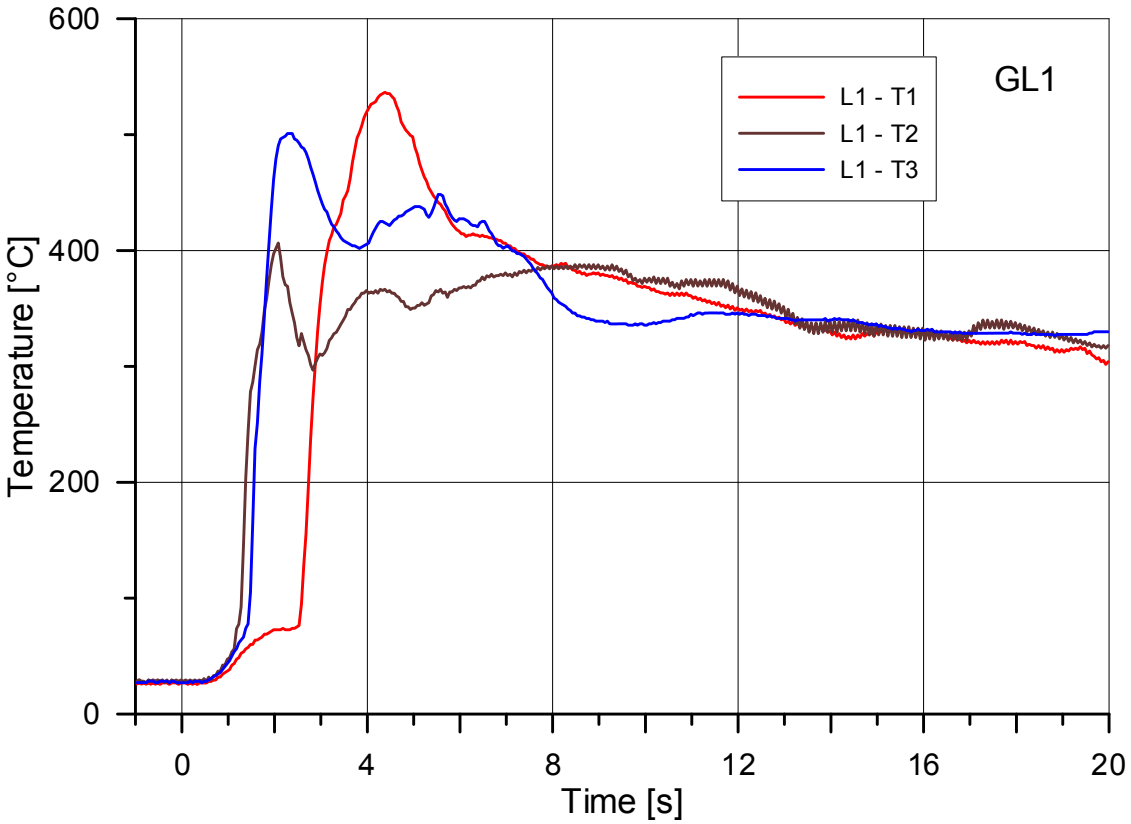

Fig. 36. Temperatures at Level 1 in Test GL1

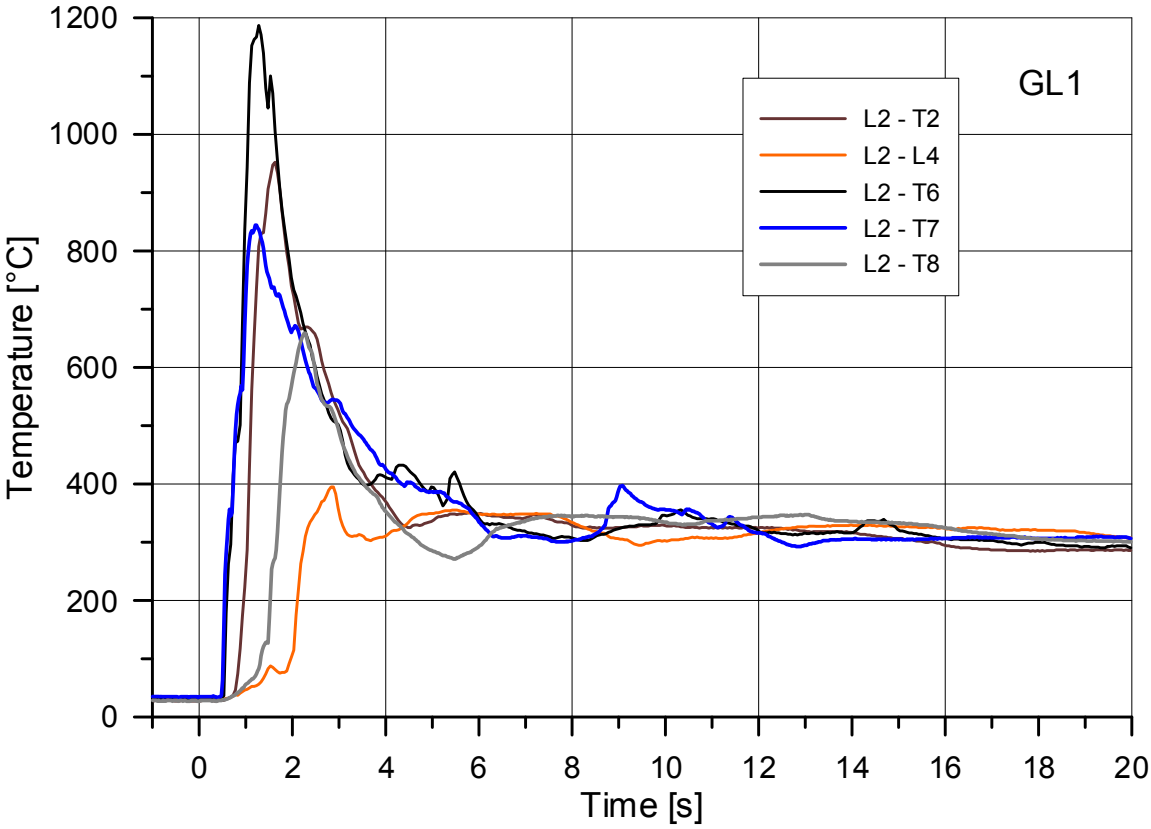

Fig. 37. Temperatures at Level 2 in Test GL1

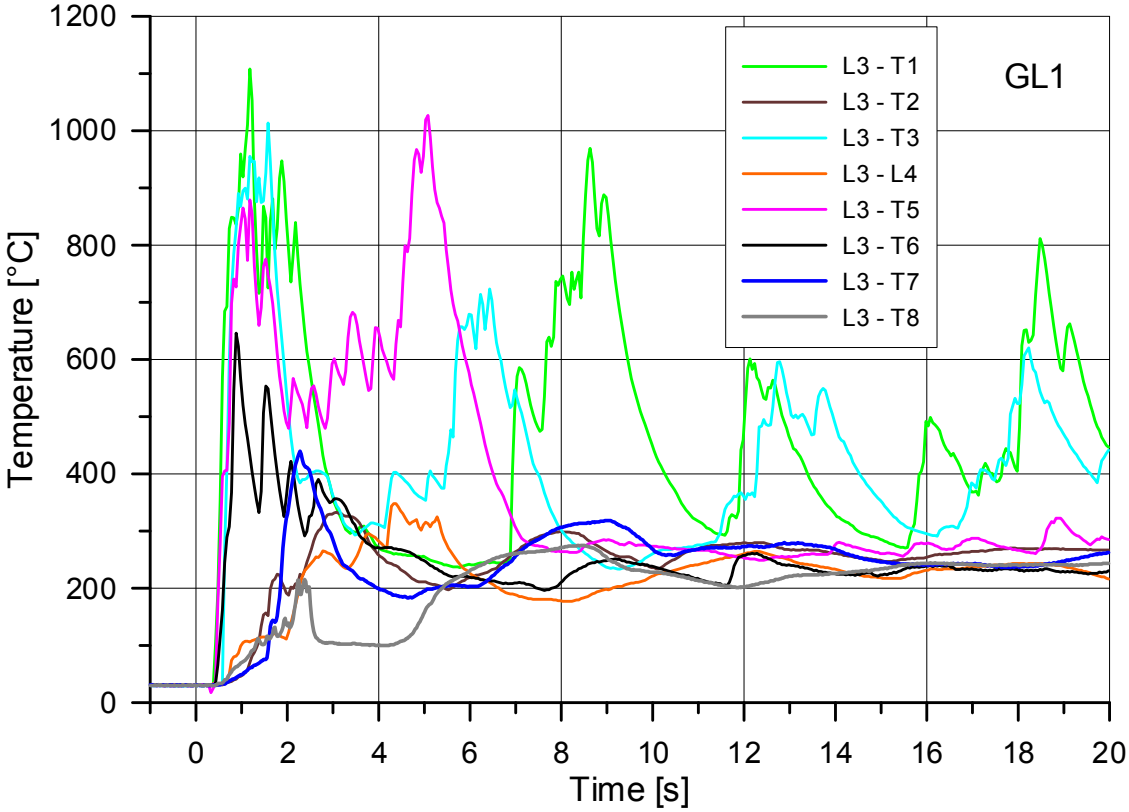

Fig. 38. Temperatures at Level 3 in Test GL1

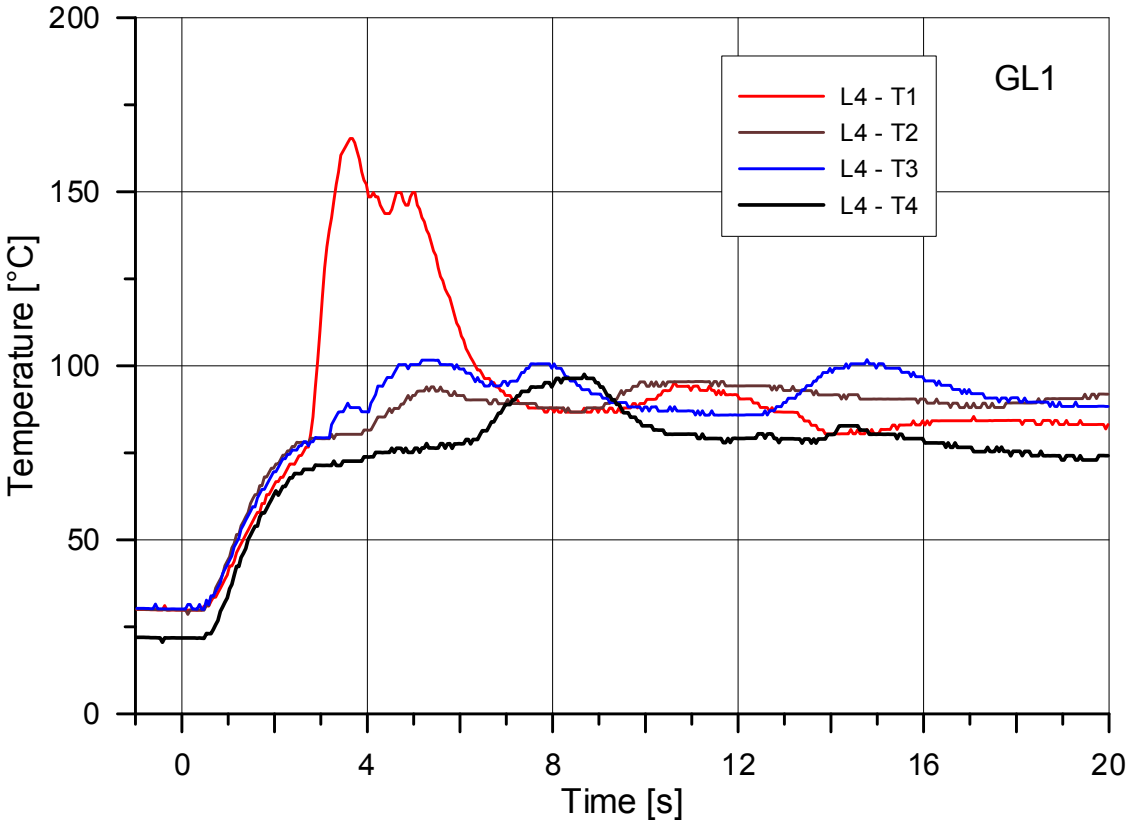

Fig. 39. Temperatures at Level 4 in Test GL1

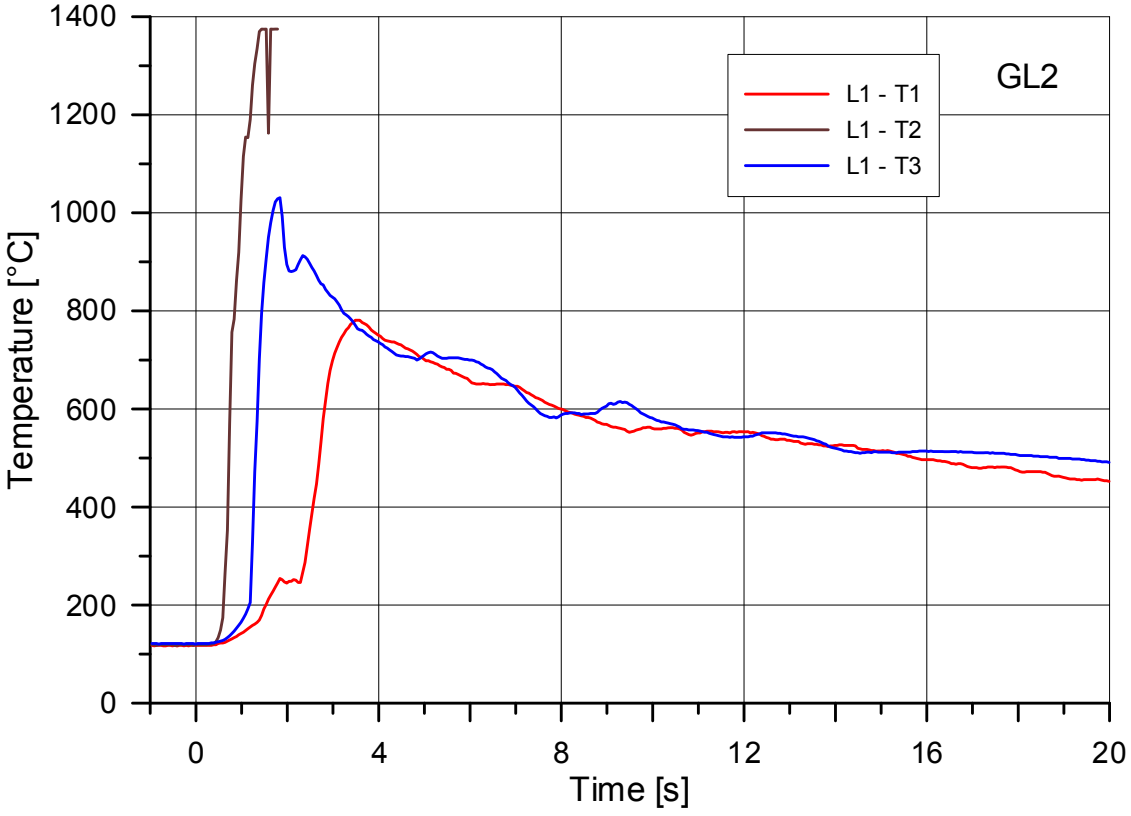

Fig. 40. Temperatures at Level 1 in Test GL2

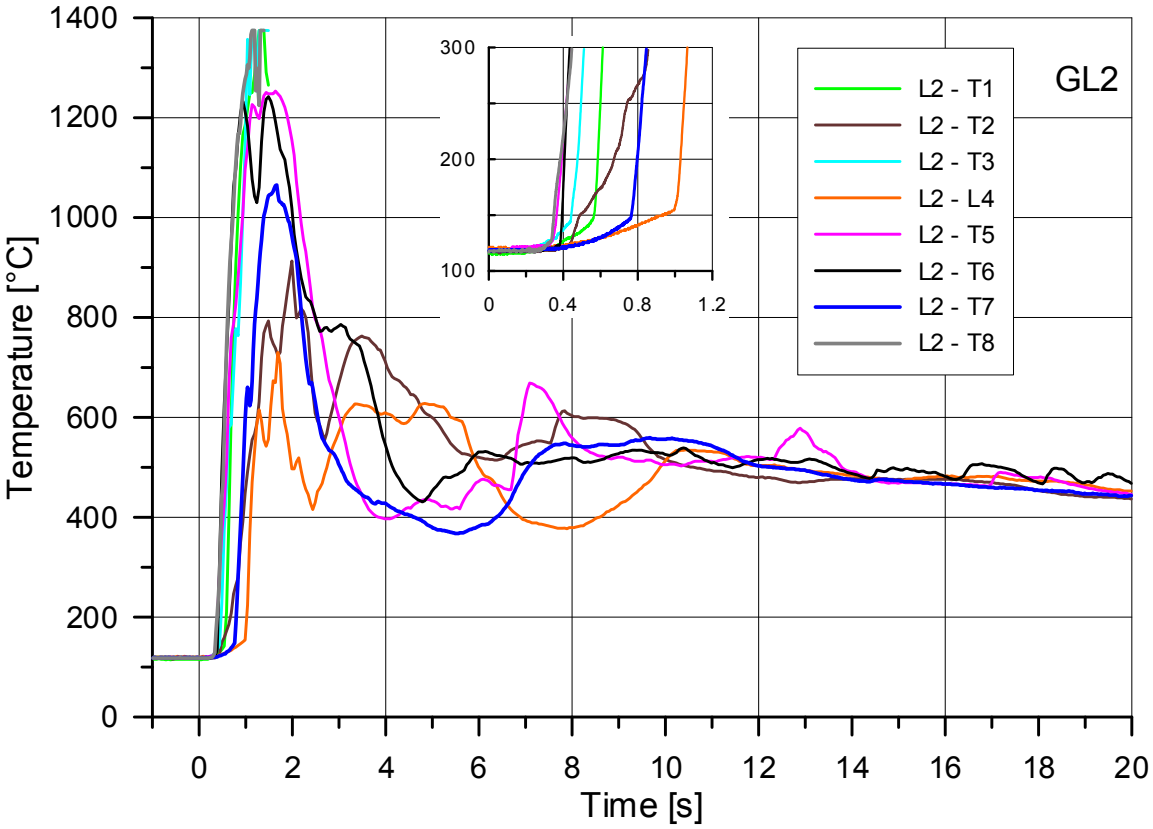

Fig. 41. Temperatures at Level 2 in Test GL2

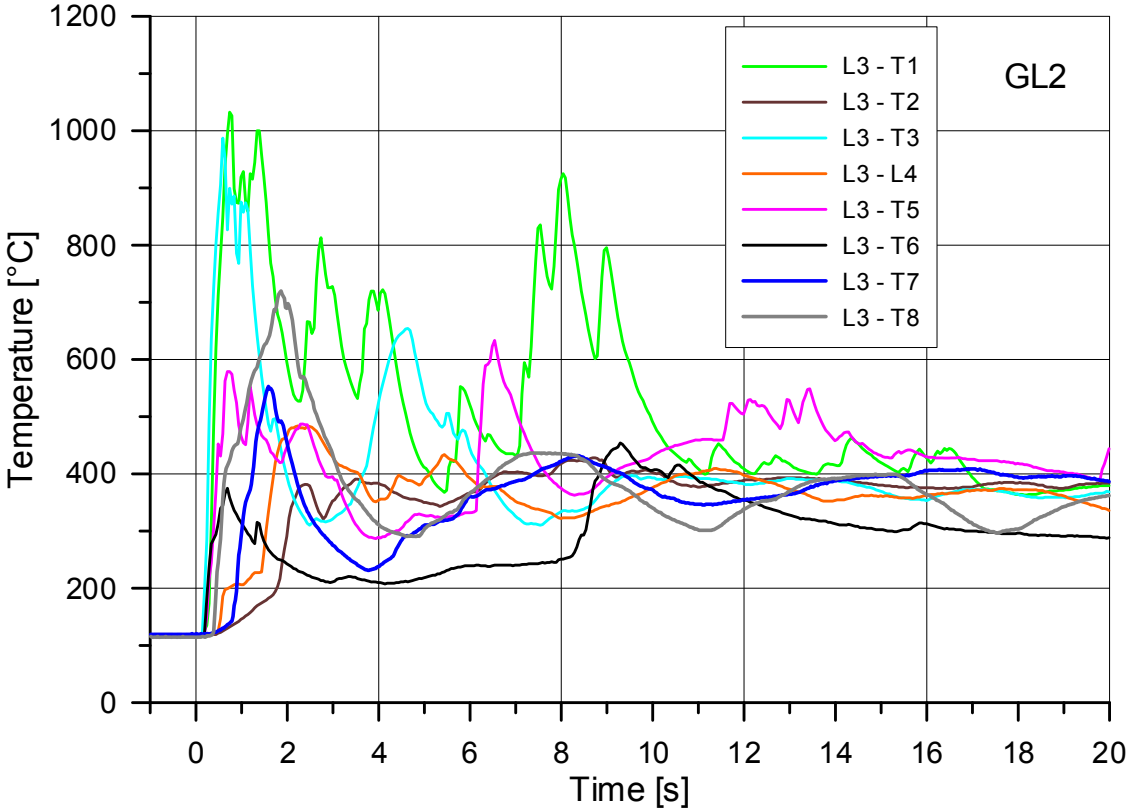

Fig. 42. Temperatures at Level 3 in Test GL2

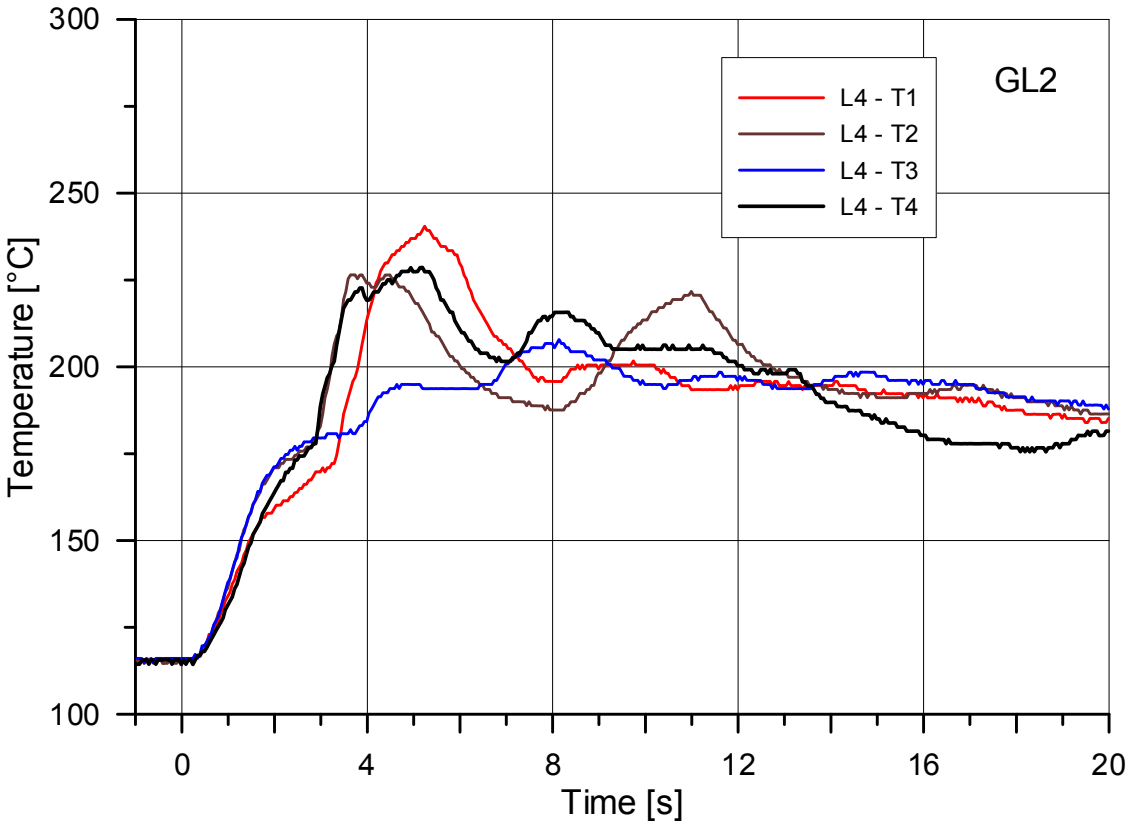

Fig. 43. Temperatures at Level 4 in Test GL2

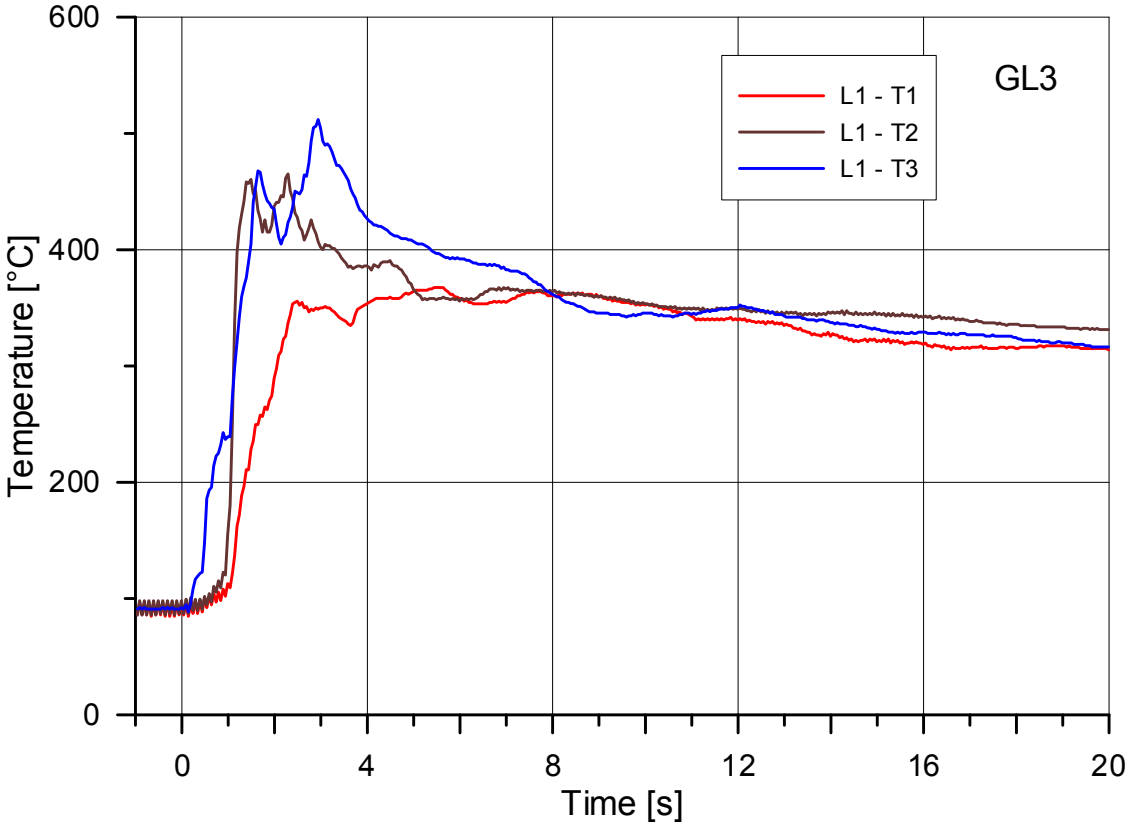

Fig. 44. Temperatures at Level 1 in Test GL3

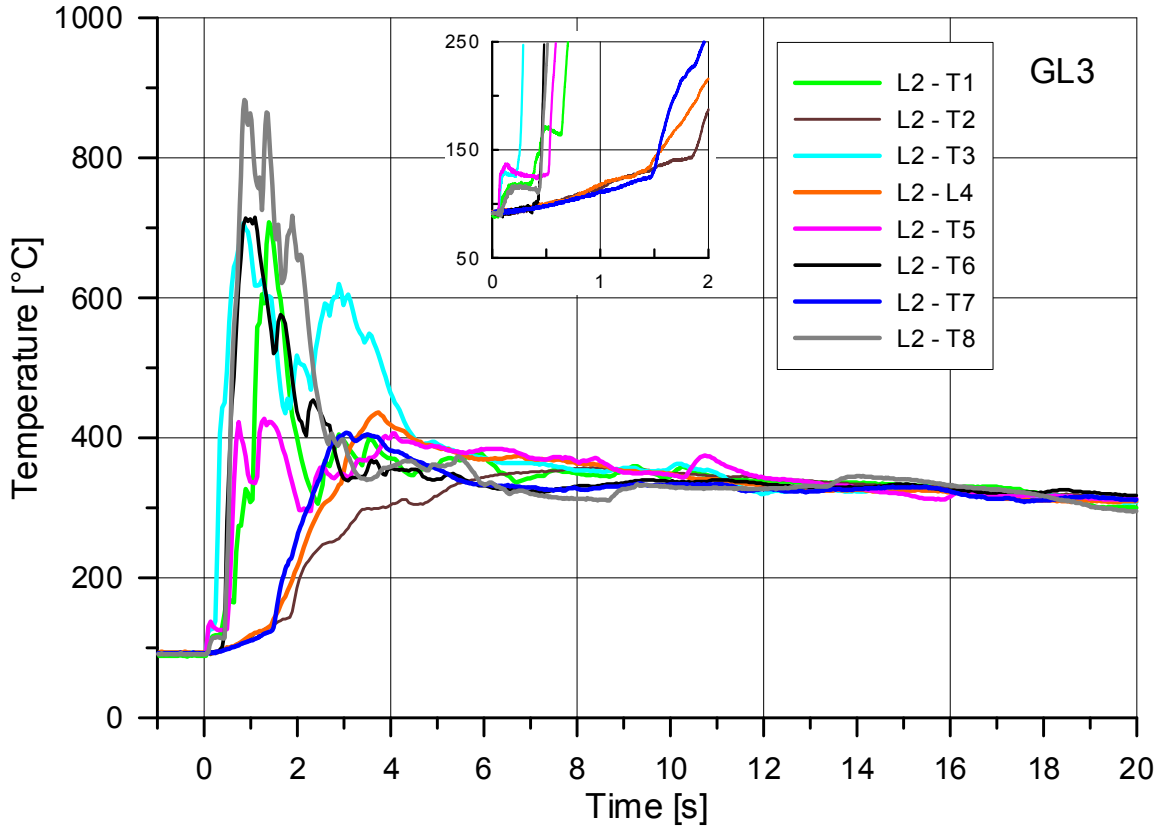

Fig. 45. Temperatures at Level 2 in Test GL3

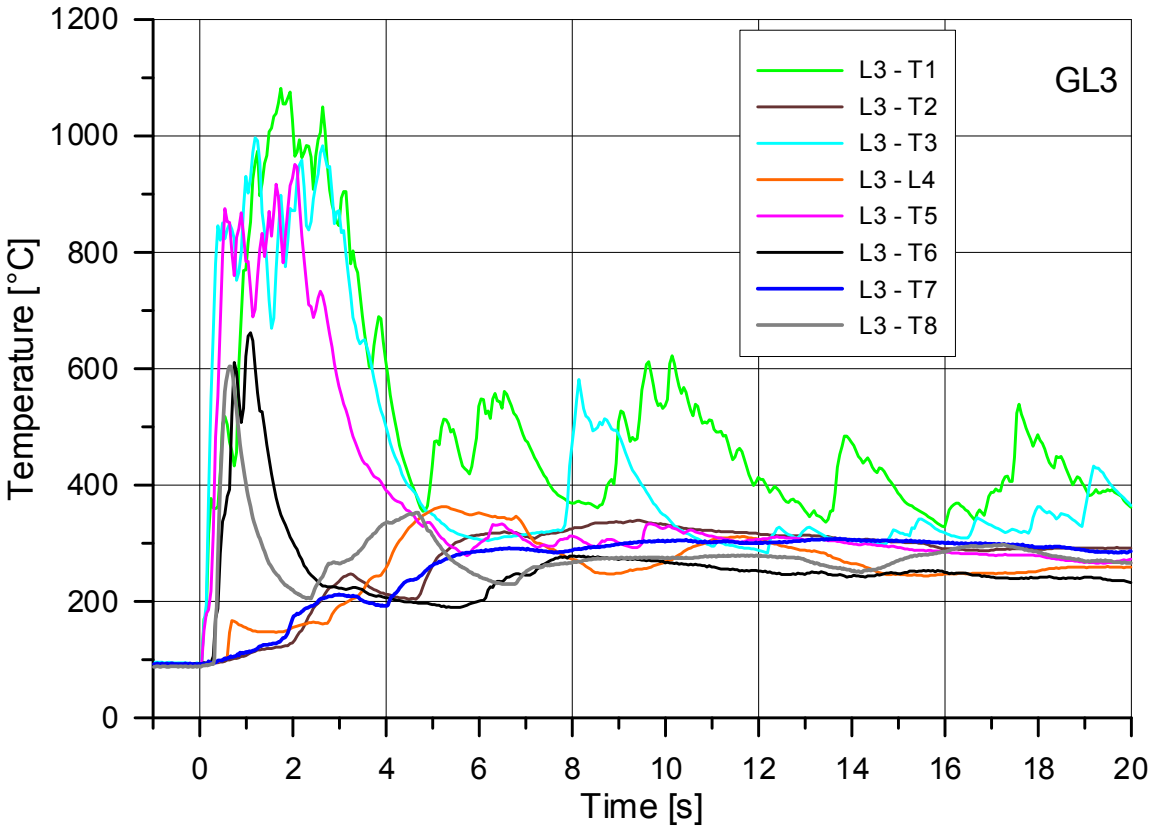

Fig. 46. Temperatures at Level 3 in Test GL3

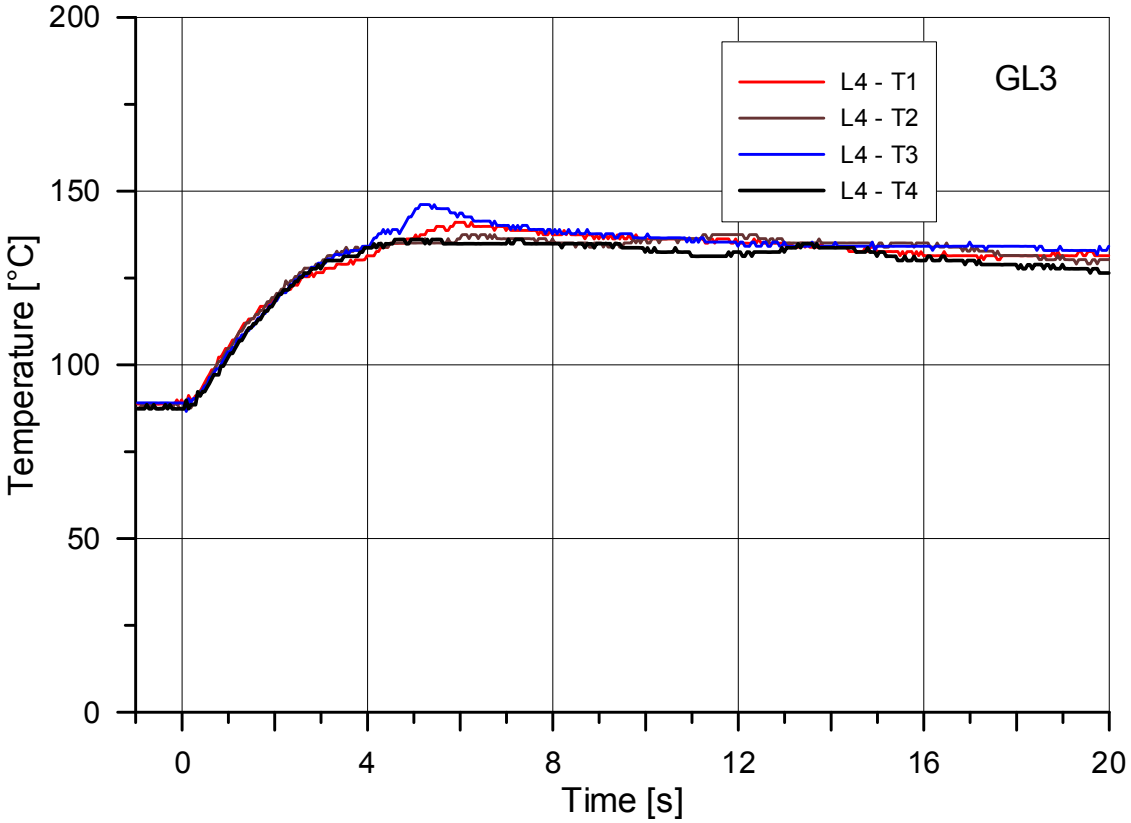

Fig. 47. Temperatures at Level 4 in Test GL3

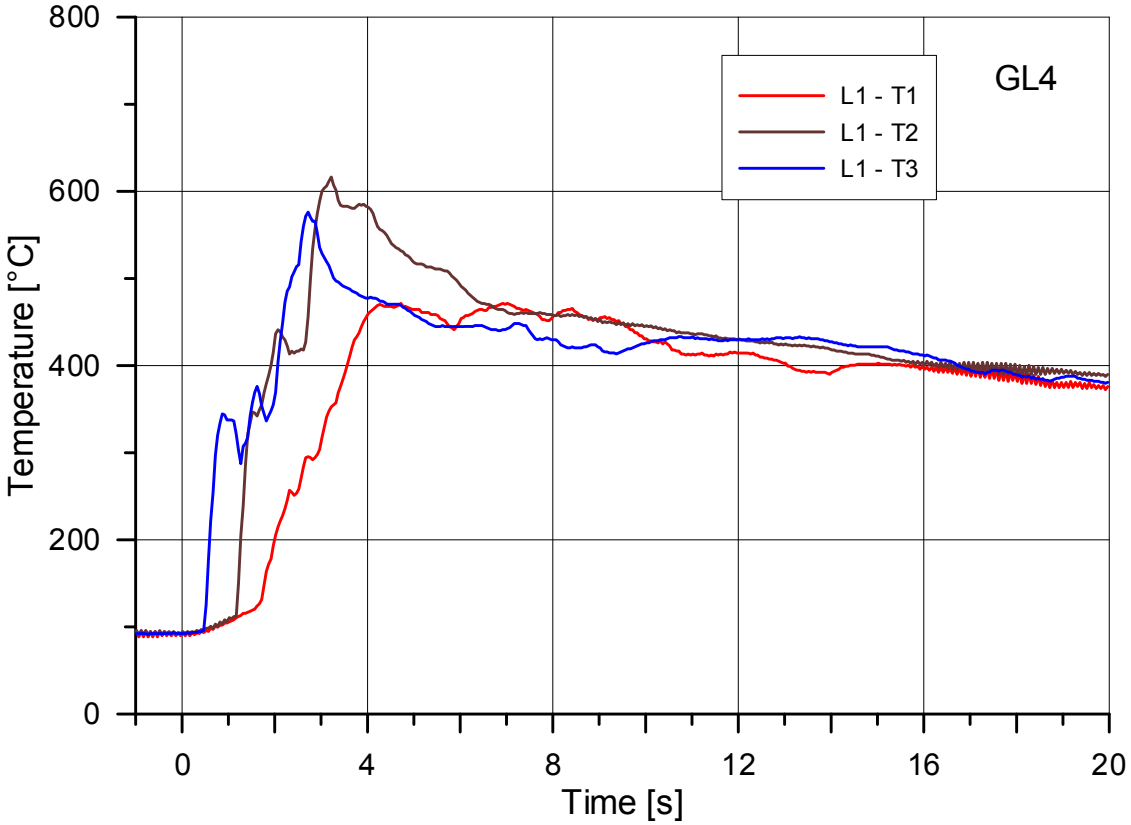

Fig. 48. Temperatures at Level 1 in Test GL4

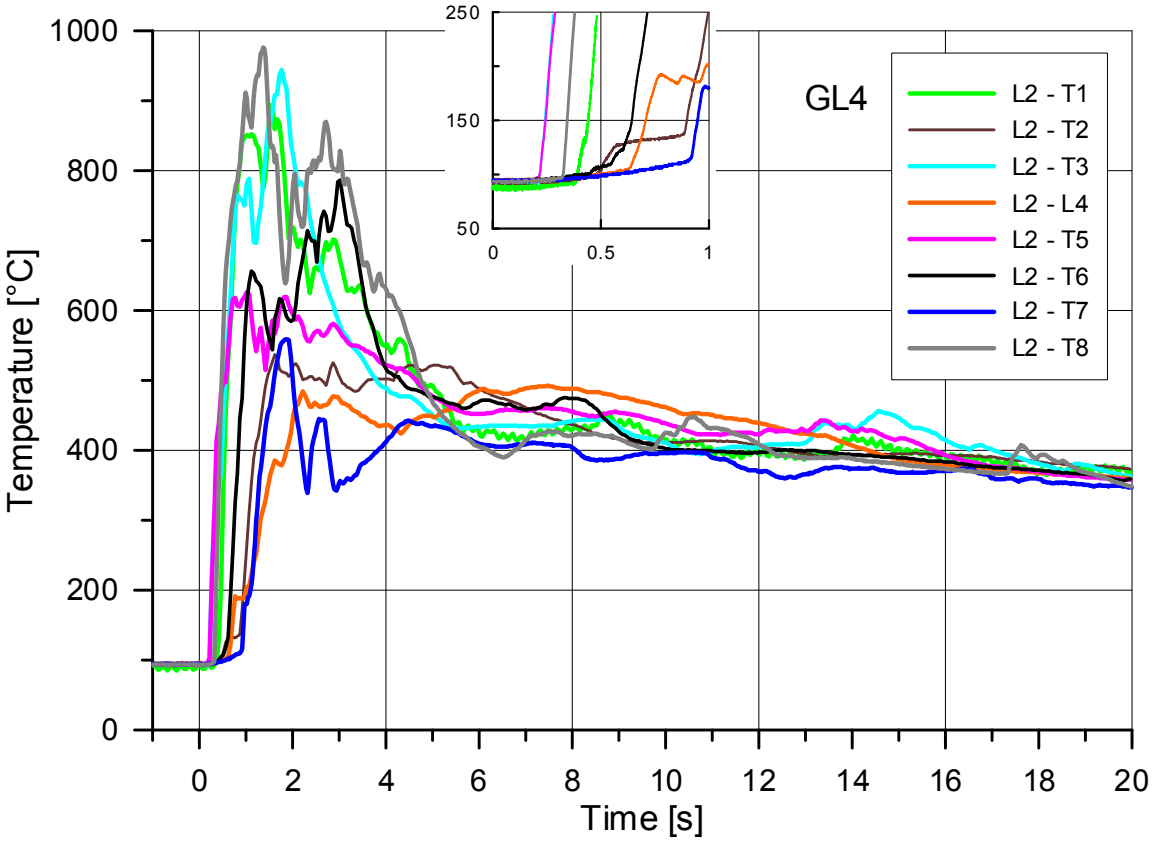

Fig. 49. Temperatures at Level 2 in Test GL4

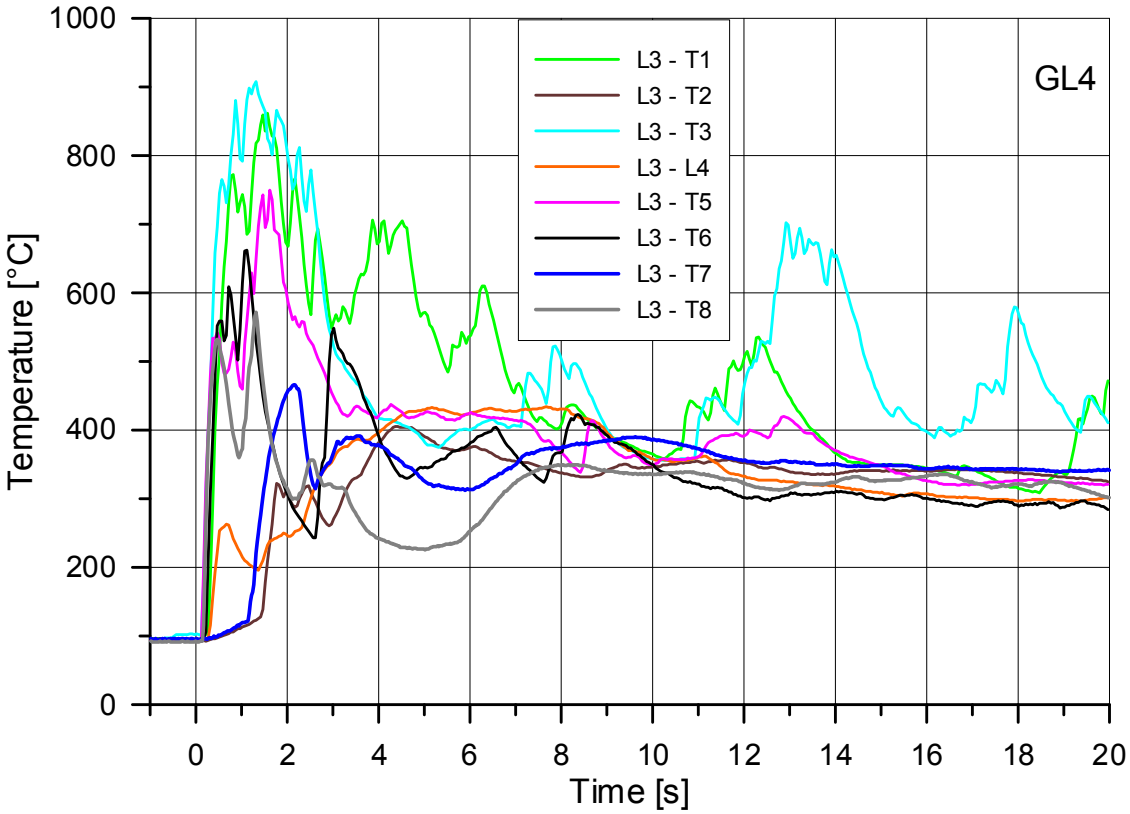

Fig. 50. Temperatures at Level 3 in Test GL4

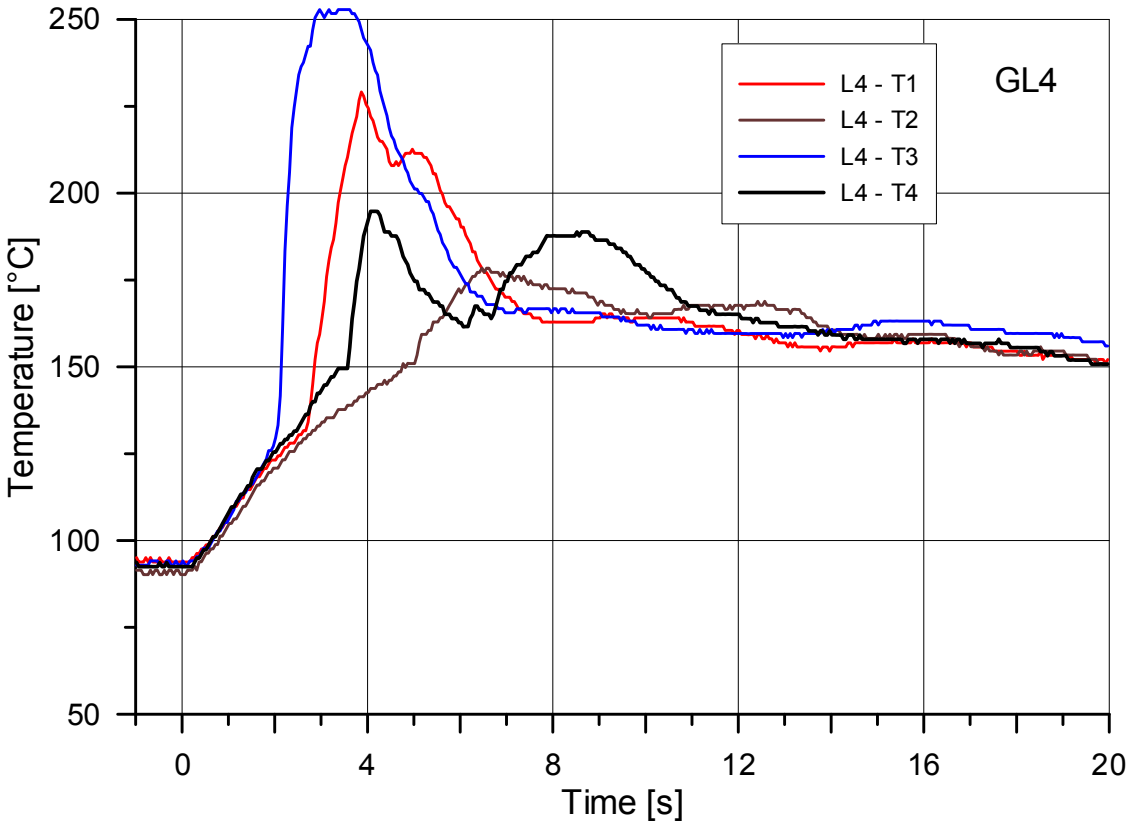

Fig. 51. Temperatures at Level 4 in Test GL4

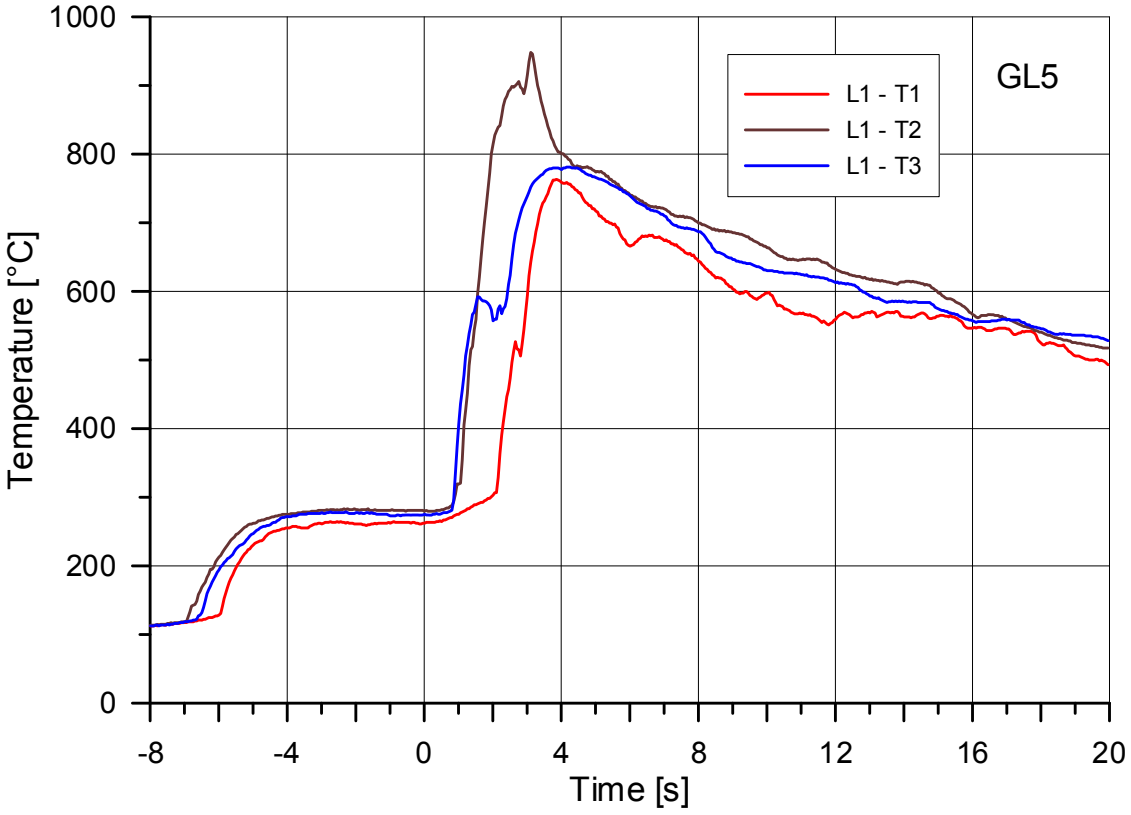

Fig. 52. Temperatures at Level 1 in Test GL5

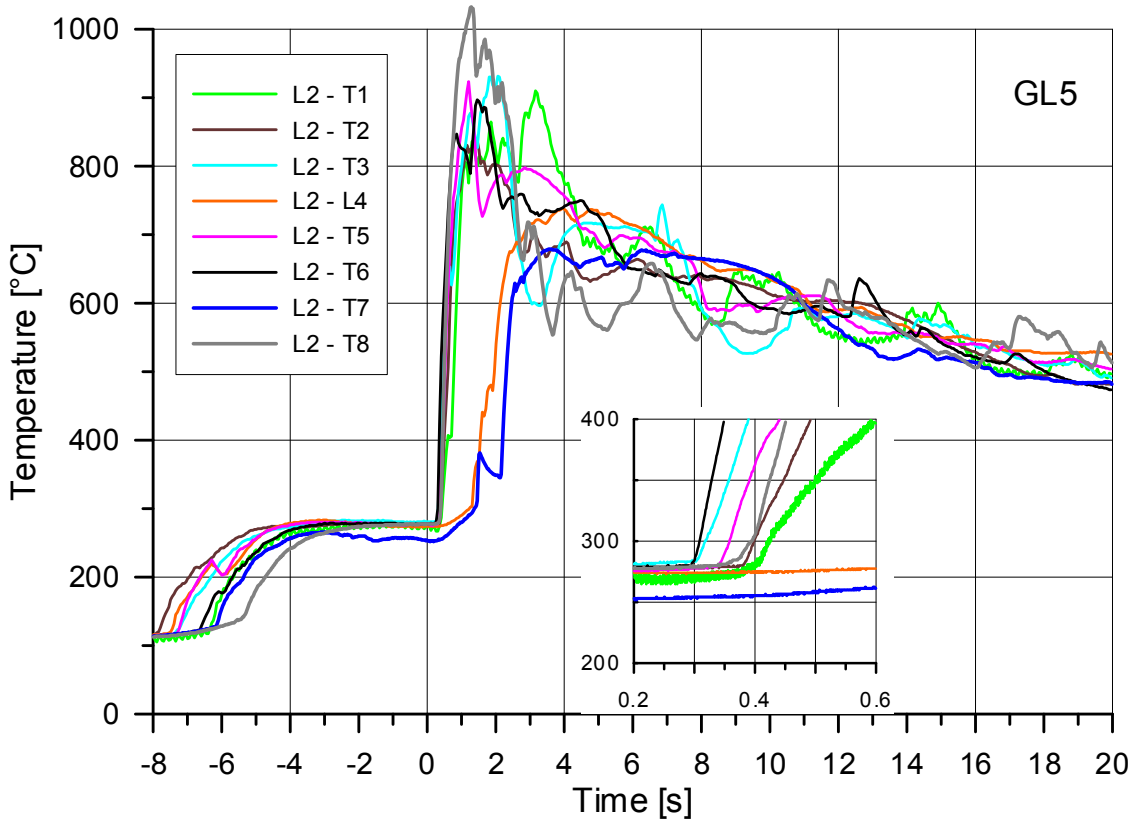

Fig. 53. Temperatures at Level 2 in Test GL5

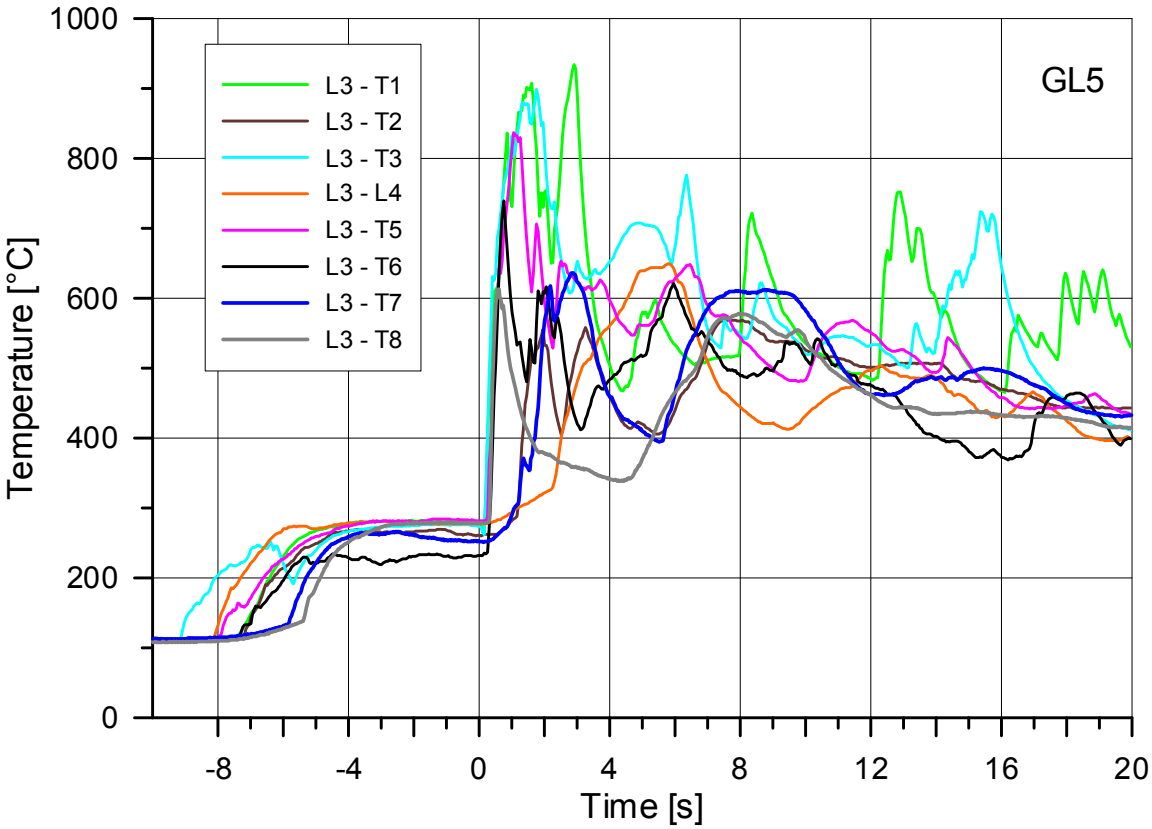

Fig. 54. Temperatures at Level 3 in Test GL5

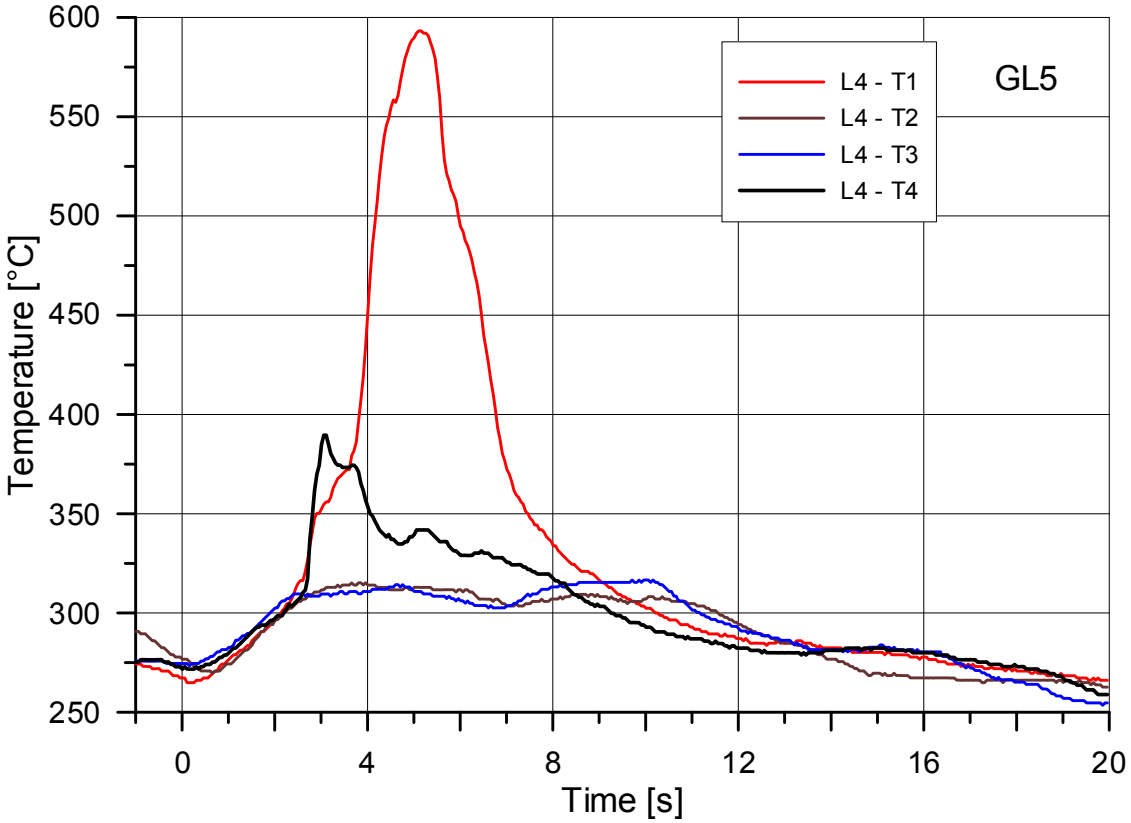

Fig. 55. Temperatures at Level 4 in Test GL5

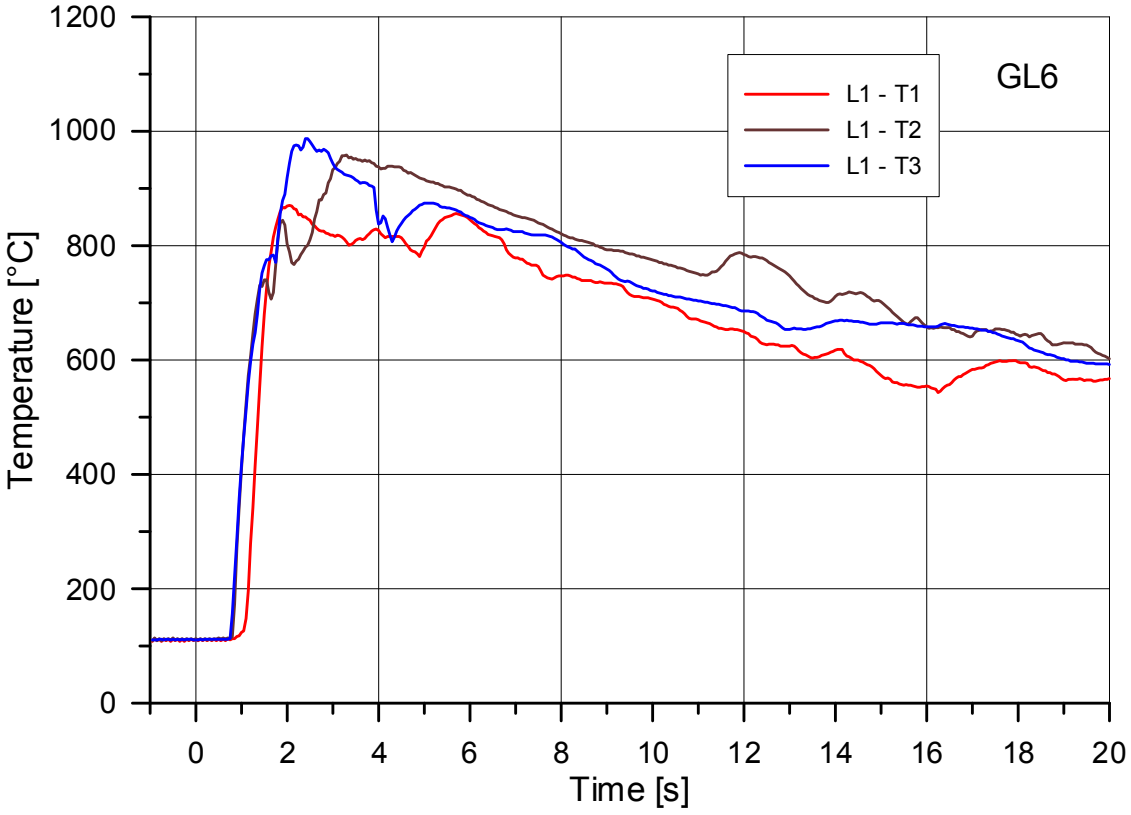

Fig. 56. Temperatures at Level 1 in Test GL6

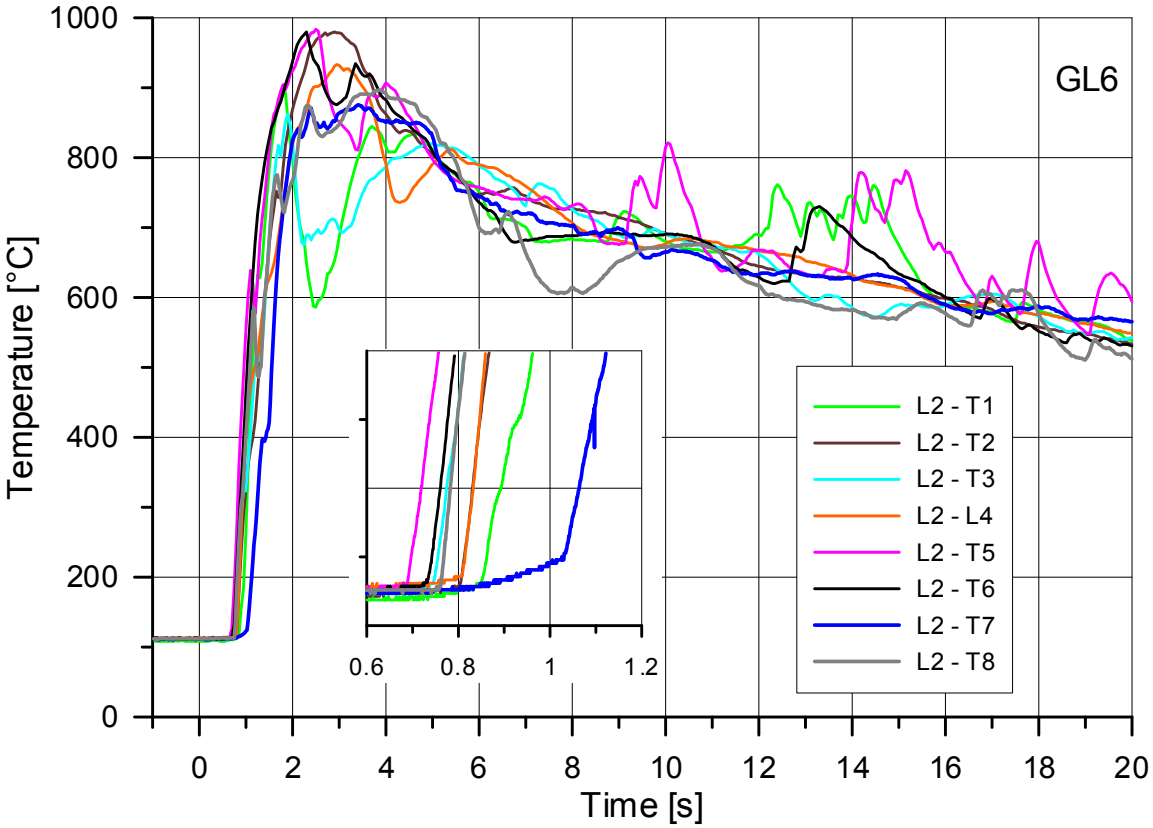

Fig. 57. Temperatures at Level 2 in Test GL6

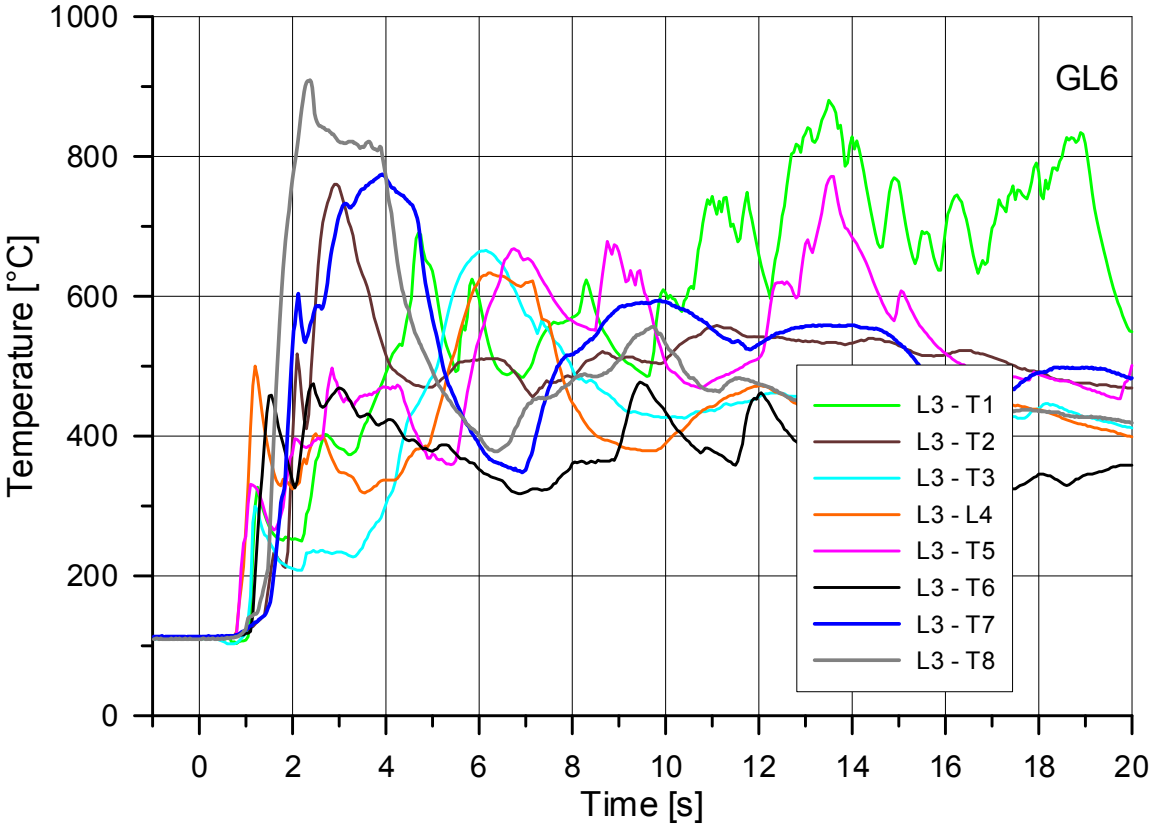

Fig. 58. Temperatures at Level 3 in Test GL6

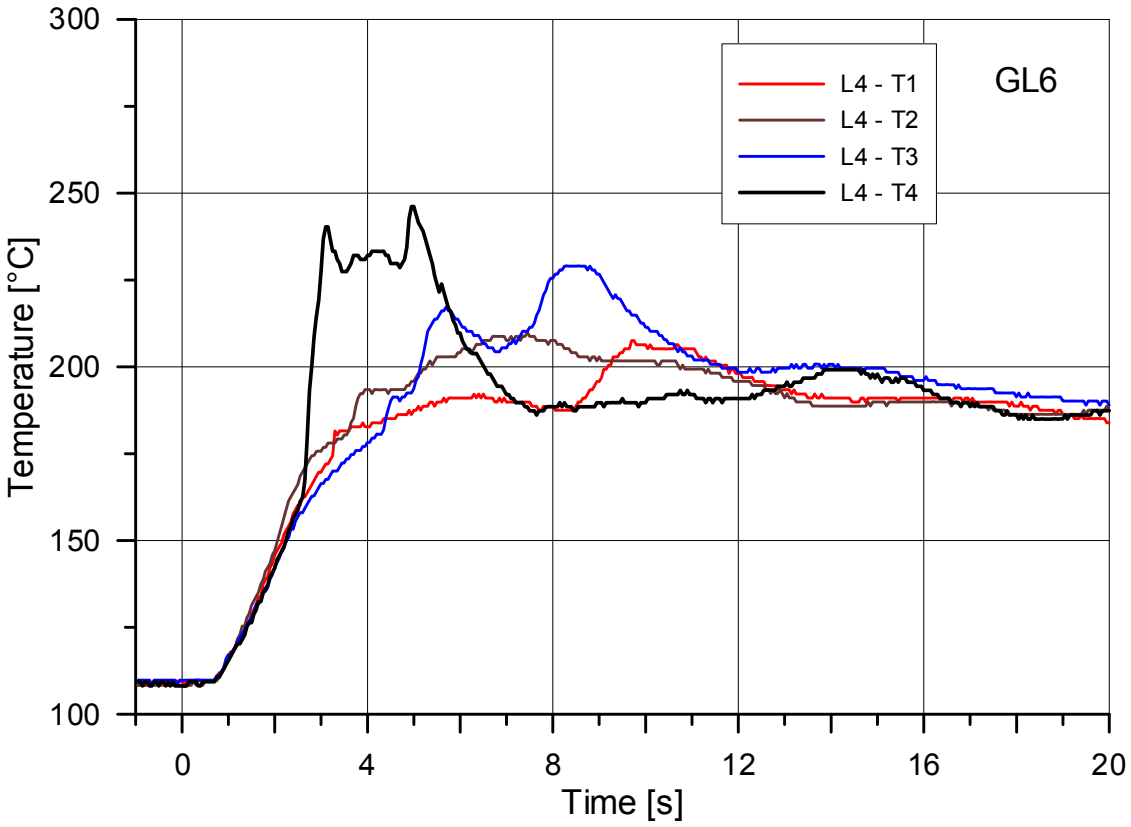

Fig. 59. Temperatures at Level 4 in Test GL6

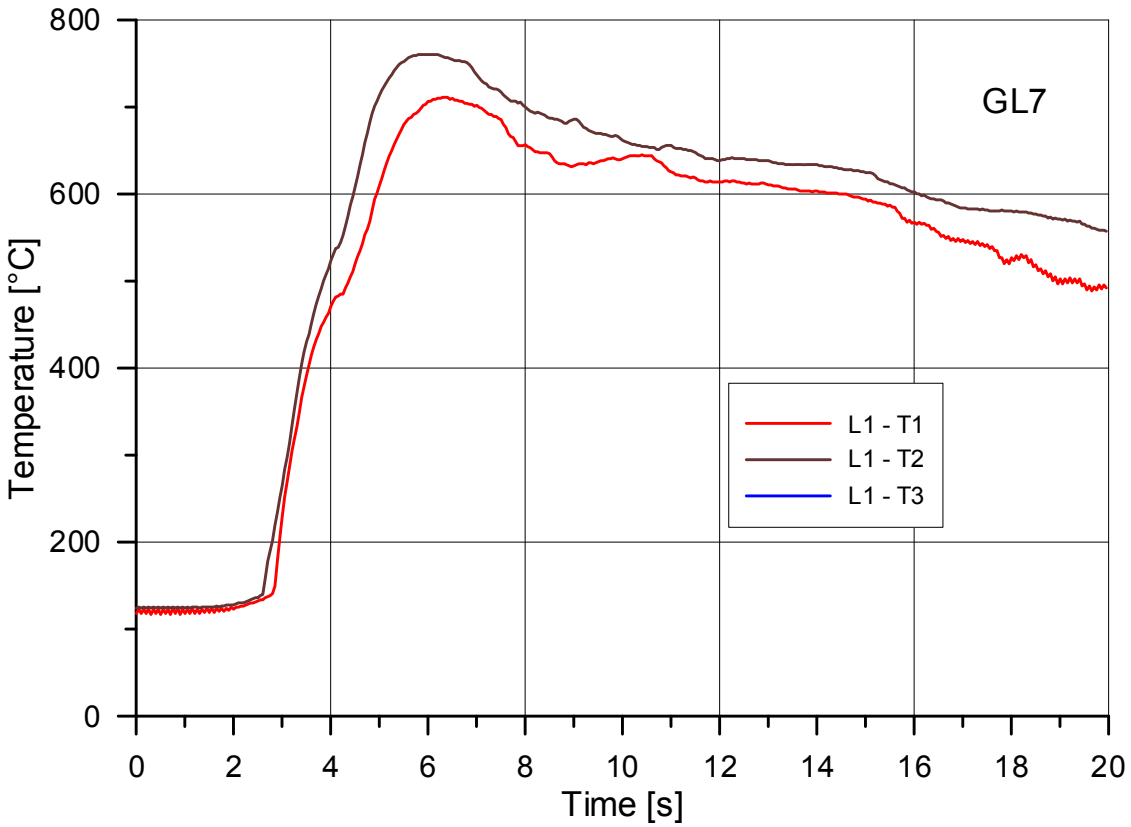

Fig. 60. Temperatures at Level 1 in Test GL7

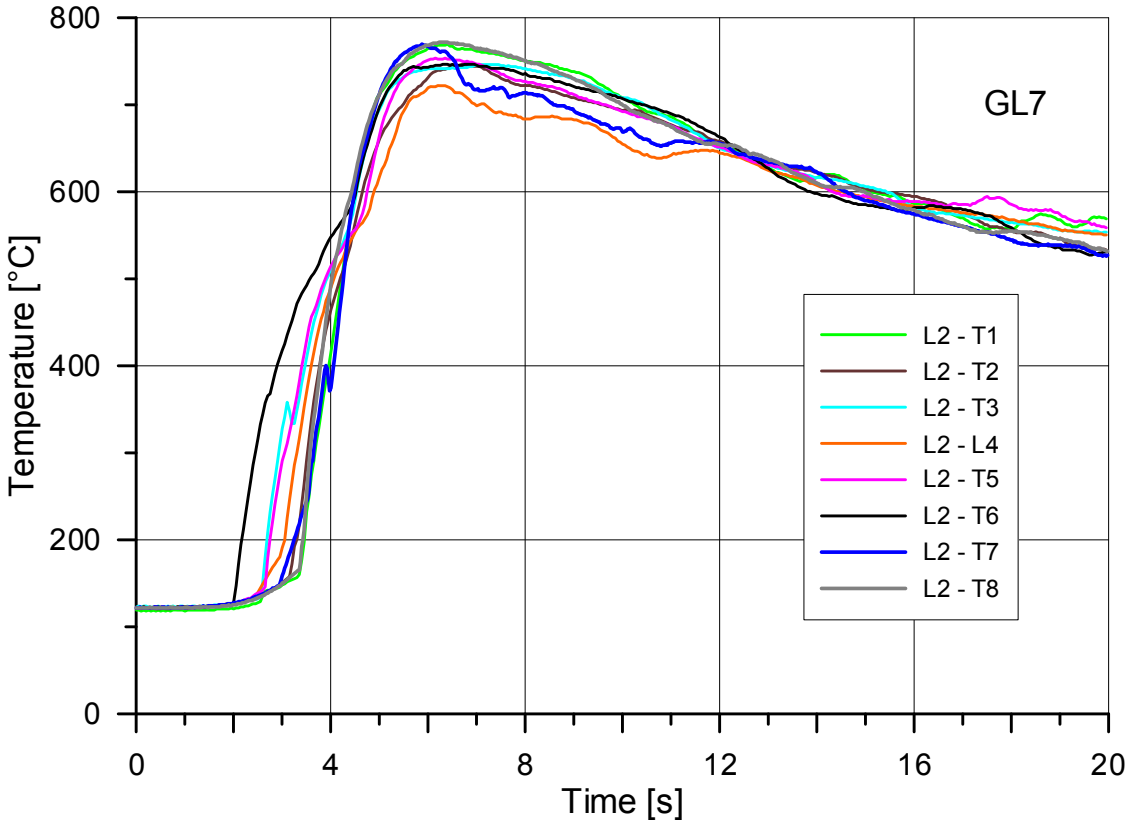

Fig. 61. Temperatures at Level 2 in Test GL7

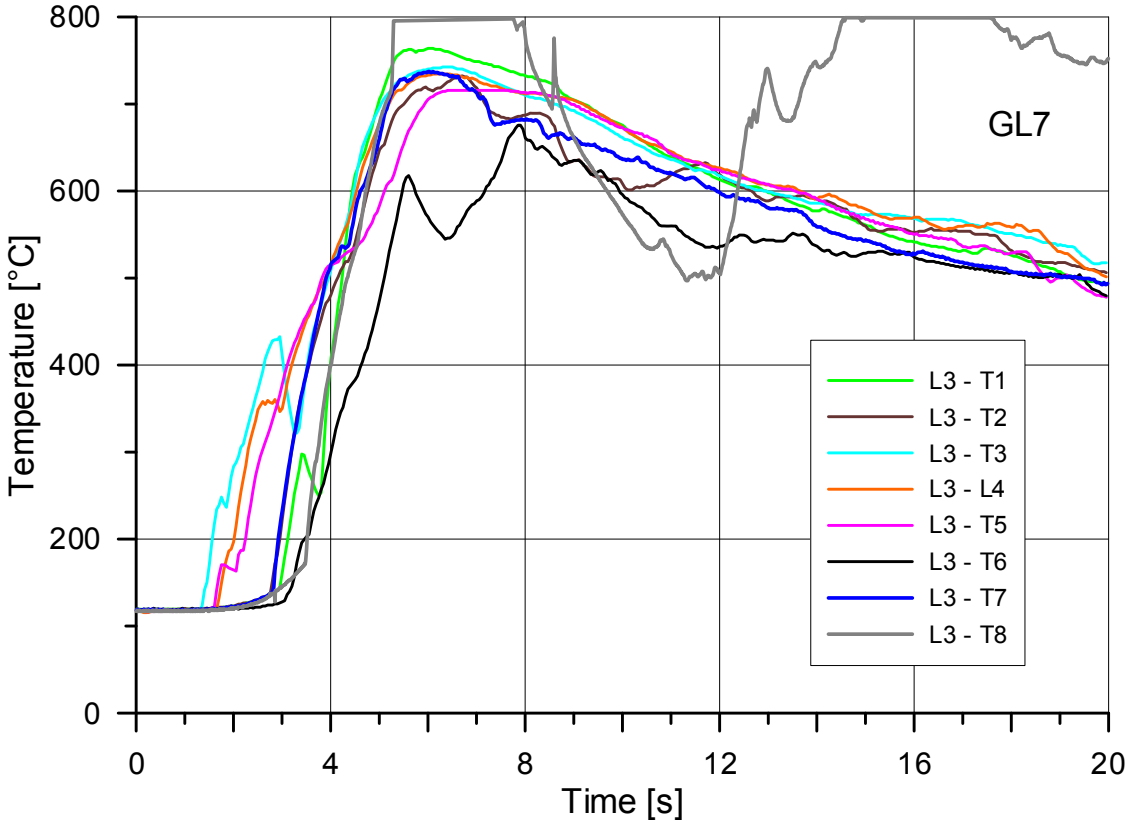

Fig. 62. Temperatures at Level 3 in Test GL7

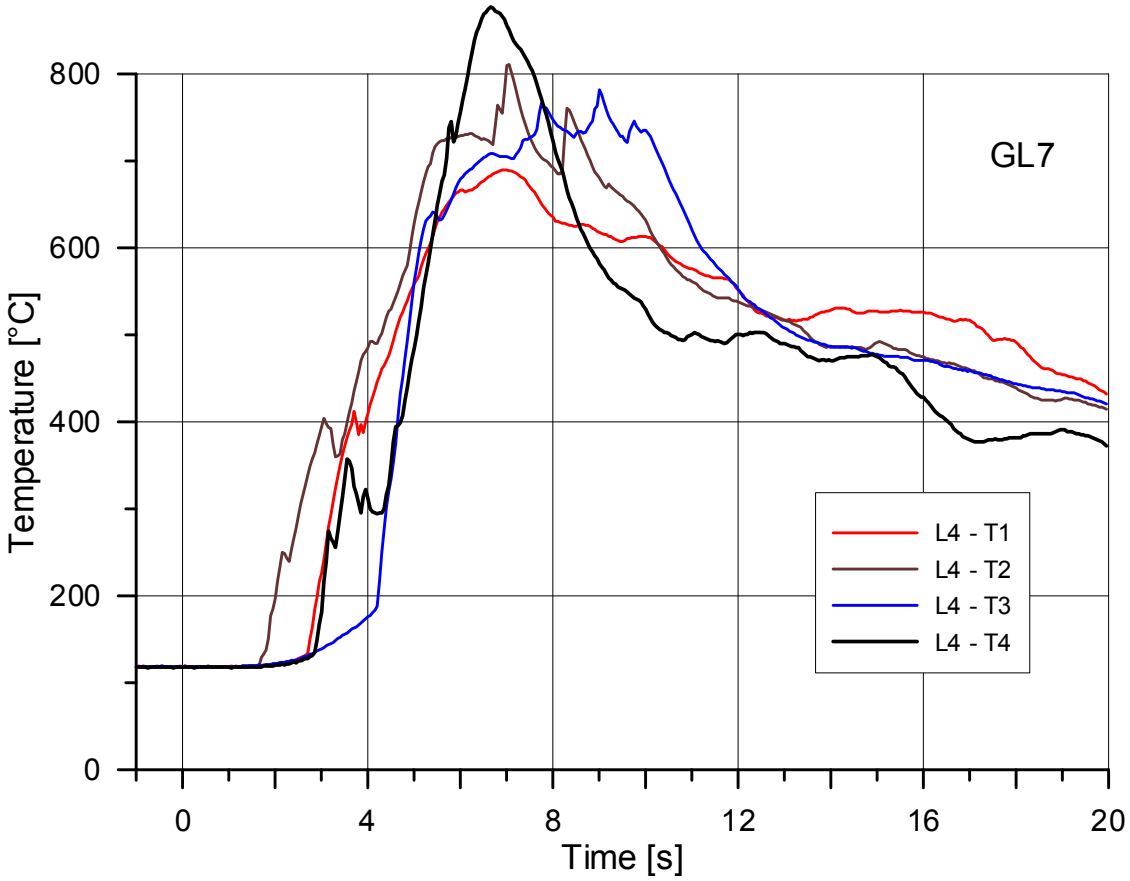

Fig. 63. Temperatures at Level 4 in Test GL7

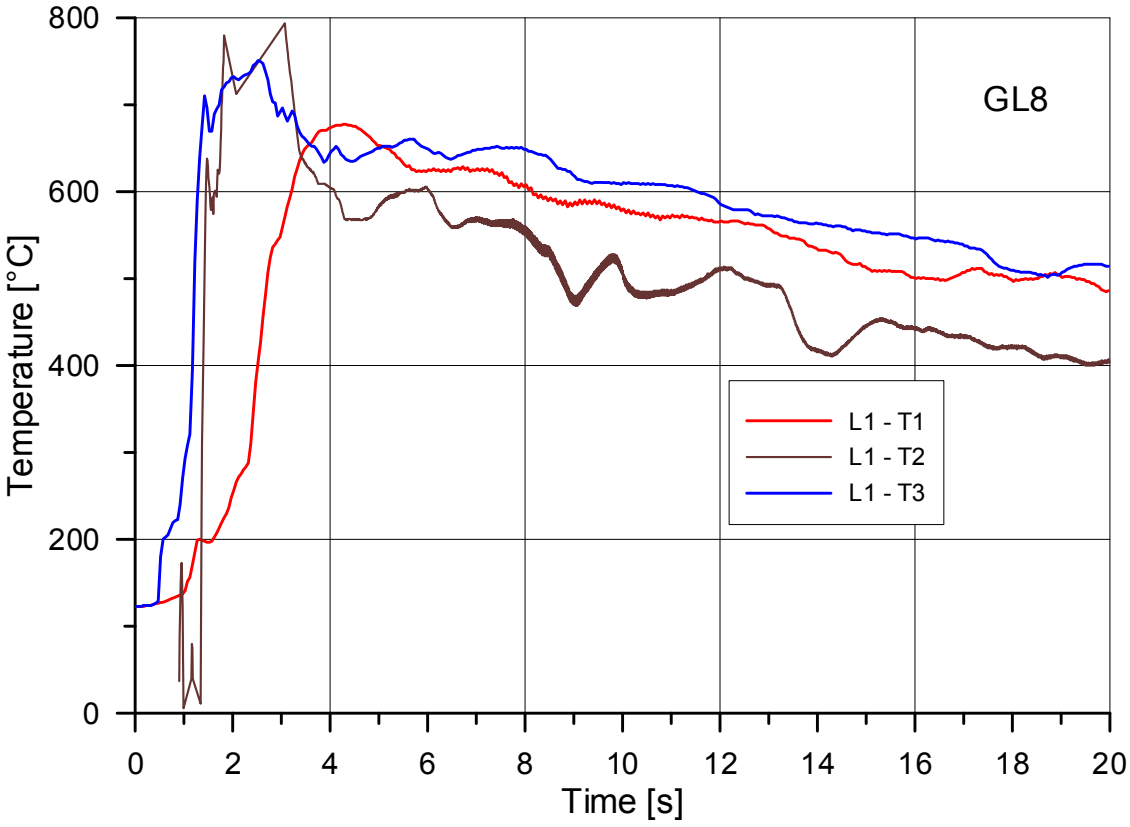

Fig. 64. Temperatures at Level 1 in Test GL8

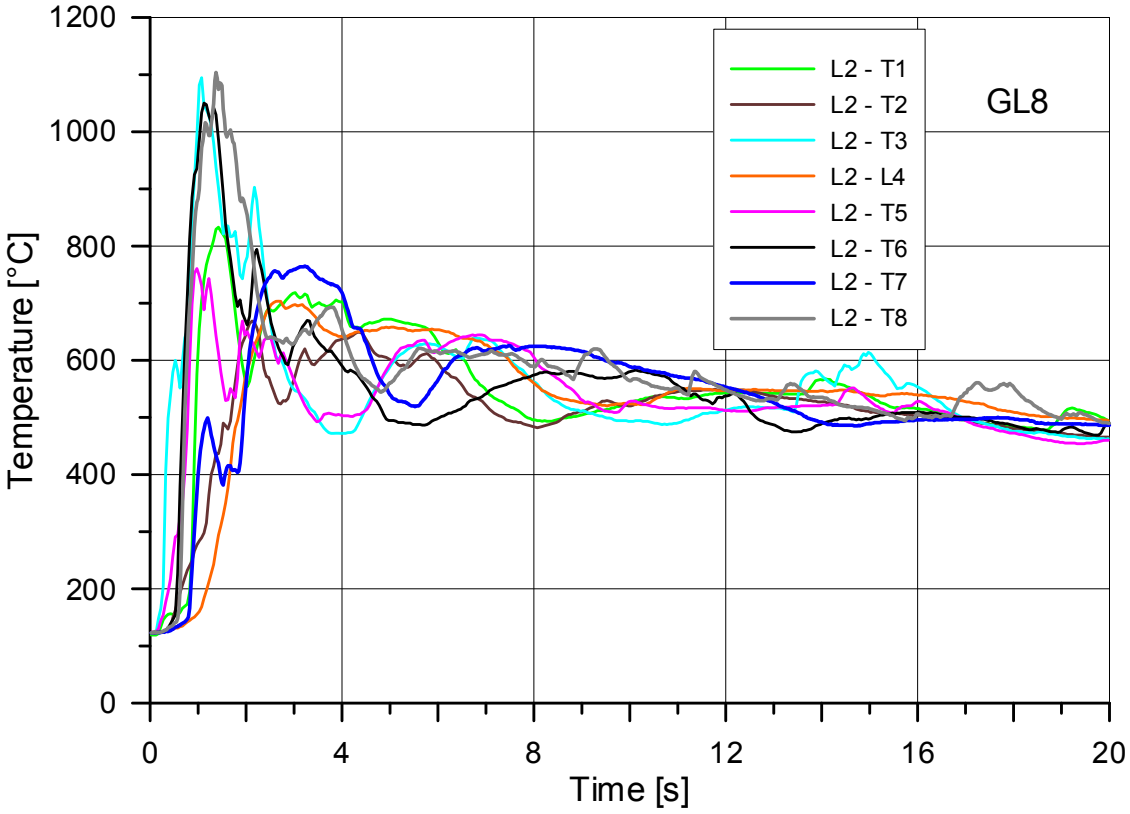

Fig. 65. Temperatures at Level 2 in Test GL8

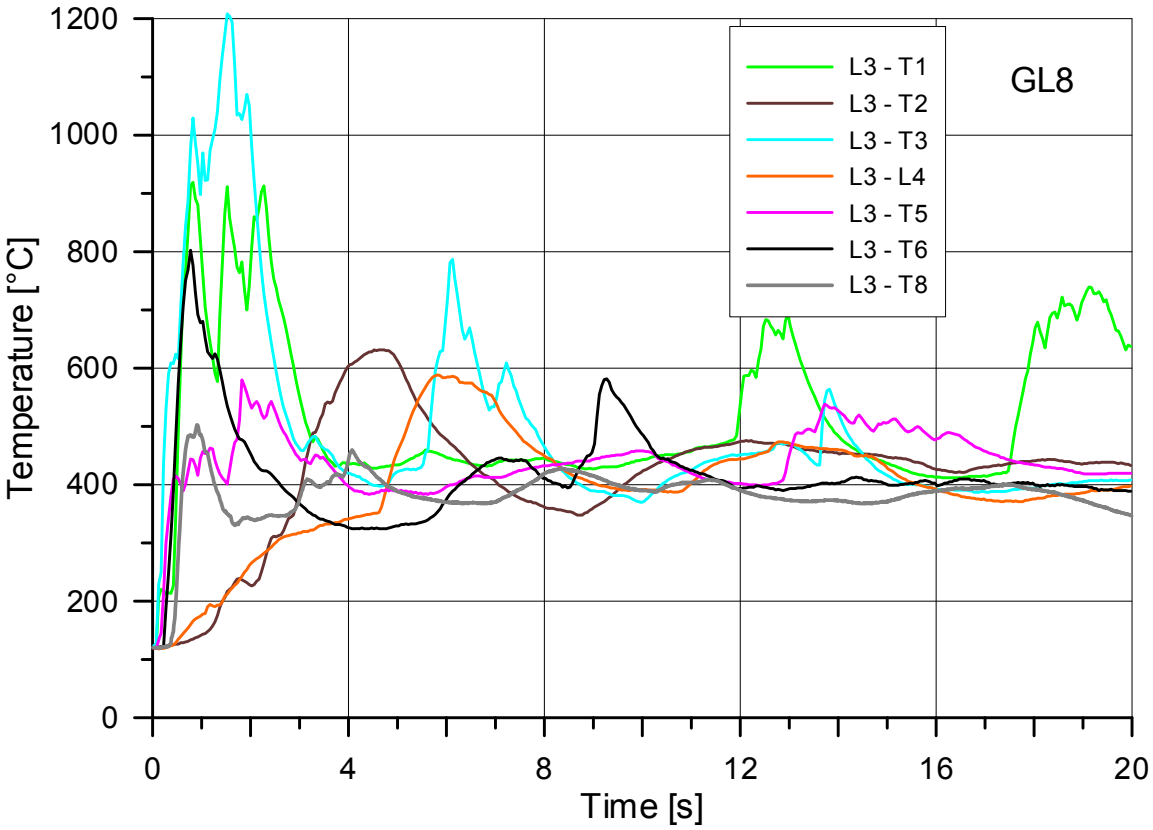

Fig. 66. Temperatures at Level 3 in Test GL8

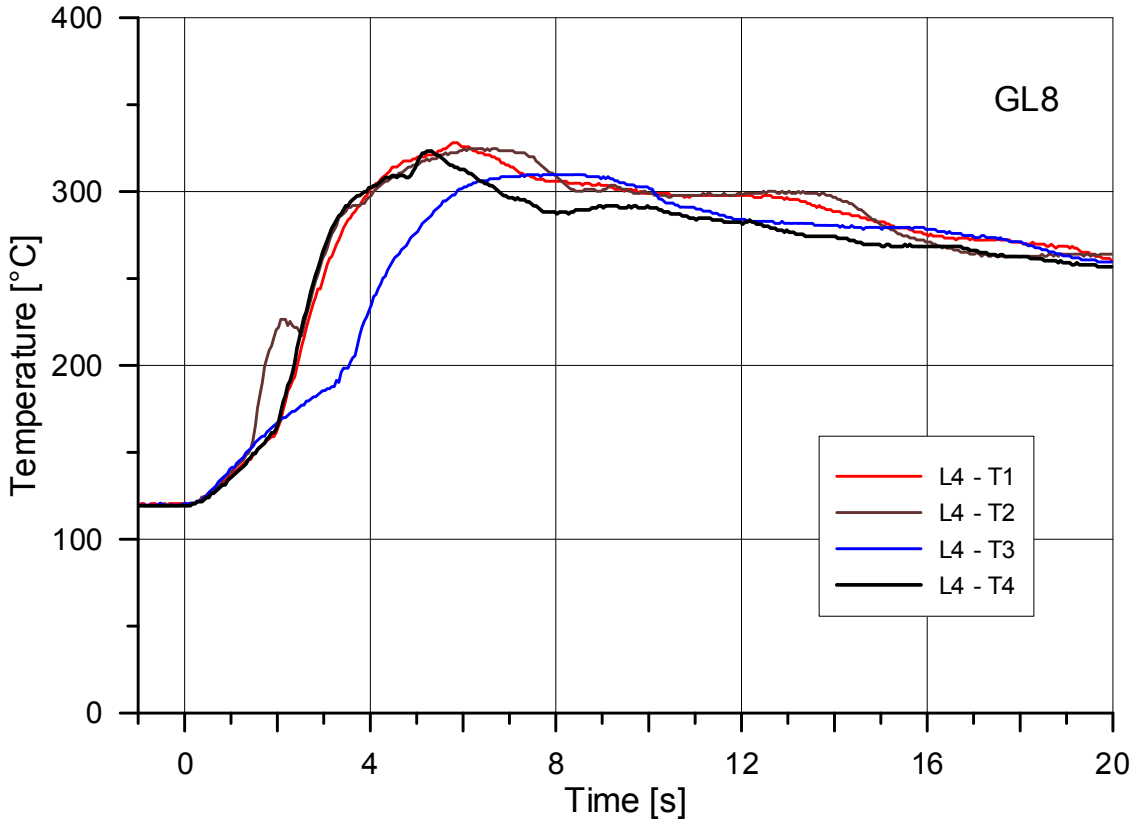

Fig. 67. Temperatures at Level 4 in Test GL8

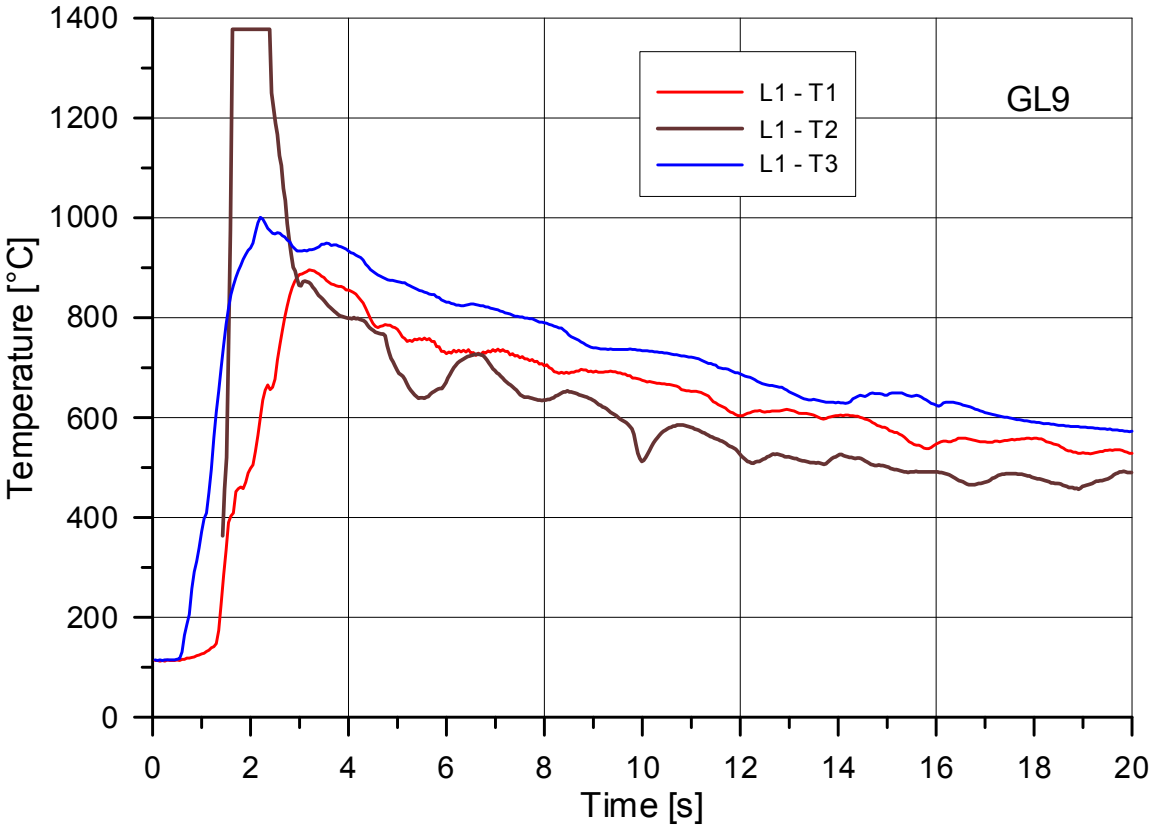

Fig. 68. Temperatures at Level 1 in Test GL9

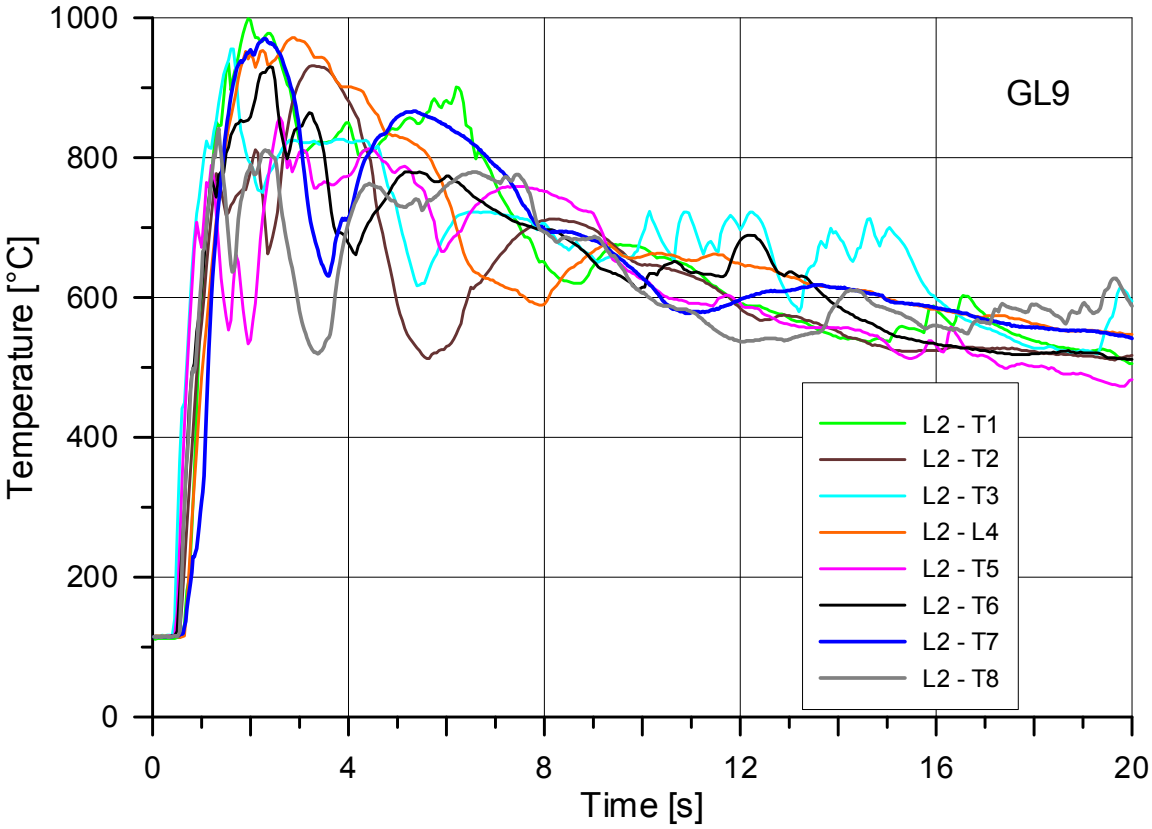

Fig. 69. Temperatures at Level 2 in Test GL9

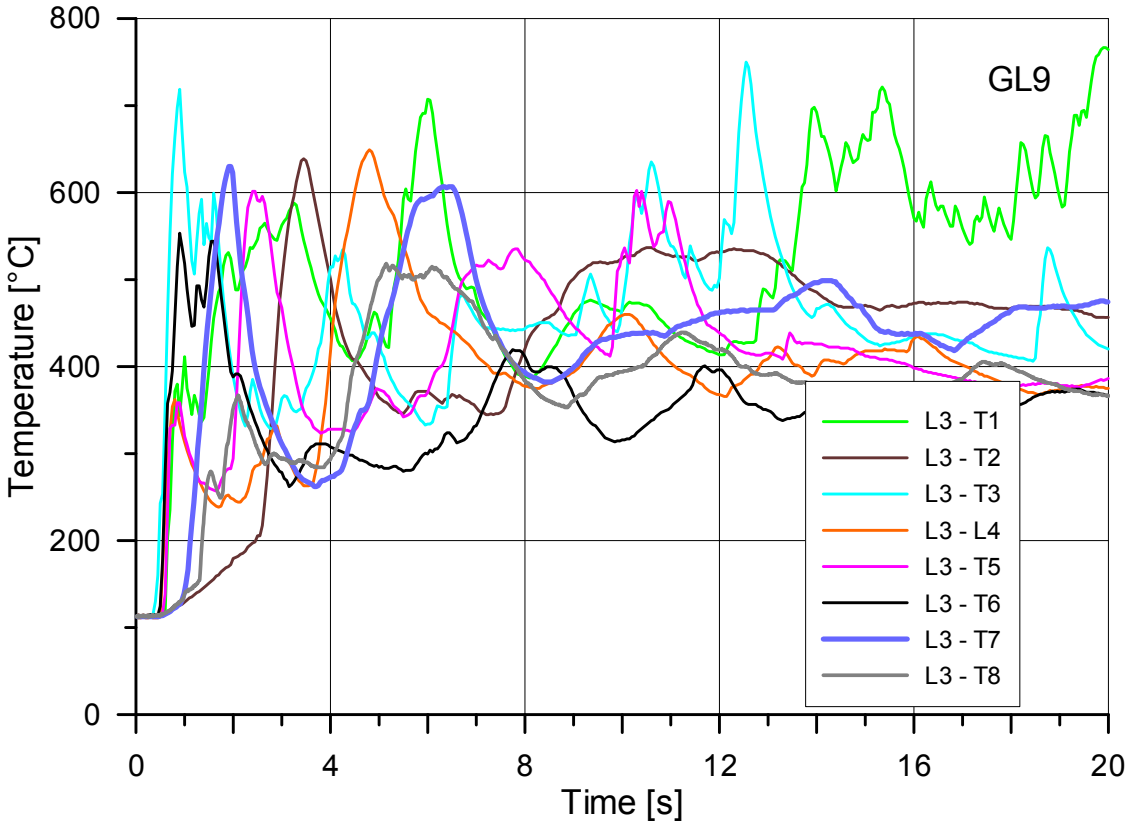

Fig. 70. Temperatures at Level 3 in Test GL9

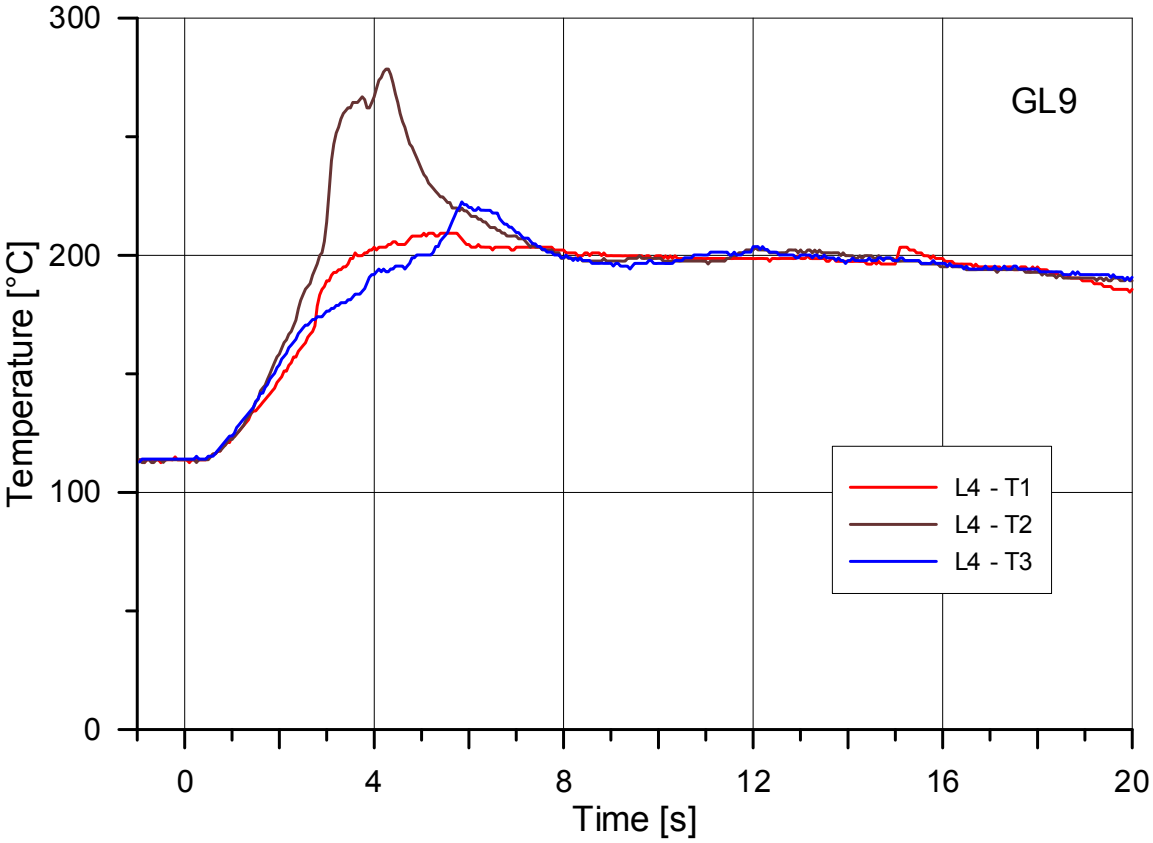

Fig. 71. Temperatures at Level 4 in Test GL9

Annex A Gas analysis

The objective of the gas composition measurements and gas analysis is to obtain data on the chemical reactions taking place during the blow-down, that is, the production of hydrogen by the metal/steam reaction and the hydrogen combustion. We cannot distinguish these processes from direct metal/oxygen reactions, but in terms of total energy release, it makes little difference that direct metal/oxygen reaction initially deposits more energy in the debris and less in the gas, because, for small particles that react efficiently, heat transfer is also efficient.

The composition of the gas in the vessel is measured by taking gas samples. The gas samples are taken from an atmosphere containing a mixture of steam and noncondensible gases. Since the steam condenses the measured mole % of nitrogen, oxygen and hydrogen are given relative to the noncondensible part of the mixture. The uncertainty in the evaluation of the gas samples has been improved lately, and is 0.1 vol% for H_2, 0.3 for O_2 and 0.4 for N_2.

The pretest composition of the vessel atmosphere is known and the amount of each gas in moles can be calculated with the volume of the vessel V, the atmosphere pressure p_0 and temperature T_0, and the measured amount of added hydrogen:

Initial number of moles of hydrogen	[kmol]	$N^0_{H2} = m_{H2} / M_{H2}$	(1)
Initial number of moles of air	[kmol]	$N^0_{air} = p_0 V / (\mathbf{R} T_0)$	(2)
Initial mass of air	[kg]	$m_{air} = N^0_{air} \cdot M_{air}$	(3)
Pre-test partial pressure of air	[MPa]	$p_{1\,air} = p_0 T_1 / T_0$	(4)
Pre-test partial pressure of hydrogen	[MPa]	$p_{1\,H2} = m_{H2} R_{H2} T_1 / V$	(5)
Pre-test partial pressure of steam	[MPa]	$p_{1\,steam} = p_1 – p_{1\,air} – p_{1\,H2}$	(6)
Number of steam moles	[kmol]	$N^0_{steam} = p_{1steam} V / (\mathbf{R} T_1)$	(7)
Mass of steam	[kg]	$m_{steam} = N^0_{steam} M_{H2O}$	(8)
Total number of gas moles	[kmol]	$N_{total} = N_{air} + N_{H2} + N_{steam}$	(9)
Number of nitrogen moles	[kmol]	$N_{N2} = 0.7803\, N_{air}$	(10)
Number of oxygen moles	[kmol]	$N_{O2} = 0.2099\, N_{air}$	(11)
Number of argon moles	[kmol]	$N_{Ar} = 0.0093\, N_{air}$	(12)

The constants are the molecular weights, M_{H2} = 2.02 kg/kmol, M_{air} = 28.96 kg/kmol, M_{H2O}=18.02 kg/kmol, and the gas constants, **R** = 8314 J/kmol/K and R_{H2} = 4116 J/kg/K.

The amount of hydrogen, that is produced and burned during the test, can be determined by the nitrogen ratio method [A1]. The data and assumptions required for this method are listed below:

1. The total pretest moles of noncondensible gases must be known.

2. The measured ratios of the pretest and posttest noncondensible gases must be known.

3. It must be assumed that nitrogen is neither produced nor consumed by chemical reactions.

With the measured data of the pretest mole fractions of species i, X^0_i, the initial number of gas moles N^0_i is:

$$N^0_i = X^0_i \, (N^0_{air} + N^0_{H2} + N_{N2\ RPV/RCS}) \tag{13}$$

The calculation is usually performed separately for the subcompartment and the rest of the containment volume. The sum of moles per species determined by gas sampling may deviate from the values determined by the theoretical determination of pretest composition, due to incomplete mixing of the components and the uncertainty in the acquisition and analysis of the gas samples. With the assumption that the number of nitrogen moles has not changed, the post test number of moles of oxygen and hydrogen can be determined from the measured post test mole fractions X^2_i:

$$N^2_{O2} = N^0_{N2} \, X^2_{O2} / X^2_{N2} \tag{14}$$

$$N^2_{H2} = N^0_{N2} \, X^2_{H2} / X^2_{N2} \tag{15}$$

The number of moles of burned hydrogen is linked to the decrease of oxygen moles,

$$N^2_{H2\ burned} = 2 \, (N^0_{O2} - N^2_{O2}) \tag{16}$$

and the balance of hydrogen gives the moles of produced hydrogen:

$$N^2_{H2\ produced} = N^2_{H2} - N^0_{H2} + N^2_{H2\ burned}. \tag{17}$$

The fraction burned is $$F_{H2} = N^2_{H2\ burned} / (N^0_{H2} + N^2_{H2\ produced}). \tag{18}$$

The ratio of hydrogen moles produced to iron moles oxidized depends on the kind of iron oxide formed. Based on the experience at the Sandia National Laboratories, Blanchat [A2] gives a ratio of 1:1, which implies that in a first step only FeO is formed. For aluminum it is 1.5:1, 3 moles of hydrogen are produced by the oxidation of 2 moles of aluminum with water.

References

[A1] T.K. Blanchat, M.D. Allen, M.M. Pilch, R.T. Nichols, "Experiments to Investigate Direct Containment Heating Phenomena with Scaled Models of the Surry Nuclear Power Plant", *NUREG/CR-6152, SAND93-2519*, Sandia Laboratories, Albuquerque, N.M., (1994)

[A2] T.K. Blanchat, M.M. Pilch, R.Y. Lee, L. Meyer, and M. Petit, “Direct Containment Heating Experiments at Low Reactor Coolant System Pressure in the Surtsey Test Facility,” *NUREG/CR-5746, SAND99-1634*, Sandia National Laboratories, Albuquerque, N.M., (1999).

ISSN 1869-9669
ISBN 978-3-7315-0195-4

ISBN 978-3-7315-0195-4